UC Davis
UC Davis Electronic Theses and Dissertations

Title

Engineering Microorganisms for Carbon Capture and Chemical Production

Permalink

Author

Treece, Tanner Robert

Publication Date

2023

Peer reviewed|Thesis/dissertation

Engineering Microorganisms for Carbon Capture and Chemical Production

BY

Tanner Robert Treece

DISSERTATION

Submitted in partial satisfaction of the requirements for the degree of

DOCTOR IN PHILOSOPHY

in

Chemistry

in the

OFFICE OF GRADUATE STUDIES

of the

UNIVERSITY OF CALIFORNIA

DAVIS

Approved:

_____

Dr. Shota Atsumi, Chair

_____

Dr. Justin Siegel

_____

Dr. Patrick Shih

Committee in charge

2023

i

Dedication

To my loving wife and parents

Table of contents

Abstract

Engineered microorganisms capable of producing commodity chemicals have gained traction as viable alternative to traditional petrochemical approaches. Expanded feedstock pools, engineering regulatory elements of metabolism, and fermentation optimization are all methods employed to increase productivity in these microbial hosts. Plant biomass refined into pure sugars are commonly used as a substrate for these fermentations. Heterotrophic hosts can convert these pure sugars into various chemical compounds, however, using sugars for fermentation directly competes with global food supply. One alternative carbon source to these sugars is using atmospheric CO_2 to power biochemical production in these organisms. However, native biological CO_2 fixation is slow, limiting growth and production rates. This dissertation seeks to address the challenges intrinsic to using CO_2 as a chemical production feedstock. First, by engineering photomixotrophy into the naturally photosynthetic microorganism cyanobacteria to supplement chemical production and growth by directing the excess carbon from sugars towards the substrate for the dominant CO_2 fixing enzyme ribulose-1,5-bisphosphate carboxylase/oxygenase. Second, by engineering a non-canonical CO_2 fixing pathway known as the reductive glycine pathway into the heterotroph, *Escherichia coli*, in conjunction with using formate produced in a novel electrocatalytic setting and optimizing biochemical production in *E. coli* from this electrocatalytic reaction mixture. Both strategies demonstrate methods where chemical production can be made more renewable with the aid of engineered microorganisms capable of utilizing CO_2 from the atmosphere to make industrially relevant chemicals such as isobutanol and succinate.

Chapter 1: Introduction
Engineering Microorganisms for the Production of Chemicals

Portions of this chapter are reproduced with permission from:

Treece, T. R., Gonzales, J. N., Pressley, J. R., & Atsumi, S. (2022). Synthetic biology approaches for improving chemical production in cyanobacteria. *Frontiers in Bioengineering and Biotechnology*, *10*.

1.1 Microbial Production as an Alternative to Petrochemistry

It is well established that rising atmospheric CO_2 levels are the primary cause for unprecedented climate change impacting the globe[1]. Despite this, chemical production still relies mostly on petroleum-based synthesis[2]. In response to the growing concern over greenhouse gases, research with a focus on more sustainable chemical production has become a high priority. The fields of synthetic biology and metabolic engineering aim to achieve a more sustainable method for chemical production using engineered organisms. These efforts include the use of both heterotrophic and photosynthetic microorganisms. Heterotrophic chemical production involves a carbon input of a sugar feedstock to a microorganism to generate a biochemical product as an output. Alternatively, using photosynthetic microorganisms offers the advantage of eliminating the need for sugar feedstocks and the ability to generate valuable chemical commodities from CO_2 and sunlight. The two predominant categories of photosynthetic microorganisms being investigated for chemical production are microalgae and cyanobacteria. Microalgae are a diverse group of photosynthetic eukaryotes that have been shown to be viable production hosts for a wide array of useful chemical commodities ranging from biofuels to lipids and vitamins[3]. Cyanobacteria are a group of prokaryotic microorganisms with some of the fastest carboxylation rates present in photosynthetic organisms[4].

Despite the burgeoning interest in these photosynthetic microorganisms, the field still faces many challenges that have yet to be addressed. The primary concern is the inefficient nature of photosynthesis and CO_2 fixation. Attempts to improve upon the central carbon fixation enzyme ribulose-1,5-bisphosphate carboxylase-oxygenase (RuBisCO) have been met with little success[4,5]. Part of the challenge with RuBisCO is its inability to distinguish between CO_2 and O_2 with high specificity. The oxygenase activity of RuBisCO results in an energetically costly pathway known as photorespiration which has widespread effects on the growth and metabolic needs of many species of photosynthetic organisms[6]. Recent research suggests that photorespiration is a symptom of RuBisCO evolving in a high CO_2 environment where enzymatic specificity was not as vital, with this in mind, recent studies are investigating the possibilities of by reviving ancestral forms of the protein and subjecting it to new environments in the hopes of

generating biologically important variants[7]. Other efforts are looking towards natural adaptations of CO_2 fixation for inspiration with a focus on the carboxysome, a bacterial microcompartment that acts to localize RuBisCO with high concentrations of CO_2[8]. An additional engineering strategy aims to avoid photorespiration by engineering synthetic protein structures to mimic cyanobacterial carboxysomes to concentrate CO_2 near RuBisCO and competitively inhibit the reaction with oxygen[8].

Plastics, a major product of the petroleum industry, have caused additional harm to the environment beyond the aforementioned greenhouse gas emissions[2]. Petroleum based plastics are a major source of pollution in our waterways due to the prolonged degradation periods associated with these products[2,9]. One alternative to these petroleum-based plastics is to use engineered microorganisms. The engineered microbe can produce various chemical commodities that can be used as monomers to synthesize a wide array of biodegradable plastics[10,11]. In the works presented in this dissertation, succinate and isobutanol are the target products synthesized by microbes. Both succinate and isobutanol are relevant chemicals to the plastics industry and can be used to make various polymers that can replace petroleum-based products[9,12]. By investigating the production of these chemicals in microbes, we can achieve an efficient synthesis platform that can not only sequester or reduce greenhouse gases but also help to replace highly polluting everyday products with greener alternatives.

1.2 Rewiring Photosynthetic Metabolism

Efforts have been made to overcome the intrinsic shortcomings of photosynthetic microorganisms by rewiring metabolism related to carbon fixation and photosynthesis. While efforts to improve RuBisCO have not been met with much success, current research has shifted focus towards rerouting metabolism to improve overall photosynthetic efficiency by focusing on key aspects of the Calvin-Benson cycle or the photosynthetic electron transport chain (PETC). One strategy used to accomplish this is rerouting excess energy from the PETC towards hydrogen production[13]. Excess energy from the PETC is generally lost as heat to the environment. Rewiring the PETC to capture this wasted energy can effectively convert excess

light energy into high energy chemical bonds that can be used as an eco-friendly alternative to other greenhouse gases such as methane. In the aforementioned study, *Chlamydomonas reinhardtii,* was successfully used for continuous hydrogen production for 14 days by fusing a naturally occurring [FeFe] hydrogenase to another enzyme known as superoxide dismutase, representing a large step forward in the viability of using this hydrogen production strategy to harness the excess reductive energy from the PETC[13].

An inherent drawback of RuBisCO is its promiscuous nature, when RuBisCO undergoes oxygenase activity a costly side pathway known as photorespiration occurs where the oxygenase product is recycled back into usable metabolism consuming energy and losing CO_2 in the process. As much as 30% of energy produced by photosynthesis has been observed to be lost through photorespiration in plants[6]. Rewiring or preventing photorespiration represents a promising way to improve the overall efficiency of carbon fixation in photosynthetic organisms. Efforts to rewire photorespiration generally involve deleting energetically costly steps, circumventing steps where CO_2 is lost, and rerouting metabolites towards central carbon metabolism[6]. One of the more ambitious efforts to ameliorate the cost of photorespiration was the expression of a synthetic carbon capture pathway to serve as both a photorespiratory bypass and as a supplement to the Calvin-Benson cycle, this was shown to be a viable use of synthetic biology to counteract the costly natural photorespiration pathway[14].

It should be noted that photorespiration is not the sole pathway responsible for carbon inefficiencies, many metabolic processes include steps where CO_2 is lost to the environment. An important way to engineer microorganisms for sustainability involves carbon conservation, focusing on rerouting metabolism to circumvent decarboxylation reactions[15]. Of the more notable strategies is the non-oxidate glycolysis pathway (NOG) which has been shown to function in *E.* coli and which can effectively conserve all carbon associated with sugar catabolism to acetyl-CoA[16]. While carbon conservation is a powerful methodology for engineering metabolism, the field is still in its infancy and further work is required to evaluate the industrial viability of many carbon conservation strategies. Additionally, *de-novo* carbon fixation pathways, which will be addressed later, are currently being developed and may prove to be a better methodology for the development of sustainable production hosts.

1.3 Photomixotrophy

Another approach to increase chemical production capacity in cyanobacteria is to supplement CO_2 with carbohydrates as an auxiliary carbon source for the Calvin-Benson cycle, thereby making the organism photomixotrophic. By re-engineering glucose catabolism to direct carbon flux into the Calvin-Benson cycle, more ribulose-1,5-bisphosphate can be supplied to RuBisCO, accelerating CO_2 fixation. This ultimately results in faster growth and production of downstream targets, as well as a 6- fold increase in titer once metabolism was rewired to accommodate photomixotrophy[17]. The addition of a heterotrophic mode further enhances the industrial potential of this approach by permitting CO_2 fixation in darkness, allowing for 24-hour production under natural diurnal conditions. Glucose can be readily obtained from the acid hydrolysis of agricultural waste products such as corn stover, in conjunction with other sugars: xylose, arabinose, and galacturonic acid[18]. By installing catabolic pathways for these non-glucose sugars, these agricultural waste products can be used more efficiently. Xylose, the second most abundant sugar in corn stover lysate, has successfully been used to achieve photomixotrophic production of 2,3-butanediol in light and dark conditions with significant improvements in growth and product titer over the equivalent photoautotrophic organism[19].

1.4 Non-RuBisCO Carbon Fixation

In contrast to research centering on canonical CO_2 fixation, investigations into *de novo* CO_2 fixation pathways have been explored and theorized in recent years as more efficient alternatives to traditional RuBisCO based CO_2 assimilation. These pathways may provide advantages in chemical production hosts by offering insight into carboxylation reactions that could work in tandem with RuBisCO. The expression of formate dehydrogenase in the cyanobacterium, *Anabaena* sp. PCC 7120, was shown to successfully increase intracellular formate concentration, representing an alternative to the photo-reduction of CO_2 and can act to supplement natural carbon fixation pathways[20].

Many of these *de-novo* CO_2 fixation pathways have had limited success when installed into model organisms such as *E. coli* and yeast and it has yet to be shown if these pathways can function effectively in photosynthetic hosts. One pathway of note that has been shown to work in *E. coli* is the reductive glycine pathway, hereafter RGP[21]. This pathway leverages the native glycine cleavage system in the reverse direction to combine one equivalent of CO_2 with 5,10-methylenetetrahydrofolate that has been produced from formate to produce pyruvate. This method allows *E. coli* to directly assimilate CO_2 into central metabolic pathways and is a more efficient method for CO_2 fixation than traditional RuBisCO [22]. This inorganic carbon can then be leveraged for biochemical synthesis. Additional work has also recently shown that the expression of formate dehydrogenase confers further renewable characteristics to strains harboring the RGP by removing the need for glucose supplementation[23]. Other notable CO_2 fixation pathways include the crotonyl-CoA/ethylmalonyl-CoA/hydroxybutyryl-CoA (CETCH) cycle and the tartronyl-CoA (TaCo) pathways[24]. While the RGP has proven to be a viable carbon fixation pathway that was shown to function in *E. coli,* the growth exhibited by this CO_2 fixing *E. coli* is slower than its traditional heterotrophic phenotype[21,23]. Advancements in modeling and metabolomics may allow for an increase in the creation of *de novo* carbon fixation pathways that may prove to be both more efficient than traditional pathways and capable of functioning in a wider array of chemical production hosts.

1.5 Metabolic Engineering Tools for *Escherichia coli* and Cyanobacteria

The metabolic engineering toolkit for *E. coli* is vast. With access to plasmid expression systems, to the genomic integration of an engineered protein via CRISPR, the ability to engineer *E. coli* to produce chemical commodities is unmatched. The ability to rewire metabolism towards the extremes of introducing *de novo* carbon fixation methods is also made easier by the abundance of work performed on the overall metabolism of *E. coli.* This is what makes *E. coli* the perfect host for investigating if alternative CO_2 fixation pathways can be integrated into metabolism to generate a host that can perform the renewable synthesis of chemicals from CO_2 more efficiently than natural methods.

In cyanobacteria, traditional genomic modifications are a labor-intensive task and limiting in nature due to the polyploidal nature of these organisms and the need for antibiotic resistance markers[25]. The current methodology for genomic integration involves constructing a plasmid with an antibiotic selection marker in a plasmid host such as *E. coli.* After introduction of this plasmid to cyanobacteria, several rounds of antibiotic screening are required to ensure complete genome segregation[26]. This process generally limits the number of modifications that can be performed in a single strain due to the physiological constraints of expressing multiple different antibiotic resistance genes.

The overall task of metabolic engineering in cyanobacteria has been made dramatically more efficient thanks to the advent of CRISPR gene editing which allows for efficient markerless edits[27]. However, the protein Cas9 is toxic to a number of cyanobacteria species[28]. Researchers have recently uncovered other endonucleases that are similarly capable of CRISPR gene editing. The main endonuclease of interest is Cpf1 which, while similar to Cas9, is better tolerated by photosynthetic hosts[29]. As the body of research grows around Cpf1, more engineering strategies will be made available in the realm of photosynthetic chemical production and should offer a boon towards the viability of these organisms to begin replacing their non-CO_2 fixing brethren in the realm of biochemical production[30,31]. Additionally, having the ability to perform markerless genomic modifications unlocks the potential to engineer these microorganisms far more ambitiously than what was previously possible.

Other work on CRISPR technologies in cyanobacteria includes the use of CRISPR inhibition (CRISPRi) by using dead Cas9 (dCas9)[32]. While the endonuclease activity of the intact Cas9 protein seems to be toxic to these production hosts, dCas9 is able to function in the same manner in photosynthetic hosts as it is able to in heterotrophic hosts such as *E. coli*[33]. While the use of dCas9 may not be as broadly useful as traditional CRISPR, dCas9 has been shown to be invaluable in certain chemical production applications where more traditional gene knockouts would otherwise be toxic. Overall, as the field of metabolic engineering continues to grow, organisms like *E. coli* or species of cyanobacteria will become more widespread as alternative production hosts for chemical commodities that ideally can sequester large amounts of carbon

dioxide and will hopefully usurp petrochemistry as the *de facto* method for the synthesis of everyday products.

1.6 References

(1)   Solomon, S.; Plattner, G. K.; Knutti, R.; Friedlingstein, P. Irreversible Climate Change Due to Carbon Dioxide Emissions. *Proc. Natl. Acad. Sci. U. S. A.* **2009**, *106* (6), 1704–1709. https://doi.org/10.1073/pnas.0812721106.

(2)   Levi, P. G.; Cullen, J. M. Mapping Global Flows of Chemicals: From Fossil Fuel Feedstocks to Chemical Products. *Environ. Sci. Technol.* **2018**, *52* (4), 1725–1734. https://doi.org/10.1021/acs.est.7b04573.

(3)   Sproles, A. E.; Fields, F. J.; Smalley, T. N.; Le, C. H.; Badary, A.; Mayfield, S. P. Recent Advancements in the Genetic Engineering of Microalgae. *Algal Res.* **2021**, *53* (December 2020), 102158. https://doi.org/10.1016/j.algal.2020.102158.

(4)   Flamholz, A. I.; Prywes, N.; Moran, U.; Davidi, D.; Bar-On, Y. M.; Oltrogge, L. M.; Alves, R.; Savage, D.; Milo, R. Revisiting Trade-Offs between Rubisco Kinetic Parameters. *Biochemistry* **2019**, *58* (31), 3365–3376. https://doi.org/10.1021/acs.biochem.9b00237.

(5)   Erb, T. J.; Zarzycki, J. A Short History of RubisCO: The Rise and Fall (?) Of Nature's Predominant CO_2 Fixing Enzyme. *Curr. Opin. Biotechnol.* **2018**, *49*, 100–107. https://doi.org/10.1016/j.copbio.2017.07.017.

(6)   Hagemann, M.; Bauwe, H. Photorespiration and the Potential to Improve Photosynthesis. *Curr. Opin. Chem. Biol.* **2016**, *35*, 109–116. https://doi.org/10.1016/j.cbpa.2016.09.014.

(7)   Shih, P. M.; Occhialini, A.; Cameron, J. C.; Andralojc, P. J.; Parry, M. A. J.; Kerfeld, C. A. Biochemical Characterization of Predicted Precambrian RuBisCO. *Nat. Commun.* **2016**, *7*, 1–11. https://doi.org/10.1038/ncomms10382.

(8)   Kerfeld, C. A.; Melnicki, M. R. ScienceDirect Assembly , Function and Evolution of Cyanobacterial Carboxysomes. *Curr. Opin. Plant Biol.* **2016**, *31*, 66–75. https://doi.org/10.1016/j.pbi.2016.03.009.

(9)   Lan, E. I.; Wei, C. T. Metabolic Engineering of Cyanobacteria for the Photosynthetic Production of Succinate. *Metab. Eng.* **2016**, *38*, 483–493. https://doi.org/10.1016/j.ymben.2016.10.014.

(10)   Sirohi, R.; Prakash Pandey, J.; Kumar Gaur, V.; Gnansounou, E.; Sindhu, R. Critical Overview of Biomass Feedstocks as Sustainable Substrates for the Production of Polyhydroxybutyrate (PHB). *Bioresour. Technol.* **2020**, *311* (May), 123536. https://doi.org/10.1016/j.biortech.2020.123536.

(11)   Nduko, J. M.; Taguchi, S. Microbial Production of Biodegradable Lactate-Based Polymers

and Oligomeric Building Blocks From Renewable and Waste Resources. *Front. Bioeng. Biotechnol.* **2021**, *8* (February), 1–18. https://doi.org/10.3389/fbioe.2020.618077.

(12)   Atsumi, S.; Hanai, T.; Liao, J. C. Non-Fermentative Pathways for Synthesis of Branched-Chain Higher Alcohols as Biofuels. *Nature* **2008**, *451* (7174), 86–89. https://doi.org/10.1038/nature06450.

(13)   Ben-Zvi, O.; Dafni, E.; Feldman, Y.; Yacoby, I. Re-Routing Photosynthetic Energy for Continuous Hydrogen Production in Vivo. *Biotechnol. Biofuels* **2019**, *12* (1), 1–13. https://doi.org/10.1186/s13068-019-1608-3.

(14)   Shih, P. M.; Zarzycki, J.; Niyogi, K. K.; Kerfeld, C. A. Introduction of a Synthetic CO2-Fixing Photorespiratory Bypass into a Cyanobacterium. *J. Biol. Chem.* **2014**, *289* (14), 9493–9500. https://doi.org/10.1074/jbc.C113.543132.

(15)   François, J. M.; Lachaux, C.; Morin, N. Synthetic Biology Applied to Carbon Conservative and Carbon Dioxide Recycling Pathways. *Front. Bioeng. Biotechnol.* **2020**, *7* (January), 1–16. https://doi.org/10.3389/fbioe.2019.00446.

(16)   Bogorad, I. W.; Lin, T. S.; Liao, J. C. Synthetic Non-Oxidative Glycolysis Enables Complete Carbon Conservation. *Nature* **2013**, *502* (7473), 693–697. https://doi.org/10.1038/nature12575.

(17)   Kanno, M.; Carroll, A. L.; Atsumi, S. Global Metabolic Rewiring for Improved CO2 Fixation and Chemical Production in Cyanobacteria. *Nat. Commun.* **2017**, *8*, 1–11. https://doi.org/10.1038/ncomms14724.

(18)   Mourtzinis, S.; Cantrell, K. B.; Arriaga, F. J.; Balkcom, K. S.; Novak, J. M.; Frederick, J. R.; Karlen, D. L. Carbohydrate and Nutrient Composition of Corn Stover from Three Southeastern USA Locations. *Biomass and Bioenergy* **2016**, *85*, 153–158. https://doi.org/10.1016/j.biombioe.2015.11.031.

(19)   McEwen, J. T.; Kanno, M.; Atsumi, S. 2,3 Butanediol Production in an Obligate Photoautotrophic Cyanobacterium in Dark Conditions via Diverse Sugar Consumption. *Metab. Eng.* **2016**, *36*, 28–36. https://doi.org/10.1016/j.ymben.2016.03.004.

(20)   Ihara, M.; Kawano, Y.; Urano, M.; Okabe, A. Light Driven CO 2 Fixation by Using Cyanobacterial Photosystem I and NADPH-Dependent Formate Dehydrogenase. **2013**, *8* (8), 1–8. https://doi.org/10.1371/journal.pone.0071581.

(21)   Tashiro, Y.; Hirano, S.; Matson, M. M.; Atsumi, S.; Kondo, A. Electrical-Biological Hybrid System for CO2 Reduction. *Metab. Eng.* **2018**, *47* (March), 211–218. https://doi.org/10.1016/j.ymben.2018.03.015.

(22)   Bar-Even, A.; Noor, E.; Flamholz, A.; Milo, R. Design and Analysis of Metabolic Pathways Supporting Formatotrophic Growth for Electricity-Dependent Cultivation of Microbes. *Biochim. Biophys. Acta - Bioenerg.* **2013**, *1827* (8–9), 1039–1047. https://doi.org/10.1016/j.bbabio.2012.10.013.

(23)   Bang, J.; Hwang, C. H.; Ahn, J. H.; Lee, J. A.; Lee, S. Y. Escherichia Coli Is Engineered to Grow on CO2 and Formic Acid. *Nat. Microbiol.* **2020**, *5* (12), 1459–1463. https://doi.org/10.1038/s41564-020-00793-9.

(24)   Scheffen, M.; Marchal, D. G.; Beneyton, T.; Schuller, S. K.; Klose, M.; Diehl, C.; Lehmann, J.; Pfister, P.; Carrillo, M.; He, H.; Aslan, S.; Cortina, N. S.; Claus, P.; Bollschweiler, D.; Baret, J. C.; Schuller, J. M.; Zarzycki, J.; Bar-Even, A.; Erb, T. J. A New-to-Nature Carboxylation Module to Improve Natural and Synthetic CO2 Fixation. *Nat. Catal.* **2021**, *4* (2), 105–115. https://doi.org/10.1038/s41929-020-00557-y.

(25)   Griese, M.; Lange, C.; Soppa, J. Ploidy in Cyanobacteria. *FEMS Microbiol. Lett.* **2011**, *323* (2), 124–131. https://doi.org/10.1111/j.1574-6968.2011.02368.x.

(26)   Golden, S. S.; Brusslan, J.; Haselkorn, R. Genetic Engineering of the Cyanobacterial Chromosome. *Methods Enzymol.* **1987**, *153* (C), 215–231. https://doi.org/10.1016/0076-6879(87)53055-5.

(27)   Behler, J.; Vijay, D.; Hess, W. R.; Akhtar, M. K. CRISPR-Based Technologies for Metabolic Engineering in Cyanobacteria. *Trends Biotechnol.* **2018**, *36* (10), 996–1010. https://doi.org/10.1016/j.tibtech.2018.05.011.

(28)   Wendt, K. E.; Ungerer, J.; Cobb, R. E.; Zhao, H.; Pakrasi, H. B. CRISPR/Cas9 Mediated Targeted Mutagenesis of the Fast Growing Cyanobacterium Synechococcus Elongatus UTEX 2973. *Microb. Cell Fact.* **2016**, *15* (1), 1–8. https://doi.org/10.1186/s12934-016-0514-7.

(29)   Ungerer, J.; Pakrasi, H. B. Cpf1 Is A Versatile Tool for CRISPR Genome Editing Across Diverse Species of Cyanobacteria. *Sci. Rep.* **2016**, *6* (December), 1–9. https://doi.org/10.1038/srep39681.

(30)   Niu, T. C.; Lin, G. M.; Xie, L. R.; Wang, Z. Q.; Xing, W. Y.; Zhang, J. Y.; Zhang, C. C. Expanding the Potential of CRISPR-Cpf1-Based Genome Editing Technology in the Cyanobacterium Anabaena PCC 7120. *ACS Synth. Biol.* **2019**, *8* (1), 170–180. https://doi.org/10.1021/acssynbio.8b00437.

(31)   Bishé, B.; Taton, A.; Golden, J. W. Modification of RSF1010-Based Broad-Host-Range Plasmids for Improved Conjugation and Cyanobacterial Bioprospecting. *iScience* **2019**, *20*, 216–228. https://doi.org/10.1016/j.isci.2019.09.002.

(32)   Qi, L. S.; Larson, M. H.; Gilbert, L. A.; Doudna, J. A.; Weissman, J. S.; Arkin, A. P.; Lim, W. A. Repurposing CRISPR as an RNA-Гuided Platform for Sequence-Specific Control of Gene Expression. *Cell* **2013**, *152* (5), 1173–1183. https://doi.org/10.1016/j.cell.2013.02.022.

(33)   Santos, M.; Pacheco, C. C.; Yao, L.; Hudson, E. P.; Tamagnini, P. Crispri as a Tool to Repress Multiple Copies of Extracellular Polymeric Substances (Eps)-Related Genes in the Cyanobacterium Synechocystis Sp. Pcc 6803. *Life* **2021**, *11* (11). https://doi.org/10.3390/life11111198.

Chapter 2: Succinate Production in Cyanobacteria

2.1 Abstract

Cyanobacteria are attracting increasing attention as a photosynthetic chassis organism for diverse biochemical production, however, photoautotrophic production remains inefficient. Photomixotrophy, a method where sugar is used to supplement baseline autotrophic metabolism in photosynthetic hosts, is becoming increasingly popular for enhancing sustainable bioproduction with multiple input energy streams. In this study, the commercially relevant diacid, succinate, was produced photomixotrophically. Succinate is an important industrial chemical that can be used for the production of a wide array of products, from pharmaceuticals to biopolymers. In this system, the substrate, glucose, is transported by a proton symporter and the product, succinate, is hypothesized to be transported by another proton symporter, but in the opposite direction. Thus, low pH is required for the import of glucose and high pH is required for the export of succinate. Succinate production was initiated in a pH 7 medium containing bicarbonate. Glucose was efficiently imported at around neutral pH. Utilization of bicarbonate by CO_2 fixation raised the pH of the medium. As succinate, a diacid, was produced, the pH of the medium dropped. By repeating this cycle with additional pH adjustment, those contradictory requirements for transport were overcome. pH affects a variety of biological factors and by cycling from high pH to neutral pH processes such as CO_2 fixation rates and CO_2 solubility can vary. In this study the engineered strains produced succinate during fluctuating pH conditions, achieving a titer of 5.0 g L^{-1} after 10 days under shake flask conditions. These results demonstrate the potential for photomixotrophic production as a viable option for the large-scale production of succinate.

2.2 Introduction

Despite efforts towards carbon remediation, atmospheric CO_2 levels continue to rise, in large part due to the current petroleum-based economy[1]. Many studies envisage that chemical commodities directly derived from biomass will play a large role in converting our petroleum-based industries to a more sustainable production platform[2,3]. Photoautotrophic production of chemical commodities is an important aspect of a biobased economy. Improving technologies to

directly convert CO_2 towards industrially relevant titers of chemical commodities would be a boon to sustainability efforts globally. Photomixotrophy is a strategy that can be leveraged to improve production from CO_2 to chemicals in photosynthetic hosts by supplementing photoautotrophic metabolism with carbohydrate substrates sourced from waste biomass. Engineered organisms tend to leverage decarboxylation steps to produce chemical targets, therefore developing carbon conserving pathways towards these chemical products is of great interest[4]. Using a photosynthetic bacterium allows for a carbon efficient chemical production route by harnessing the naturally occurring CO_2 fixation process to incorporate CO_2 into the chemical of interest[5,6].

Succinic acid or succinate, has a large market today, valued at 223 million USD in 2021[7]. Succinate has a wide range of applications from pharmaceuticals to bioplastic production. Commercialization of biologically-derived succinate, produced through microbial fermentation of biologically-sourced sugars, has been implemented by many companies such as Corbion, BASF, Roquette, and BioAmber. Succinate based bioplastics in particular can replace several everyday products, which can further decrease our carbon footprint by replacing polymer-based products that are difficult to recycle. Several bio-based platforms have been used to generate succinate industrially, including using heterotrophic organisms capable of high natural production, such as *Mannheimia succiniciproducens*, or engineering traditional model organisms, such as *Escherichia coli*.

Photoautotrophic production of succinate has been accomplished in recent studies focusing on engineering various cyanobacteria[8,9]. The TCA cycle in most cyanobacteria is bisected into two branches because these organisms are missing key enzymes to produce succinate from α-ketoglutarate and complete the cycle[10]. The cyanobacterium *Synechococcus elongatus* PCC 7002 (hereafter, 7002) possesses a unique pathway for succinate production via a succinate semialdehyde intermediate[10]. Recent studies have established that other species of cyanobacteria can produce succinate when equipped with the succinate semialdehyde pathway from 7002[8,9]. This pathway includes two key steps, an oxoglutarate decarboxylase and a succinate semialdehyde dehydrogenase[10]. These two enzymes alone are not sufficient for significant production of succinate and these engineered strains are further equipped with

upstream modifications including overexpression of the genes encoding for a phosphoenol pyruvate carboxylase and a citrate synthase to enhance carbon flux into the TCA cycle[8,9]. However, photoautotrophic production rates and yields of succinate significantly lag behind heterotrophic systems[11,12]. The cyanobacterium *Synechocystis* sp. PCC 6803 (6803) is naturally capable of succinate production under nutrient limiting and dark anoxic conditions through auto-fermentation, wherein intracellular glycogen is catabolized to produce necessary cellular energy requirements. One study using this strategy was able to achieve a titer of 1.8 g L^{-1} succinate after 72 hours under dark anaerobic and high biomass conditions (25g DCW L^{-1})[13]. Another recent study further improved succinate production in 6803 and achieved a titer of 4.2 g L^{-1} [14]. One study in 7942 achieved a cumulative titer of 8.9 g L^{-1} succinate photoautotrophically after 112 days when using CRISPR inhibition to knockdown the activities of *sdhB* and *glgC*[15]. While these studies show potential as a means to convert CO_2 into succinate, auto-fermentation requires multiple cultivation steps, anoxic conditions are often difficult to successfully implement and long production periods can be difficult to monitor. Additionally, heterotrophic organisms still outpace photoautotrophic organisms; one study using an engineered *E. coli* produced ~12 g L^{-1} succinate with a productivity of 0.17 g L^{-1} h^{-1} heterotrophically in minimum media under shake flask conditions[16].

In a previous study, the model cyanobacterium, *Synechococcus elongatus* PCC 7942 (hereafter, 7942), was engineered to consume glucose resulting in a photomixotrophic strain[5]. Notably, this strain was able to continue carbon fixation and chemical production during dark conditions, providing a significant milestone in the efforts to make a commercially viable microbe that can directly convert CO_2 into valuable chemicals[5,17,18]. Ideally, the photomixotrophic strains would be utilizing glucose from lignocellulosic hydrolysate, a strategy which allows for enhanced chemical production without competing against food supply and provides a route for recycling biomass that would otherwise be burned as waste.

This work demonstrates that photomixotrophy can be applied to enhance succinate production in cyanobacteria. The glucose utilization[5] and succinate production[9] pathways were introduced into 7942. Additionally, the Calvin-Benson (CB) cycle was deregulated by removing *cp12* encoding for the CB regulatory protein Cp12, which was previously shown to improve

photomixotrophic production of chemicals[5].The gene *sdhB,* which encodes for succinate dehydrogenase subunit B was deleted to prevent conversion of succinate to its major downstream product, fumarate. This photomixotrophic strain uses two proton symporters in opposite directions, glucose import requires a low or neutral pH for efficient consumption and the succinate transporter requires high pH in order to export the product to the media. Thus, it was determined that a fluctuating pH would be required for efficient succinate production. The results provide useful insights into the viability of expanding photomixotrophic production platforms to scale up chemical bioproduction.

2.3 Methods

2.3.1 Reagents

The following reagents were obtained from Research Products International (RPI): glucose, cycloheximide, gentamycin, spectinomycin, kanamycin, thiamine and IPTG. Phusion polymerase was purchased from New England Biolabs. All synthetic oligonucleotides were synthesized by Integrated DNA Technologies.

2.3.2 Plasmid construction

All plasmids and primers used in this study are listed in **Tables 2.S1** and **2.S2**, respectively. The target genes and vector fragments used to construct plasmids were amplified using PCR with the primers and templates described in **Table 2.S3**. The gene *ppc* was cloned from a codon optimized gene fragment purchased from Genewiz from Azenta Life Sciences. The resulting fragments were assembled by sequence and ligation-independent cloning[19]. All constructed plasmids were verified via Sanger sequencing.

2.3.3 Strain construction

Strains used in this study are listed in **Table 2.1**. Transformation and integration via double homologous recombination were performed as previously described[20]. In brief, cells at OD_{730} ~0.4 were collected from 2 ml of culture by centrifugation, washed, and concentrated in 300 μl

of BG-11 medium. After adding plasmid DNA (2 µg) to the concentrated cells, the tube was wrapped in foil and incubated overnight at 30 °C. Cells were plated on a BG-11-agar solid media containing appropriate antibiotics and incubated at 30 °C under constant light until colonies appear. Complete chromosomal segregation for the introduced fragments was achieved through propagation of multiple generations on selective agar plates. Correct recombinants were confirmed for double crossover and gene fidelity by PCR and Sanger sequencing.

Table 2.1 List of strains used in this study

Strain no.	Key genotype	Ref
1	NSI:: P_{trc}:*galP-zwf-gnd*; Spec^R NSIII:: P_{trc}:*gabD* (MG1655)-*kgd* (7002); Gent^R	This work
2	NSI:: P_{trc}:*gabD* (MG1655)-*kgd* (7002); Spec^R	[9]
3	2 + NSII:: P_{trc}:*galP-zwf-gnd*; Kan^R	This work
4	3 + *sdhB*::Gent^R	This work
5	3 + *sdhB*::P_{LlacO1}:*ppc (Cg*); Gent^R	This work
6	3 + *sdhB*::P_{LlacO1}:*ppc (*MG1655*)*; Gent^R	This work
7	3 + *sdhB*::P_{LlacO1}:*ppc* (7942*)*; Gent^R	This work
8	3 + *sdhB*::P_{LlacO1}:*ppc* (7942)–*gltA* (*Cg*); Gent^R	This work
9	3 + *sdhB*::P_{LlacO1}:*ppc* (7942)–*gltA* (MG1655); Gent^R	This work
10	3 + *sdhB*::P_{LlacO1}:*ppc* (7942)–*gltA* (7942); Gent^R	This work
11	2 + *cp12*::P_{LlacO1}:*prk* P_{trc}:*galP-zwf-gnd*; Kan^R	This work
12	11 + *sdhB*::P_{LlacO1}:*ppc* (7942); Gent^R	This work
13	11 + *sdhB*::P_{LlacO1}:*ppc* (7942)–*gltA* (*Cg*); Gent^R	This work
14	2 + Synpcc7942_0366*::*Tn*5*; Kan^R	This work

2.3.4 Culture conditions

Unless otherwise specified, 7942 cells were cultured in BG-11 medium[20] with the addition of 50 mM $NaHCO_3$ without the addition of HEPES buffer. For production experiments, the production media was either 2x BG-11 or 5x BG-11, which were composed of doubled or quintupled 1x BG-11 medium component concentrations, respectively, with the exception of HEPES-KOH, which was excluded from all conditions, and the addition of glucose, $NaHCO_3$ (20 mM), IPTG (1 mM), thiamine (10 mg l^{-1}), and appropriate antibiotics. Cells were grown at 30 °C with rotary shaking (100 rpm) and light (80 µmol photons·m^{-2} s^{-1} in the PAR range) provided by 86 cm 20 W fluorescent tubes. Light intensity was measured using a PAR quantum flux meter (Model MQ-200, Apogee Instruments). Cell growth was monitored by measuring OD_{730} in a Microtek Synergy H1 plate reader (BioTek). Antibiotics concentrations were as follows: cycloheximide (50 mg l^{-1}), spectinomycin (20 mg l^{-1}), kanamycin (20 mg l^{-1}), gentamycin (10 mg l^{-1}) and chloramphenicol (5 mg l^{-1}).

Prior to succinate production, colonies were inoculated in BG-11 medium containing 50 mM $NaHCO_3$ and appropriate antibiotics and grown photoautotrophically. Cells at the exponential growth phase were adjusted to an OD_{730} of 0.5 in 10 ml BG-11 medium including 20 mM $NaHCO_3$ (unless otherwise stated), 1 mM IPTG, 10 mg l^{-1} thiamine and appropriate antibiotics in 20 ml glass tubes with a height of 15 cm and a diameter of 1.5 cm. For high-density production experiments, cells were adjusted to an OD_{730} of 5.0 in 25 ml of 2x BG-11 or 5x BG-11 medium in 250 ml baffled glass flasks with a maximum circumference of 83 cm^2. Appropriate concentrations of glucose were added as required. Every 24 h, 10% of the culture volume was removed, the pH was adjusted to 7.0 with 3.6 N HCl, and the removed volume was replaced with production media containing 200 mM $NaHCO_3$ if bicarbonate was included for that experimental condition. For Fig. 2.4, cells were collected by centrifugation and resuspended with fresh production media on day 3 and resuspended at an OD_{730} of 5.0 in production media on day 6. For Fig. 2.5, the cells were harvested by centrifugation and resuspended in fresh media at a target OD_{730} of 5. For Fig. 2.7, the cultures were maintained at an alkaline pH, the

sampling volume was replaced daily, and no cell harvesting, or resuspension was performed. For Fig. 2.8, 5x BG-11 was used and no cell harvesting was performed.

2.3.5 Genome sequencing

Photoautotrophically grown cultures at an approximate OD_{730} of 0.8 were collected via centrifugation (20,000 x g for 3 min) and genomic DNA was extracted using a phenol-chloroform and ethanol precipitation protocol, as previously described[21]. Purified genomic DNA was analyzed by nanodrop for purity and concentration, and then submitted to the UC San Diego IGM Genomics Center for standard Illimuna library preparation according to the manufacturer's instructions and sequencing using an Illumina NovaSeq 6000. Resulting sequence data for wild-type 7942 and Strain 2 were analyzed for SNPs with BreSeq[22] using default parameters.

2.3.6 Quantification of extracellular metabolites

Glucose and succinate concentrations in culture supernatants were determined using a high-performance liquid chromatography (20A HPLC Shimadzu) equipped with a differential refractive detector 10A and an Agilent Hi-Plex H organic acid analysis column (Agilent). The mobile phase was 5 mM of H_2SO_4, maintained at a flow rate of 0.2 ml min^{-1} at 55 °C for 18 min.

To prepare samples for HPLC analysis, 1 mL of cell culture was centrifuged at 20,000 x g for 10 min at 25 °C. 10 µL of filtered culture supernatant was injected into the column for analysis.

Glucose consumption was determined by measuring glucose concentration in culture supernatants at each sampling point and subtracting it from the previous measurement. Glucose concentration was also measured after resuspension in fresh media.

For analysis of Strain 14, fumarate and succinate were analyzed via UV-HPLC (UV at 210 nm) using an ACE C18-PFP 3 µm particle size, 150x2.1mm Ultra-Inert HPLC Column (MacMod Analytical, Chadds Ford) with an isocratic method using 0.1% formic acid in MilliQ water, pH 3.5 on an Ultimate 3000 HPLC. Prior to HPLC analysis, 1 mL of cell culture was centrifuged at 20,000 x g for 3 min at room temperature and the supernatant was filtered through a 0.22 µm filter.

10 μL of filtered culture supernatant was injected into the column for analysis. Between samples, the column is washed with acetonitrile (ACN) for 8 min followed by a 5 min linear gradient back to the 0.1% formic acid solution and a 10 min equilibration step.

2.4 Results & Discussion

2.4.1 Installation of the glucose and succinate pathways to 7942

To utilize glucose, a glucose pathway that consists of three enzymes from *E. coli*; a galactose-proton symporter encoded by *galP*, a glucose-6-phosphate dehydrogenase encoded by *zwf*, and a 6-phosphogluconate dehydrogenase encoded by *gnd* was introduced to 7942 (**Fig. 2.1**)[5]. An isopropylthio-β-galactoside (IPTG)-inducible P_{LlacO1}[23] was utilized to express *galP-zwf-gnd* (**Table 2.1**). The glucose pathway was observed in a previous study to enable a cyanobacterial strain to efficiently incorporate glucose into central carbon metabolism via the oxidative branch of the pentose phosphate pathway. This pathway also improved the carbon fixing ability of the cyanobacterial strain by increasing the substrate pool for the CO_2 fixing enzyme, ribulose-1,5-bisphosphate carboxylase/oxygenase (RuBisCO)[5]. 7942 has an incomplete TCA cycle, thus the succinate semialdehyde shunt which includes *kgd* cloned from 7002 gDNA (Synpcc7002_A2770) and *gabD* cloned from *E. coli* MG1655 (hereafter, MG1655) gDNA encoding for an α-ketoglutarate decarboxylase (KGDH) and succinate semialdehyde dehydrogenase (SSDH), respectively, (P_{LlacO1}:*kgd-gabD*) was introduced to the strain with the glucose pathway, creating Strain 1 (**Table 2.1**). These variants of *gabD* and *kgd* were selected based off their reported activities and due to their successful use in producing succinate in 7942 in a previous study[9]. Strain 1 was unable to produce succinate. However, Strain 2 (**Table 2.1**), which was provided by the Lan group[9] and has the same succinate semialdehyde shunt genes, was able to produce succinate photoautotrophically (75 ± 15.2 mg L^{-1} in 5 days when induced with 1mM IPTG under photoautotrophic conditions in 1x BG-11 without bicarbonate supplementation). Because the heterologous expression cassettes in Strains 1 and 2 are equivalent, we hypothesized that background mutations may exist between the two strains. Thus, the genomes of the wild type and Strain 2 were re-sequenced to determine any genetic

differences. Three single nucleotide polymorphisms (SNPs) were present on the genome of Strain 2 as compared to the wild type strain in the loci Synpcc7942_0884 (elongation factor tu), Synpcc7942_1475 (*sbtA*), and Synpcc7942_1988 (conserved hypothetical). Based on the observed lack of production in Strain 1 and the SNPs present in Strain 2, Strain 2 was used for further modifications.
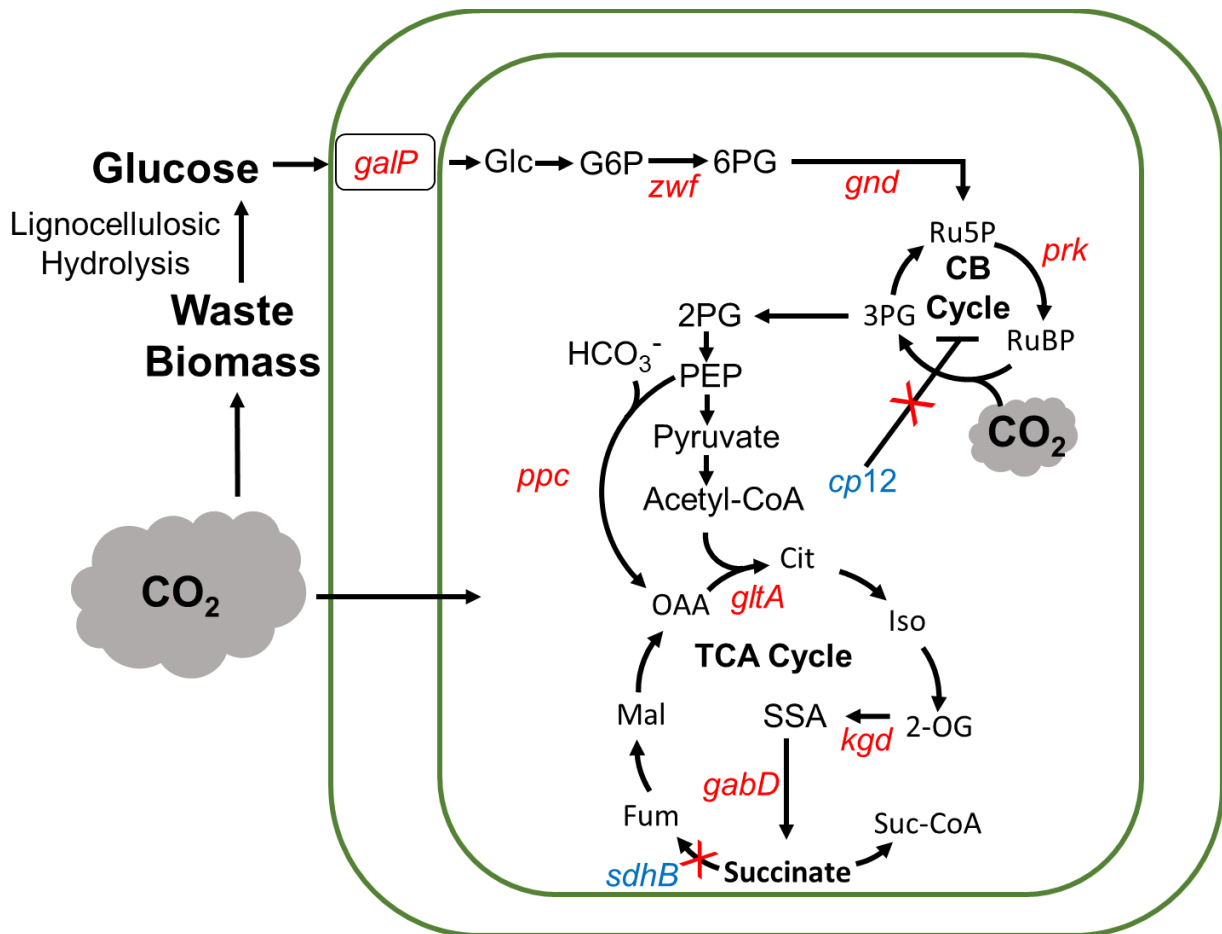
Figure 2.1 Photomixotrophic Succinate Production Pathway.

Genes in red are overexpressed and genes in blue are deleted in this study. GalP, galactose-proton symporter; Zwf, G6P dehydrogenase; Gnd, 6PG dehydrogenase; G6P, glucose-6-phosphate; 6PG, 6-phosphogluconate; Prk, phophoribulokinase; RuBP, ribulose-1,5-bisphosphate; Ru5P, ribulose-5-phosphate; Cp12, a regulatory protein of the CB cycle; 3PG, 3-phosphoglycerate; 2PG, 2-phosphoglycerate; PEP, phosphoenolpyruvate; PEPC encoded by *ppc*, phosphoenolpyruvate carboxylase; Cit, citrate; GLTA encoded by *gltA*, citrate synthase; Iso, isocitrate; 2OG, 2-oxoglutarate; KGDH encoded by *kgd*, oxoglutarate dehydrogenase; SSDH encoded by *gabD*, succinate semialdehyde dehydrogenase; Suc-CoA, succinyl-CoA; SdhB, succinate dehydrogenase subunit B; Fum, fumarate; Mal, malate; OAA, oxaloacetate.

The glucose pathway was introduced into Strain 2, creating Strain 3 (**Table 2.1**). Strain 3 with and without bicarbonate produced 352 ± 40.1 mg L^{-1} and 300 ± 20.4 mg L^{-1} succinate, respectively, after 5 days, a $4 - 4.3$ fold increase over photoautotrophic production (**Fig. 2.2a, Fig. 2.S1**). In the production experiments, Strain 3 produced fumarate as a major side product. To remove fumarate production, *sdhB* on the chromosome of Strain 3 was deleted, resulting in Strain 4. Succinate dehydrogenase (SDH) is responsible for the conversion of succinate to fumarate, as well as the generation of electrons that ultimately impact the redox state of the plastoquinone pool[8,24,25]. Strain 4 with and without bicarbonate produced 516 ± 48.4 mg L^{-1} and 543 ± 12.3 mg L^{-1} succinate, respectively, and no fumarate was detected via HPLC after 5 days (**Fig. 2.2a**). However, the addition of bicarbonate inhibited growth of Strain 4 (**Fig. 2.2c**). Although growth inhibition occurred, the *sdhB* knockout was used for further study due to its benefit to specific productivity in experiments with bicarbonate present, 0.012 ± 0.001 g L^{-1} OD_{730}^{-1} day^{-1} for Strain 3 and 0.054 ± 0.002 g L^{-1} OD_{730}^{-1} day^{-1} for Strain 4 (**Fig. 2.2abc**). Because these strains have a mutation in *sbtA*, we hypothesize that the synthetic combination of this transporter mutation and a redox imbalance from an incomplete reductive branch of the TCA cycle causes the observed bicarbonate-dependent growth inhibition of Strain 4. Further studies are needed to elucidate the inhibition mechanisms.
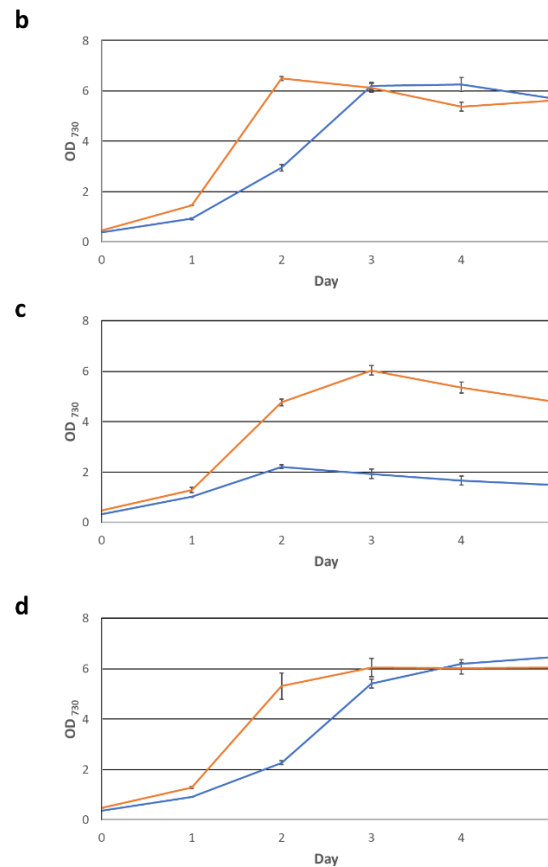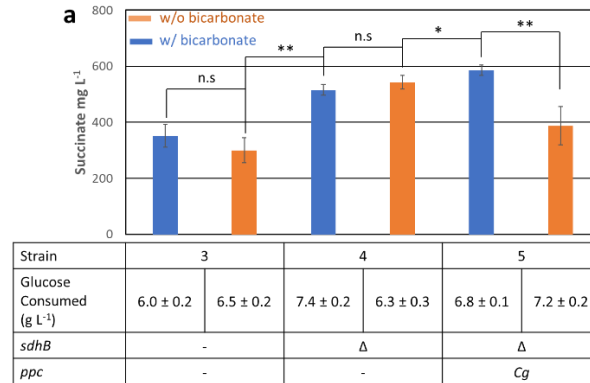
Figure 2.2 Photomixotrophic succinate production and growth of strains 3, 4, and 5.

a) production b-d) Growth of Strains 3, 4, and 5 (**Table 1**) with (blue) and without (orange) 20 mM bicarbonate. Error bars indicate s.d. (n = 3 biological replicates). For significance calculations, n.s represents no significant difference P > 0.05, (*) represents P ≤ 0.05, (**) represents P ≤ 0.01, (***) P ≤ 0.001 using an unpaired t-test. Experiment was performed in 1x BG-11 with 10 g L^{-1} glucose.

2.4.2 Increased carbon flux toward the TCA cycle

We hypothesized that increased carbon flux from central metabolism to the TCA cycle would remedy the growth detriment with bicarbonate. The *ppc* gene from *Corynebacterium glutamicum* (hereafter, *Cg*) under P_{LlacO1} was introduced to Strain 4, creating Strain 5 (**Table 2.1**). Phosphoenol pyruvate carboxylase (PEPC) encoded by *ppc* converts phosphoenolpyruvate to oxaloacetate through reaction with bicarbonate, thus potentially impacting the bicarbonate-dependent growth defect[26]. The *Cg* variant of *ppc* was chosen because *Cg* is a known glutamate overproducer and it has been hypothesized that enzymes related to the TCA cycle from *Cg* would have a higher activity[9,26]. Strain 5 did not show the growth detriment present in Strain 4 in the presence of bicarbonate (**Fig. 2.2d**). Succinate production was also improved in Strain 5 (**Fig. 2.2a**). Strain 5 with and without bicarbonate produced 586 ± 9.88 mg L^{-1} and 388 ± 55.0 mg L^{-1} succinate, respectively, after 5 days (**Fig. 2.2a**).

To identify efficient PEPC for succinate production, additional strains were constructed with *ppc* from MG1655 and 7942 (Strains 6 and 7 respectively (**Table 2.1**)). Overexpression of *ppc* in MG1655 is a well-established method for regenerating TCA cycle intermediates via carboxylation of intracellular pools of phosphoenol pyruvate towards oxaloacetate and this reaction catalyzed by PEPC is highly favorable among other anaplerotic reactions[9,27]. We hypothesized that this variant would enhance succinate production in 7942. Additionally, we hypothesized that overexpression of native 7942 *ppc* would achieve similar results. Indeed, Strain 7 with 7942 *ppc* produced more succinate than Strain 5 (**Fig. 2.3a, Fig. 2.S2**). In contrast, Strain 6 with *ppc* from MG1655 did not produce detectable levels of succinate (**Fig. 2.3a**). The MG1655 PEPC is allosterically inhibited by aspartate and citrate which may be one reason for the observed lack of succinate production in Strain 6. Additionally, PEPC from different species can be sensitive or insensitive to regulation by various metabolites, such as cyclic-di-AMP, which may not be present at relevant concentrations in 7942[28–30]. Thus Strain 7 was used for further modifications.
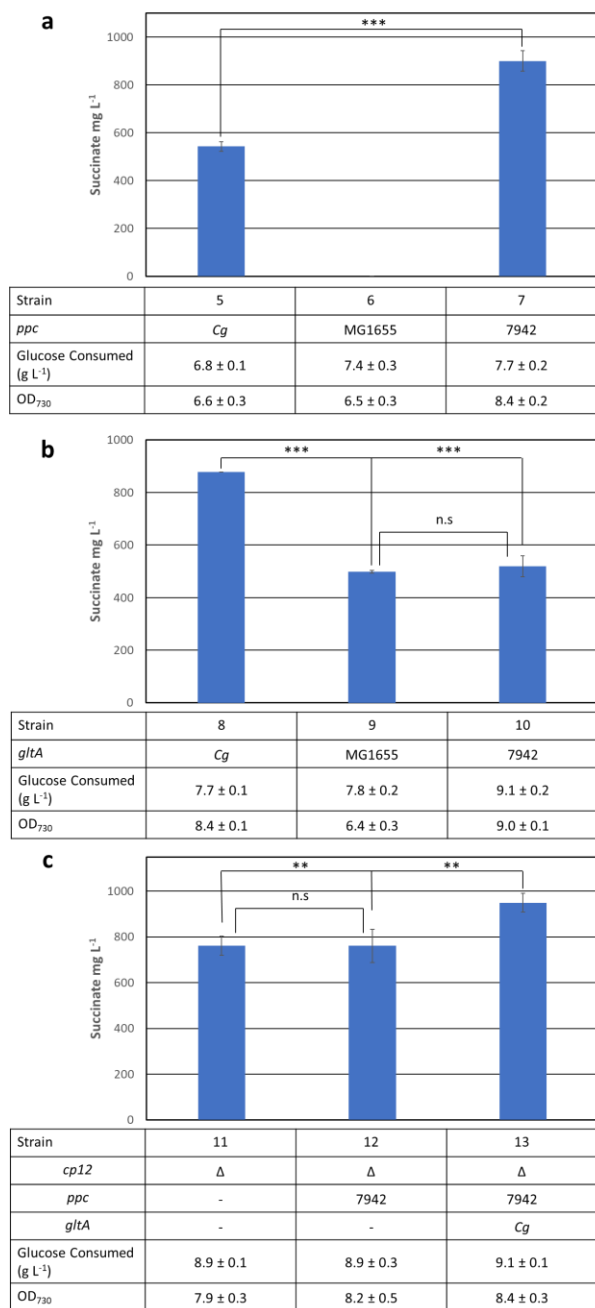
Figure 2.3 Low density photomixotrophic succinate production of strains 5-13.

a) Production of succinate in strains 5, 6, and 7 (**Table 1**) to evaluate optimal *ppc* variant. b) Production of succinate in Strains 8, 9 and 10 (**Table 1**) to evaluate optimal *gltA* variant. c) Production of succinate in Strains 11, 12 and 13 (**Table 1**). Each strain was cultivated in BG-11 supplemented with 20 mM sodium bicarbonate and 10g L^{-1} glucose. Appropriate antibiotics and inducers were also added. Error bars indicate standard deviation (n = 3 biological replicates). For

significance calculations, n.s represents no significant difference $P > 0.05$, (*) represents $P \leq$ 0.05, (**) represents $P \leq 0.01$, (***) $P \leq 0.001$ using an unpaired t-test.

To identify an efficient citrate synthase (GLTA) for succinate production, Strains 8, 9, and 10 were constructed using variants of *gltA* from *Cg*, MG1655, and 7942 along with the 7942 *ppc* (**Table 2.1**). GLTA converts oxaloacetate to citrate. We hypothesized that the additional expression of *gltA* would increase the carbon flux toward succinate. Strain 8 produced similarly to Strain 7, while Strains 9 and 10 produced much less than Strains 7 and 8 (**Fig. 2.3b, Fig. 2.S3**). These results suggest that *gltA* is not the rate-limiting step in these strains and that there may be a bottleneck in upstream metabolism, in fact, overexpression of *gltA* in Strains 9 and 10 likely overburdened the cell causing the observed decrease in production. Additionally, GLTA requires two substrates, acetyl-CoA and oxaloacetate, since overexpression of *ppc* likely competes for the available phosphoenolpyruvate substrate pool, acetyl-CoA pools may be depleted compared to oxaloacetate in Strains 8 through 10, therefore the limitation is substrate availability not availability of the free GLTA enzyme.

2.4.3 Deregulation of the CB cycle

We have previously shown that the deletion of *cp12* and the additional expression of *prk* improved CO_2 fixation, glucose utilization, and product formation[5]. Cp12 is a regulatory protein that represses two important enzymes of the CB cycle, glyceraldehyde-3-phosphate dehydrogenase (GAPDH) and phosphoribulokinase (PRK). PRK converts D-ribulose-5-phosphate to D-ribulose-1,5-bisphosphate, which is a substrate of RuBisCO[31,32]. The *cp12* gene was deleted and the *prk* gene was additionally expressed without or with *ppc* (7942) or *ppc* (7942)-*gltA* (*Cg*), creating Strains 11, 12, and 13 (**Table 2.1**). Strain 11, without the additional expression of *ppc* and *gltA*, produced 761 ± 20.9 mg L^{-1} succinate, nearly double that of Strain 3 which is identical to Strain 11 except for the deletion of *cp12* and overexpression of *prk* (**Fig. 2.3c, Fig. 2.S4**). Strain 12 with the additional expression of *ppc* (7942) produced similarly to Strain 11, suggesting PEPC is not the limiting step in this strain. Strain 13 with the additional expression of *ppc* (7942) and *gltA* (*Cg*) produced the highest titers of succinate at 950 ± 25.0 mg L^{-1} (**Fig. 2.3c**). The observable benefit of overexpressing *gltA* in the context of Strain 13 compared to the nonbeneficial overexpression observed in Strains 8 through 10 is likely due to the upstream

bottleneck being removed, most likely caused by increasing flux through the CB cycle, allowing for an increase in acetyl-CoA pools. Thus, we used Strain 13 in the following experiments.

2.4.4 High cell density succinate production

We attempted to optimize production conditions using Strain 13. The production experiment started at OD_{730} ~5. 7942 generally cannot grow to the high OD_{730}s achieved in this study under photoautotrophic conditions due to density-dependent light deficiencies without condensing cell cultures, however, photomixotrophic conditions allow for this deficiency to be removed through sugar supplementation of metabolism[5,33]. The media were replaced at day 3 and 6 to refresh sugar and medium content. At day 6, the OD_{730} was adjusted to 5 (**Fig. 2.4**). Under these conditions, Strain 13 produced 4.0 ± 0.20 g L^{-1} in 8 days (**Fig. 2.4a**). However, the cells had an observable growth burden following centrifugation and cell harvesting at Day 3 and 6. Interestingly, succinate production and glucose consumption remained constant in spite of this growth inhibition or post-media replacement lag phase (**Fig. 2.4ab**). To test the effects of the media replacement on Strain 13, another experiment was carried out where the cells were harvested at day 3 and the OD_{730} was adjusted back to 5 (**Fig. 2.5**). The culture suffered from poor growth following centrifugation, suggesting that full media replacement by centrifugation was not optimal for these experiments (**Fig. 2.5**).

Figure 2.4 Effects of media replacement on Strain 13

a) Succinate production. b) Glucose consumed over the time course of the experiment. c) pH changes over time. pH was adjusted back to 7 every 24 hours; pH was recorded prior to adjustment. Both pH measurements prior to adjustment and post adjustment are plotted. d) OD_{730} on day 3, cells were collected by centrifugation and resuspended in fresh production media. On day 6, cells were collected by centrifugation and resuspended at an OD_{730} 5 in fresh production media. Error bars indicate s.d. (n = 3 biological replicates). Experiment was performed in 2x BG-11 with 40 g L^{-1} glucose and 20mM bicarbonate.
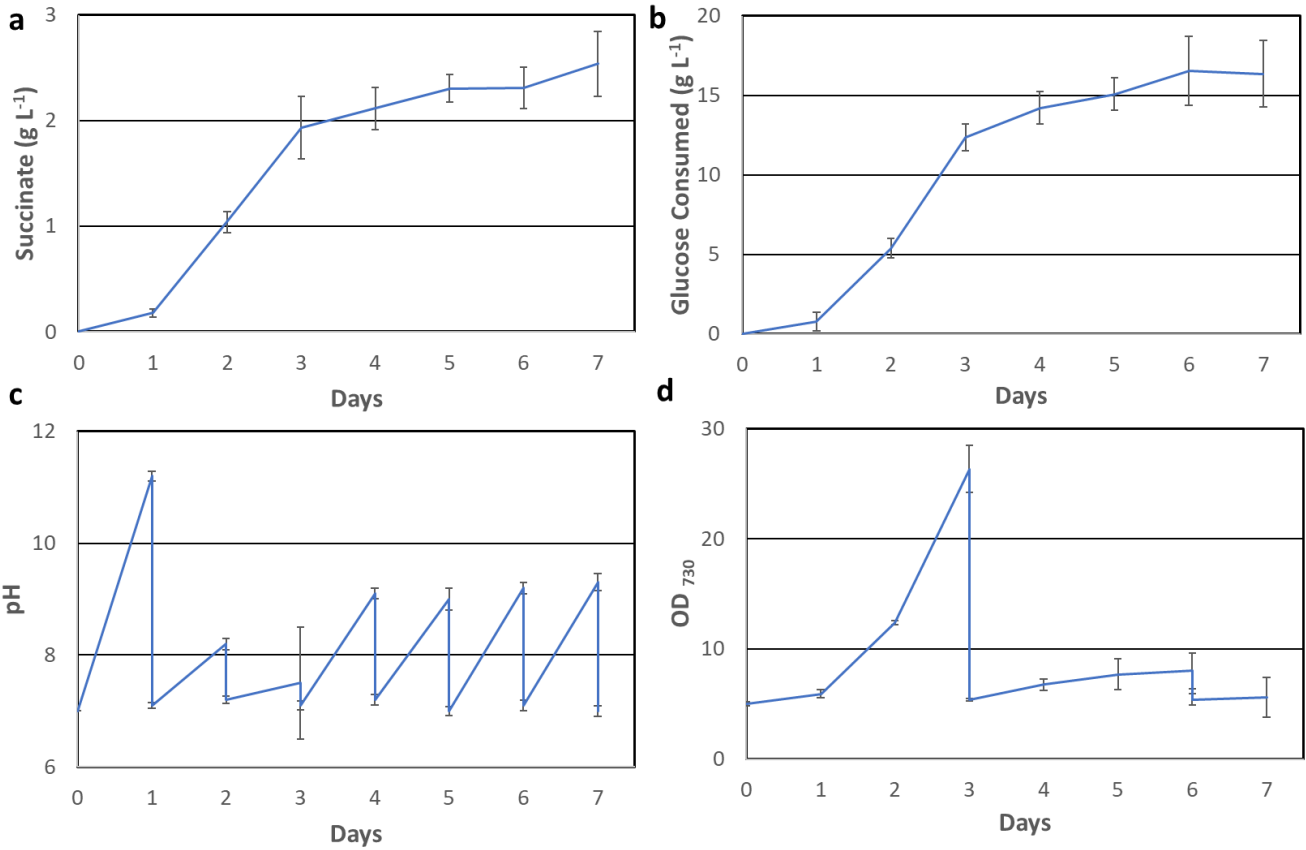
Figure 2.5 High density succinate production in Strain 13 with centrifugation and media replacement in 2x BG-11
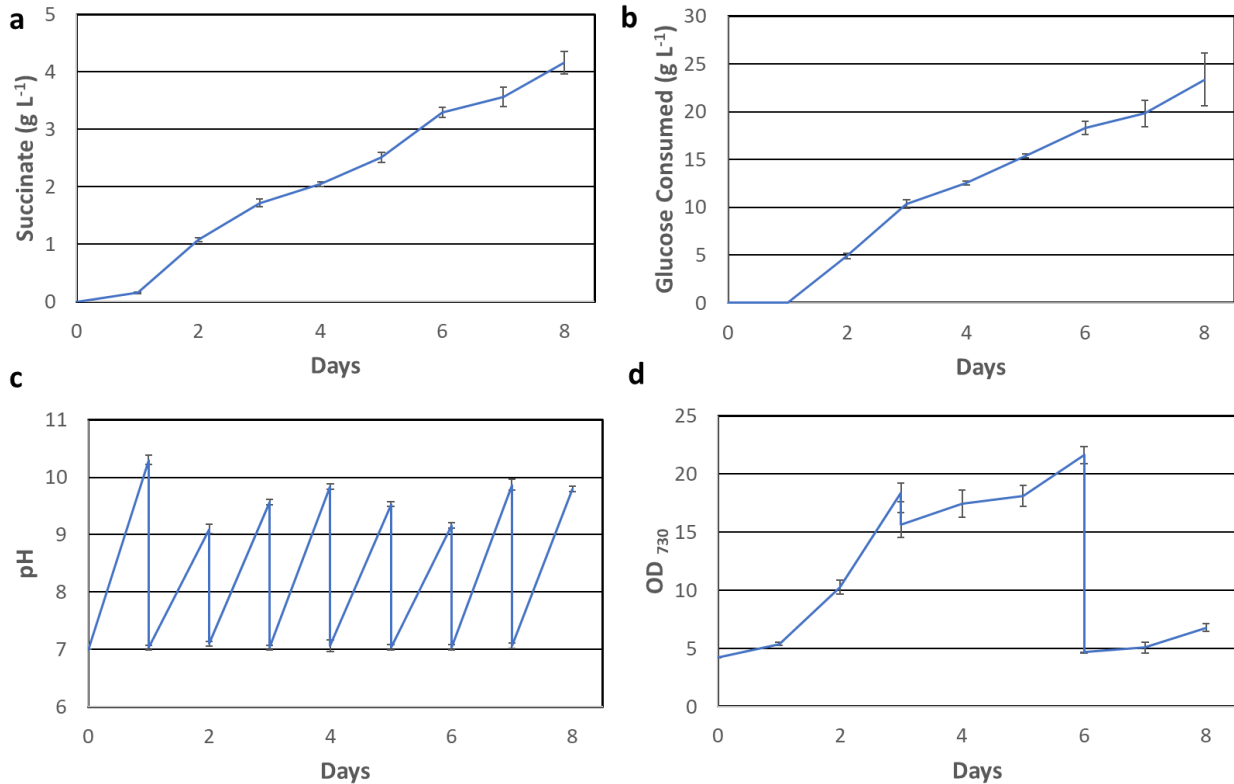
a) Succinate production. b) Glucose consumed over the time course of the experiment. c) pH changes over time. pH was adjusted back to 7 every 24 hours; pH was recorded prior to adjustment. Both pH measurements prior to adjustment and post adjustment are plotted. d) OD_{730} on day 3, cells were collected by centrifugation, resuspended, and adjusted down to an OD_{730} of 5 in fresh production media. On day 6, cells were collected by centrifugation and resuspended in fresh production media. Error bars indicate s.d. (n = 3 biological replicates). Experiment was performed in 2x BG-11 with 40 g L^{-1} glucose and 20mM bicarbonate.

3.4.5 Photomixotrophic succinate production with pH fluctuations

Both the glucose and succinate transporters are proton symporters[34,35]. A low pH is required for efficient glucose import and a high pH is required for efficient succinate export. Because an alkaline pH was found to be beneficial for photoautotrophic succinate production[9], the pH for photomixotrophic production needs to shift between low and high or maintain a pH that works for both. The secretion of succinate and other diacids to the media was previously hypothesized to occur through a diacid transporter, encoded by SynPCC7942_0366, which is predicted to rely on a proton gradient similar to the mechanism of the glucose transporter, GALP[9,34]. To test this hypothesis, we generated Strain 14 through transposon insertional knockout of SynPCC7942_0366 in Strain 2 (**Table 2.1**). HPLC analysis of the supernatant from production cultures of Strains 2 or 14 demonstrated that both succinate and fumarate secretion are greatly reduced upon knockout of SynPCC7942_0366, supporting this gene's role in encoding a transporter (**Fig. 2.6**). GALP being a proton symporter uses a proton from the media to transport glucose across the bacterial membrane, therefore a neutral or acidic pH in the media is ideal for efficient sugar consumption[35]. First, we performed a high-density experiment wherein pH was maintained at alkaline levels instead of being adjusted back to a neutral pH daily (**Fig. 2.7**). The medium pH steadily increases as CO_2 in bicarbonate is fixed, resulting in the evolution of hydroxide. When succinate is not being produced, pH increases to ~10.5, which was shown to be a beneficial pH for photoautotrophic succinate production[9]. When succinate was being produced, the medium was acidified to a pH of approximately 9.5, where pH equilibrated even as succinate continued to be produced (**Fig. 2.7**). Strain 13 under this condition produced 2.8 ± 0.056 g L^{-1} succinate in 7 days (**Fig. 2.7a**), which was lower than that with pH adjustment where 4.0 ± 0.20 g L^{-1} succinate was produced (**Fig. 2.4**). Glucose consumption was diminished under the alkaline conditions (day 0 to day 3, 3.5 ± 0.062 g L^{-1} d $^{-1}$ and day 3 to day 7, 2.3 ± 0.11 g L^{-1} d $^{-1}$, **Fig. 2.7b**) compared to glucose consumption prior to centrifugation on day 3 in a previous high-density experiment (4.1 ± 0.23 g L^{-1} d $^{-1}$, **Fig. 2.4b**). We hypothesize that the decrease in glucose consumption resulted in lower succinate titers. The previous experiment with pH adjustment (**Fig. 2.4**) was conducted in 2x BG-11 and the cultures were centrifuged. We hypothesized that 5x BG-11 would be beneficial for high density experiments. Since succinate

production and glucose consumption were both diminished in the 5x BG-11 condition compared to 2x BG-11, it became necessary to investigate if the alkaline conditions were at fault for the diminished metrics as we hypothesized. It should be noted that changes in pH can cause variation in many factors ranging from enzyme kinetics to CO_2 fixation rates and growth. Studies suggest that 7942 favors alkaline conditions for photoautotrophic growth and protein production[36,37].Further study is required to determine how photomixotrophic metabolism is affected under different pH conditions in 7942. However, intracellular pH is generally stable in 7942, ranging only from 7.16 ± 0.03 to 7.55 ± 0.02 in media with pH ranging from 5 to 10[38].
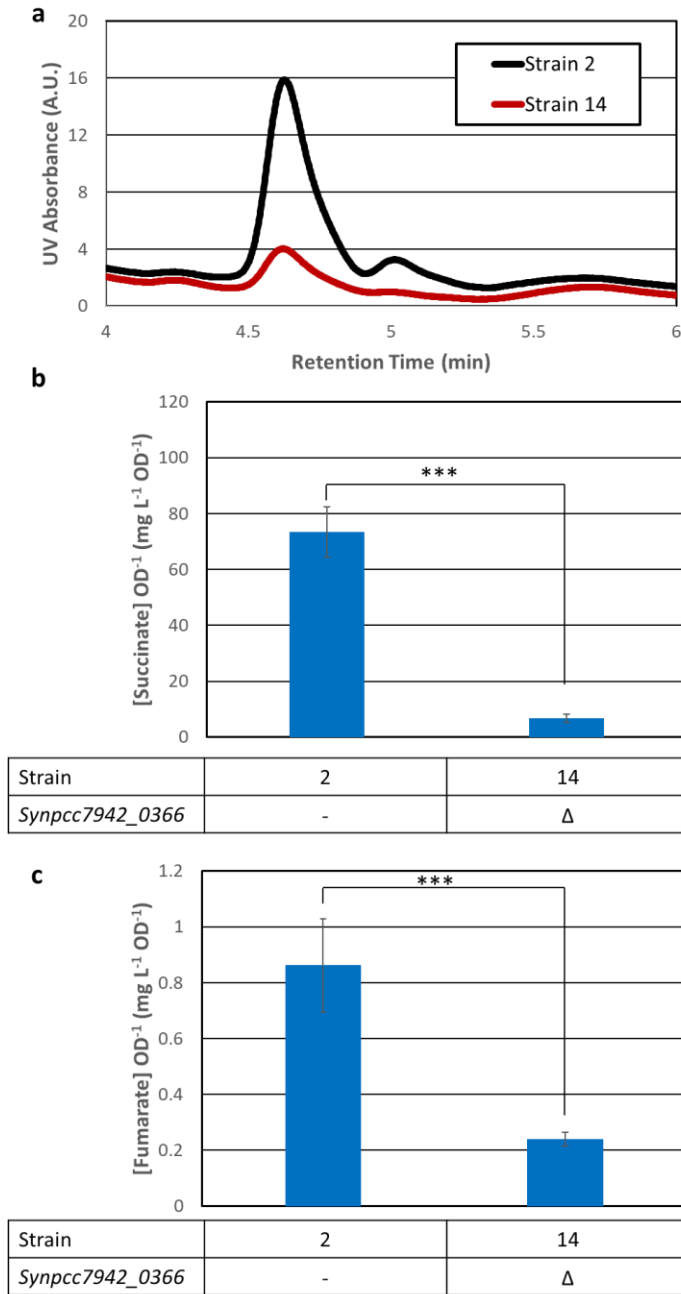
Figure 2.6 Inhibition of secretion of fumarate and succinate upon knockout of Synpcc7942_0366.

a) HPLC-UV retention traces of supernatant samples from production cultures of Strains 2 (black) and 14 (red). Spike-ins of pure fumarate or succinate demonstrate that fumarate runs at a retention time of 4.65 min and succinate runs at 5.0 min. **b)** Specific titer of succinate in strains 2 and 14. **c)** Specific titer of fumarate in strains 2 and 14. For significance calculations, n.s

represents no significant difference P > 0.05, (*) represents P ≤ 0.05, (**) represents P ≤ 0.01, (***) P ≤ 0.001 using an unpaired t-test.
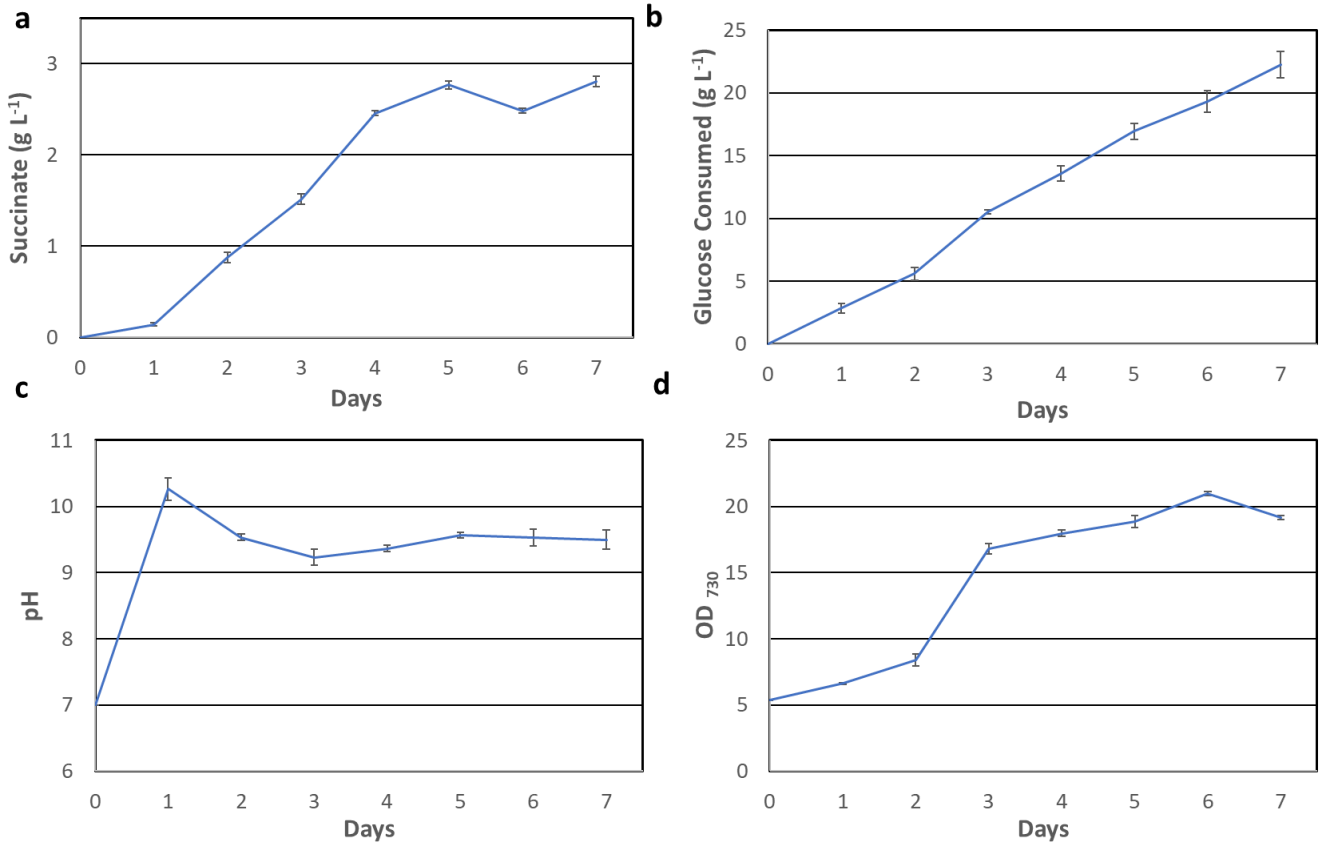
Figure 2.7 High density succinate experiment in strain 13 at high pH in 5x BG-11

a) Succinate production. **b)** Glucose consumed over the time course of the experiment. **c)** pH over time. **d)** OD_{730}. Error bars indicate s.d. (n = 3 biological replicates). Experiment was performed in 5x BG-11 with 40 g L^{-1} glucose and 20 mM bicarbonate.

Given these results, we chose to focus on enhancing glucose import by adjusting the medium pH to 7 daily since it is known that the GALP transporter functions best at acidic or neutral medium pH[35]. Bicarbonate in the media offers the ability to increase pH with hydroxide evolution. The sensitivity to bicarbonate found in Strain 4 was removed by additionally expressing *ppc* (**Fig. 2.2ad**), making Strain 13 amenable to bicarbonate-dependent pH adjustments. Additionally, succinate acidifies the culture media upon production. To investigate the pH effects of both bicarbonate and succinate, a production experiment was started at pH 7 and the pH was adjusted back to pH 7 every day (**Fig. 2.8**). In this experiment, pH was allowed to fluctuate to alkaline levels due to the evolution of hydroxide from bicarbonate and was adjusted back to neutral levels daily. The pH was measured prior to adjustment and was determined to be indicative of succinate production. By day 1, minimal succinate production had occurred, and pH remained at 10.5 (**Fig. 2.8c**). The highest succinate productivity rates were observed from day 2-5, and subsequently pH was lower (pH ~8.5) prior to adjustment during that time due to the produced succinate acidifying the medium (**Fig. 2.8ac**). By days 9-10 succinate productivity decreased, therefore, pH of the cultures was more alkaline prior to adjustment (pH ~9.5) (**Fig. 2.8ac**). Glucose consumption also correlated well with succinate production and decreased pH; glucose consumption was highest (3.9 ± 0.26 g $L^{-1}d^{-1}$) during days 2-5 where succinate production was decreasing medium pH to more neutral levels (pH ~8.5 prior to adjustment) (**Fig. 2.8b**). Glucose consumption was lower (2.2 ± 0.59 g $L^{-1}d^{-1}$) on days 9-10 when the medium was more alkaline (**Fig. 2.8b**). Increased succinate production correlated with exponential growth (**Fig. 2.8d**) while decreased rates correlated with a stationary phase of growth. Strain 13 under this condition produced 5.0 ± 0.41 g L^{-1} succinate and efficiently consumed glucose (3.5 ± 0.44 g $L^{-1}d^{-1}$) over the entire time course.
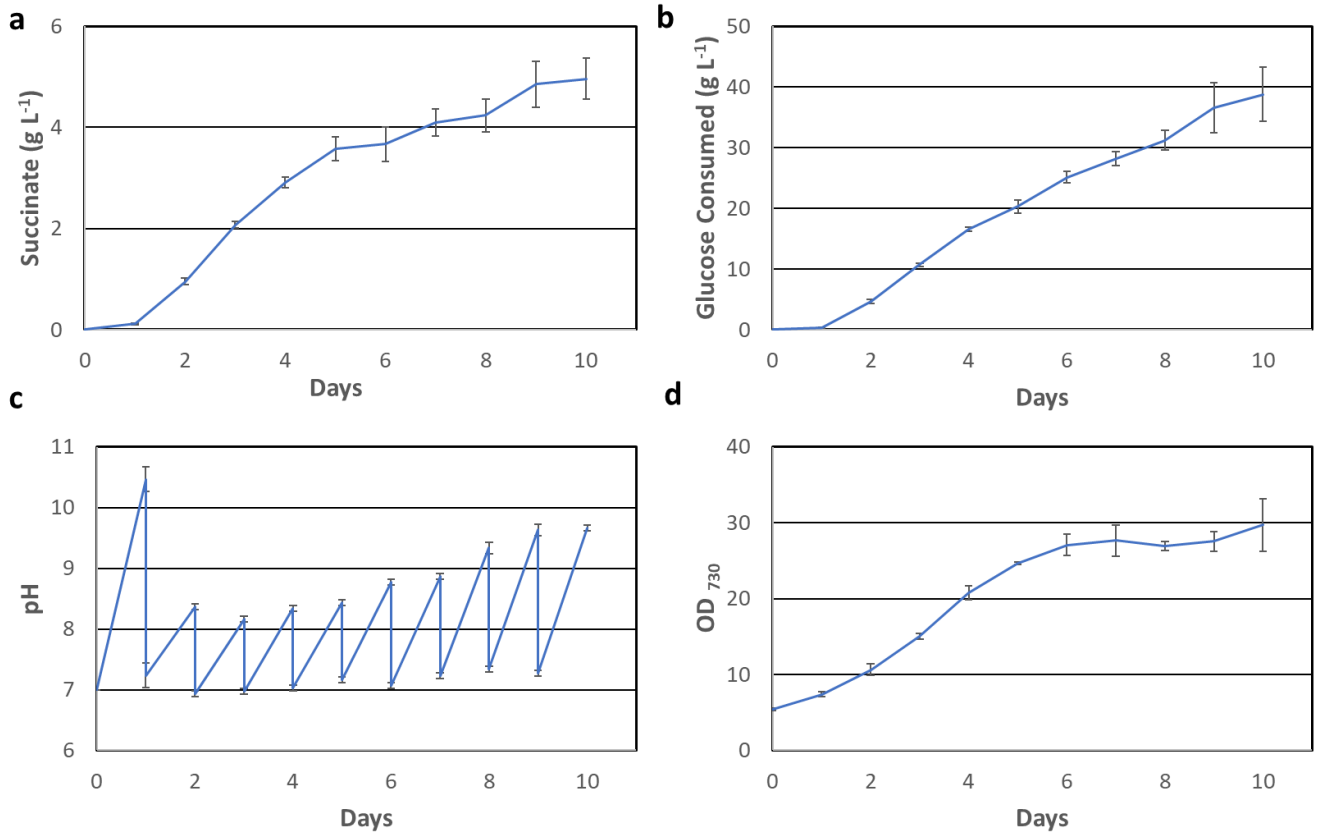
Figure 2.8 High density photomixotrophic succinate production in strain 13 with fluctuating pH

a) Succinate production. **b)** Glucose consumed over the time course of the experiment. **c)** pH changes over time. pH was adjusted back to 7 every 24 hours; pH was recorded prior to adjustment. Both pH measurements prior to adjustment and post adjustment are plotted. d) OD_{730}. Error bars indicate s.d. (n = 3 biological replicates). Experiment was performed in 5x BG-11 with 40 g L^{-1} glucose and 20 mM bicarbonate.

2.5 Conclusion

We improved glucose assimilation and succinate production through gene knockout and overexpression. The pH of the media was observed to be important to both the production of succinate and the consumption of glucose. We investigated various production conditions, our findings in this study show that a fluctuating pH enhances succinate production compared to a stable high pH. Further studies are needed to elucidate whether these results are due to the proton symporters involved in glucose import and succinate export, or to metabolic changes under these various pH conditions. We also hypothesize that a fluctuating pH is natural in an outdoor growth environment due to the diel cycle as CO_2 fixation rates naturally oscillate. This natural oscillation in medium pH was mimicked in the laboratory scale cultures and we determined that succinate can be produced under fluctuating pH conditions. Research into the effects of pH on photomixotrophic production of chemical commodities warrants further exploration to determine the next steps towards optimizing a large scale outdoor cyanobacterial cultivation process. Additionally, this study demonstrated that photomixotrophy in cyanobacteria can be applied to other production systems and is generally an effective way for enhancing production of valuable chemical commodities.

2.6 References

(1)   Uprety, D. C.; Reddy, V. R.; Mura, J. D. *Historical Analysis of Climate Change and Agriculture*; 2019. https://doi.org/10.1007/978-981-13-2014-9_2.

(2)   Sheldon, R. A. Green and Sustainable Manufacture of Chemicals from Biomass: State of the Art. *Green Chem.* **2014**, *16* (3), 950–963. https://doi.org/10.1039/c3gc41935e.

(3)   Cozier, M. Business Highlights: Collaboration: Bigger and Beta. *Biofuels, Bioprod. Biorefining* **2014**, *8* (6), 743. https://doi.org/10.1002/BBB.

(4)   François, J. M.; Lachaux, C.; Morin, N. Synthetic Biology Applied to Carbon Conservative and Carbon Dioxide Recycling Pathways. *Front. Bioeng. Biotechnol.* **2020**, *7* (January), 1–16. https://doi.org/10.3389/fbioe.2019.00446.

(5)   Kanno, M.; Carroll, A. L.; Atsumi, S. Global Metabolic Rewiring for Improved CO_2 Fixation and Chemical Production in Cyanobacteria. *Nat. Commun.* **2017**, *8*, 1–11. https://doi.org/10.1038/ncomms14724.

(6)   Stephens, S.; Mahadevan, R.; Allen, D. G. Engineering Photosynthetic Bioprocesses for Sustainable Chemical Production: A Review. *Front. Bioeng. Biotechnol.* **2021**, *8* (January), 1–15. https://doi.org/10.3389/fbioe.2020.610723.

(7)   Newark. *Global Succinic Acid Market is Expected to Reach USD 218.14*. https://www.globenewswire.com/news-release/2020/01/30/1977366/0/en/Global-Succinic-Acid-Market-is-Expected-to-Reach-USD-218-14-Million-by-2025-Fior-Markets.html (accessed 2023-03-21).

(8)   Sengupta, S.; Jaiswal, D.; Sengupta, A.; Shah, S.; Gadagkar, S.; Wangikar, P. P. Metabolic Engineering of a Fast-Growing Cyanobacterium Synechococcus Elongatus PCC 11801 for Photoautotrophic Production of Succinic Acid. *Biotechnol. Biofuels* **2020**, *13* (1), 1–18. https://doi.org/10.1186/s13068-020-01727-7.

(9)   Lan, E. I.; Wei, C. T. Metabolic Engineering of Cyanobacteria for the Photosynthetic Production of Succinate. *Metab. Eng.* **2016**, *38*, 483–493. https://doi.org/10.1016/j.ymben.2016.10.014.

(10)   Steinhauser, D.; Fernie, A. R.; Araújo, W. L. Unusual Cyanobacterial TCA Cycles: Not Broken Just Different. *Trends Plant Sci.* **2012**, *17* (9), 503–509. https://doi.org/10.1016/j.tplants.2012.05.005.

(11)   Lee, J. W.; Kim, H. U.; Choi, S.; Yi, J.; Lee, S. Y. Microbial Production of Building Block Chemicals and Polymers. *Curr. Opin. Biotechnol.* **2011**, *22* (6), 758–767. https://doi.org/10.1016/j.copbio.2011.02.011.

(12)   Ahn, J. H.; Jang, Y. S.; Lee, S. Y. Production of Succinic Acid by Metabolically Engineered Microorganisms. *Curr. Opin. Biotechnol.* **2016**, *42*, 54–66. https://doi.org/10.1016/j.copbio.2016.02.034.

(13)   Hasunuma, T.; Matsuda, M.; Kato, Y.; Vavricka, C. J.; Kondo, A. Temperature Enhanced
         Succinate Production Concurrent with Increased Central Metabolism Turnover in the
         Cyanobacterium Synechocystis Sp. PCC 6803. *Metab. Eng.* **2018**, *48*, 109–120.
         https://doi.org/10.1016/j.ymben.2018.05.013.

(14)   Iijima, H.; Watanabe, A.; Sukigara, H.; Iwazumi, K.; Shirai, T. Four-Carbon Dicarboxylic Acid
         Production through the Reductive Branch of the Open Cyanobacterial Tricarboxylic Acid
         Cycle in Synechocystis Sp . PCC 6803. *Metab. Eng.* **2021**, *65*, 88–98.
         https://doi.org/10.1016/j.ymben.2021.03.007.

(15)   Lai, M. J.; Tsai, J. C.; Lan, E. I. CRISPRi-Enhanced Direct Photosynthetic Conversion of
         Carbon Dioxide to Succinic Acid by Metabolically Engineered Cyanobacteria. *Bioresour.*
         Technol. **2022**, *366*, 128131. https://doi.org/10.1016/j.biortech.2022.128131.

(16)   Li, Q.; Huang, B.; Wu, H.; Li, Z.; Ye, Q. Efficient Anaerobic Production of Succinate from
         Glycerol in Engineered Escherichia Coli by Using Dual Carbon Sources and Limiting
         Oxygen Supply in Preceding Aerobic Culture. *Bioresour. Technol.* **2017**, *231*, 75–84.
         https://doi.org/10.1016/j.biortech.2017.01.051.

(17)   Nozzi, N. E.; Oliver, J. W. K.; Atsumi, S. Cyanobacteria as a Platform for Biofuel Production.
         Front. Bioeng. Biotechnol. **2013**, *1*, 1–6. https://doi.org/10.3389/fbioe.2013.00007.

(18)   Berla, B. M.; Saha, R.; Immethun, C. M.; Maranas, C. D.; Moon, T. S.; Pakrasi, H. B.
         Synthetic Biology of Cyanobacteria: Unique Challenges and Opportunities. *Front.*
         Microbiol. **2013**, *4*, 1–14. https://doi.org/10.3389/fmicb.2013.00246.

(19)   Jeong, J. Y.; Yim, H. S.; Ryu, J. Y.; Lee, H. S.; Lee, J. H.; Seen, D. S.; Kang, S. G. One-Step
         Sequence-and Ligation-Independent Cloning as a Rapid and Versatile Cloning Method for
         Functional Genomics Studies. *Appl. Environ. Microbiol.* **2012**, *78* (15), 5440–5443.
         https://doi.org/10.1128/AEM.00844-12.

(20)   Golden, S. S.; Brusslan, J.; Haselkorn, R. Genetic Engineering of the Cyanobacterial
         Chromosome. *Methods Enzymol.* **1987**, *153* (C), 215–231. https://doi.org/10.1016/0076-
         6879(87)53055-5.

(21)   Clerico, E. M.; Ditty, J. L.; Golden, S. S. Specialized Techniques for Site-Directed Mutagenesis in Cyanobacteria. *Methods Mol. Biol.* **2007**, *362*, 155–171. https://doi.org/10.1007/978-1-59745-257-1_11.

(22)   Deatherage, D. E.; Barrick, J. E. Identification of Mutations in Laboratory-Evolved Microbes from next-Generation Sequencing Data Using Breseq. *Methods Mol. Biol.* **2014**, *1151*, 165–188. https://doi.org/10.1007/978-1-4939-0554-6_12.

(23)   Till, P.; Toepel, J.; Bühler, B.; Mach, R. L.; Mach-Aigner, A. R. Regulatory Systems for Gene Expression Control in Cyanobacteria. *Appl. Microbiol. Biotechnol.* **2020**, *104* (5), 1977–1991. https://doi.org/10.1007/s00253-019-10344-w.

(24)   Zhao, Y.; Wang, C. S.; Li, F. F.; Liu, Z. N.; Zhao, G. R. Targeted Optimization of Central Carbon Metabolism for Engineering Succinate Production in Escherichia coli. *BMC Biotechnol.* **2016**, *16* (1). https://doi.org/10.1186/s12896-016-0284-7.

(25)   Cooley, J. W.; Vermaas, W. F. J. Succinate Dehydrogenase and Other Respiratory Pathways in Thylakoid Membranes of Synechocystis Sp. Strain PCC 6803: Capacity Comparisons and Physiological Function. *J. Bacteriol.* **2001**, *183* (14), 4251–4258. https://doi.org/10.1128/JB.183.14.4251-4258.2001.

(26)   Chen, Z.; Bommareddy, R. R.; Frank, D.; Rappert, S.; Zeng, A. P. Deregulation of Feedback Inhibition of Phosphoenolpyruvate Carboxylase for Improved Lysine Production in Corynebacterium Glutamicum. *Appl. Environ. Microbiol.* **2014**, *80* (4), 1388–1393. https://doi.org/10.1128/AEM.03535-13.

(27)   De Mey, M.; Lequeux, G. J.; Beauprez, J. J.; Maertens, J.; Waegeman, H. J.; Van Bogaert, I. N.; Foulquié-Moreno, M. R.; Charlier, D.; Soetaert, W. K.; Vanrolleghem, P. A.; Vandamme, E. J. Transient Metabolic Modeling of Escherichia Coli MG1655 and MG1655 ΔackA-Pta, ΔpoxB Δpppc Ppc-P37 for Recombinant β-Galactosidase Production. *J. Ind. Microbiol. Biotechnol.* **2010**, *37* (8), 793–803. https://doi.org/10.1007/s10295-010-0724-7.

(28)   Kai, Y.; Matsumura, H.; Izui, K. Phosphoenolpyruvate Carboxylase: Three-Dimensional Structure and Molecular Mechanisms. *Arch. Biochem. Biophys.* **2003**, *414* (2), 170–179.

https://doi.org/10.1016/S0003-9861(03)00170-X.

(29)   Choi, P. H.; Vu, T. M. N.; Pham, H. T.; Woodward, J. J.; Turner, M. S.; Tong, L. Structural and Functional Studies of Pyruvate Carboxylase Regulation by Cyclic Di-AMP in Lactic Acid Bacteria. *Proc. Natl. Acad. Sci. U. S. A.* **2017**, *114* (35), E7226–E7235. https://doi.org/10.1073/pnas.1704756114.

(30)   Piazza, I.; Kochanowski, K.; Cappelletti, V.; Fuhrer, T.; Noor, E.; Sauer, U.; Picotti, P. A Map of Protein-Metabolite Interactions Reveals Principles of Chemical Communication. *Cell* **2018**, *172* (1–2), 358-372.e23. https://doi.org/10.1016/j.cell.2017.12.006.

(31)   Stec, B. Structural Mechanism of RuBisCO Activation by Carbamylation of the Active Site Lysine. *Proc. Natl. Acad. Sci. U. S. A.* **2012**, *109* (46), 18785–18790. https://doi.org/10.1073/pnas.1210754109.

(32)   Spreitzer, R. J.; Salvucci, M. E. Rubisco: Structure, Regulatory Interactions, and Possibilities for a Better Enzyme. *Annu. Rev. Plant Biol.* **2002**, *53*, 449–475. https://doi.org/10.1146/annurev.arplant.53.100301.135233.

(33)   McEwen, J. T.; Machado, I. M. P.; Connor, M. R.; Atsumi, S. Engineering Synechococcus Elongatus PCC 7942 for Continuous Growth under Diurnal Conditions. *Appl. Environ. Microbiol.* **2013**, *79* (5), 1668–1675. https://doi.org/10.1128/AEM.03326-12.

(34)   Geertsma, E. R.; Chang, Y. N.; Shaik, F. R.; Neldner, Y.; Pardon, E.; Steyaert, J.; Dutzler, R. Structure of a Prokaryotic Fumarate Transporter Reveals the Architecture of the SLC26 Family. *Nat. Struct. Mol. Biol.* **2015**, *22* (10), 803–808. https://doi.org/10.1038/nsmb.3091.

(35)   Zheng, H.; Taraska, J.; Merz, A. J.; Gonen, T. The Prototypical H+/Galactose Symporter GalP Assembles into Functional Trimers. *J. Mol. Biol.* **2010**, *396* (3), 593–601. https://doi.org/10.1016/j.jmb.2009.12.010.

(36)   Martinho de Brito, M.; Bundeleva, I.; Marin, F.; Vennin, E.; Wilmotte, A.; Plasseraud, L.; Visscher, P. T. Effect of Culture PH on Properties of Exopolymeric Substances from

Synechococcus PCC7942: Implications for Carbonate Precipitation. *Geosci.* **2022**, *12* (5). https://doi.org/10.3390/geosciences12050210.

(37)   Mangan, N. M.; Flamholz, A.; Hood, R. D.; Milo, R.; Savage, D. F. PH Determines the Energetic Efficiency of the Cyanobacterial CO_2 Concentrating Mechanism. *Proc. Natl. Acad. Sci. U. S. A.* **2016**, *113* (36), E5354–E5362. https://doi.org/10.1073/pnas.1525145113.

(38)   Ritchie, R. J. Membrane Potential and PH Control in the Cyanobacterium Synechococcus R-2 (Anacystis Nidulans) PCC 7942. *J. Plant Physiol.* **1991**, *137* (4), 409–418. https://doi.org/10.1016/S0176-1617(11)80309-3.

2.7 Supplementary Information

Table 2.S1 Plasmids used in this study

Plasmid name	Contents	Relevant Strain(s)	Marker	Ref
pAL1136	NSIII targeting plasmid, P_{trc}:*alsD-alsS-adh*	-	Gent^R	Kanno et al. 2017
pAL1450	NSI targeting plasmid, P_{trc}:*galP-zwf-gnd*	1	Spec^R	Kanno et al. 2017
pAL1515	NSI targeting plasmid, P_{trc}:*galP-zwf-gnd*	All except 11-15	Kan^R	Kanno et al. 2017
pAL1618	*cp12*::P_{trc}:*prk-rbcLS*	-	Kan^R	Kanno et al. 2017
pAL1832	NSIII targeting plasmid, P_{trc}:*gabD* (MG1655)-*kgd* (7002)-*ppc* (7942)-*gltA* (MG1655)	1	Gent^R	This work
pAL2225	*sdhB*::P_{LlacO1}:*ppc* (*Cg*)	5	Gent^R	This work
pAL2229	Δ*sdhB*	4	Gent^R	This work
pAL2241	*sdhB*::P_{LlacO1}:*ppc* (MG1655)	6	Gent^R	This work
pAL2242	*sdhB*::P_{LlacO1}:*ppc* (7942)	7, 12	Gent^R	This work
pAL2276	*sdhB*::P_{LlacO1}:*ppc* (7942)–*gltA* (7942)	10	Gent^R	This work
pAL2277	*sdhB*::P_{LlacO1}:*ppc* (7942)–*gltA* (*Cg*)	8, 13	Gent^R	This work
pAL2279	*sdhB*::P_{LlacO1}:*ppc* (7942)–*gltA* (MG1655)	9	Gent^R	This work
pAL2301	*cp12*::P_{trc}:*prk, P_{trc}:galP-zwf-gnd*	11-13	Kan^R	This work
UGS-19F2	Synpcc7942_0366::Tn*5*	14	Kan^R	Chen et al. 2012

M. Kanno, A. L. Carroll, S. Atsumi. *Nat. Commun.* **8**, 1–11 (2017).

Chen Y, Holtman CK, Taton A, Golden SS. *Adv Photosynth Respir* **33**:119 –137 (2012).

Table 2.S2 Oligonucleotides used in this study

Name	Sequence 5' to 3'
TT90	GATTTAATCTGCCGTATGTAAAGATCCTCTAGAGTCGACCTG
TT111	GCGGCTGGCATGCGCAATACAGG
TT113	GCGACTTTAAAAGCGATATCAAGCGTTAAAGATCCTCTAGAGTCGACCTG
TT114	GATTTAATCTGCCGTATGTAAATTAATAAGGAGGAATTATTAGCATGAGTGCTGCTCTCCAGTC
TT116	GCATGCGCAATACAGGTTGACTTTAATTTAACGTAAATAAGGAAGTCATTATGGCTGATACAAAAGCAAAAC
TT122	CACCTGGGCAGATGTGTTGAAC
TT123	GATTGCGAGTGAGATATTTATG
TT124	GAGTTGACGCGTGCTTATCA
TT125	GCCTTTCGTTTTATCTGTTG
TT213	AATGACTTCCTTATTTACGTTAAATTAAAG
TT213	CTTTAATTTAACGTAAATAAGGAAGTCATT
TT214	AGATCCTCTAGAGTCGACCTG
TT214	ACCTGATCTGTCGTATGTAAAGATCCTCTAGAGTCGACCTGCAGG
TT221	ATTAATAAGGAGGAATTATTAGCATGAATACTGCAG
TT222	ACGTAAATAAGGAAGTCATTATGAAACTTAACGACAGTAAC
TT223	CAAATATATGTGCATCGGTCTTTAAATTAATAAGGAGGAATTATT
TT359	TGGCGAGCCTCGGAGTGTTCC
TT360	CCAAAGTGGCAGAAGACAGCACTGTATGC
TT361	CAGAAGACAGCACTGTATGCCCTAGAGGCATCAAATAAAACG
TT362	GAACACTCCGAGGCTCGCCAGCACTGGTGCTGTAGCAATC
TT363	GCCTATTGCGGCATTGTTGCTGTCA
TT364	GACTGGATCAGTAAATCTAGGATTCAGTTGTTCTAGAGACTC
TT507	CGTCACTGTCTCGAGGGATCCTATTAATAAGGAGGAATTATT
TT508	TTGCGGCATTGTTGCTGTCACGTACGCTCGAACCCCAGAG

TT509	CTGTTGTTTGTCGGTGAACGCTCTCGACTGGATCAGTAAATCTAGGATTCAGTTG
TT510	AGATCCTCTAGAGTCGACCTGCAGG
TT511	ATTAATAAGGAGGAATTATTAGCATGAACGAACAATATTCCGC
TT512	GGTATGCGTAATACCGGCTAAAGATCCTCTAGAGTCGACCT
TT513	CTGGCATGCGCAATACAGGTTGAAGATCCTCTAGAGTCGACCT
TT514	ATTAATAAGGAGGAATTATTAGCATGAGTGCTGCTCTCCAGTCATCC
TT515	TCAAATATGTATCCGCTCATGGCGGCCCAG
TT516	CAGGCAAGAACCTCGAATTTCTCATCGGATTGC
TT523	GCTTGGTTTTGGACAGTGATCTCAAATATGTATCCGCTCAT
TT524	CGAATTTCTCATCGGATTGCGATTCAGTTGTTCTAGAGACTCGAG
TT544	TAAATAAGGAAGTCATTATGGCTGATACAAAAGCAAAACTCACC
TT545	CGACTTTAAAAGCGATATCAAGCGTTAAGCAGGCATGCAAGCTTAAGCG
TT546	ACGTAAATAAGGAAGTCATTATGTTTGAACGCGATATCGTGGCCAC
TT547	GTCCCACGCGAAGAACGCTAGGCAGGCATGCAAGCTTAAGC
TT548	TAAATAAGGAAGTCATTATGACTGCCGTCAGCGAGTTTCG
TT549	CGGGATTTGGCGATCGAATCTGATTGAGCAGGCATGCAAGCTTAAGC
TT583	GCAGGCATGCAAGCTTAAGCGAGAG
TT584	GCAATACAGGTTGAAGATCCTCTAGAGTCGACCTCTTTAATTTAACGTAAATAAGGAAGTCATTATG
TT628	GTTTGTCGGTGAACGCTCTCCGACTGCACGGTGCACCAATG
TT629	CGCTCTCACGCGTTCTAGAGGCTCACCTCAATCAACGCTCAC
TT632	CTCTCACGCGTTCTAGAGGCTCACCTCAATCAACGCTCACC
TT633	GTTGTTTGTCGGTGAACGCTCTCCGACTGCACGGTGCACCAAT

Table 2.S3 Plasmid Construction Guide

| Plasmid	Vector PCR			Insert(s) PCR			
	Primer (F)	Primer (R)	Template	Primer (F)	Primer (R)	Template	Insert description
pAL1832	TT214	TT213	pAL1136	TT222	TT223	MG1655 gDNA	*gabD*
				TT221	TT90	7002 gDNA	*kgd*
				TT114	TT111	7942 gDNA	*ppc*
				TT116	TT113	MG1655 gDNA	*gltA*
pAL2225	TT361	TT362	pAL1136	TT359	TT363	7942 gDNA	Upstream sequence of *sdhB*
				TT364	TT360	7942 gDNA	Downstream sequence of *sdhB*
				TT508	TT509	Codon Optimized Gene Fragment from Genewiz	*ppc* (Cg)
pAL2229	TT524	TT523	pAL2225	TT515	TT516	pAL1136	Gent[R]
pAL2241	TT510	TT507	pAL2225	TT511	TT512	MG1655 gDNA	*ppc*
pAL2242	TT510	TT507	pAL2225	TT514	TT513	7942 gDNA	*ppc*
pAL2276	TT583	TT584	pAL2242	TT548	TT549	7942 gDNA	*gltA*
pAL2277	TT583	TT584	pAL2242	TT546	TT547	Codon Optimized Gene Fragment from Genewiz	*gltA* (Cg)
pAL2279	TT583	TT584	pAL2242	TT544	TT545	MG1655 gDNA	*gltA*
pAL2301	TT632	TT633	pAL1618	TT628	TT629	pAL1450	*galP-gnd-zwf*
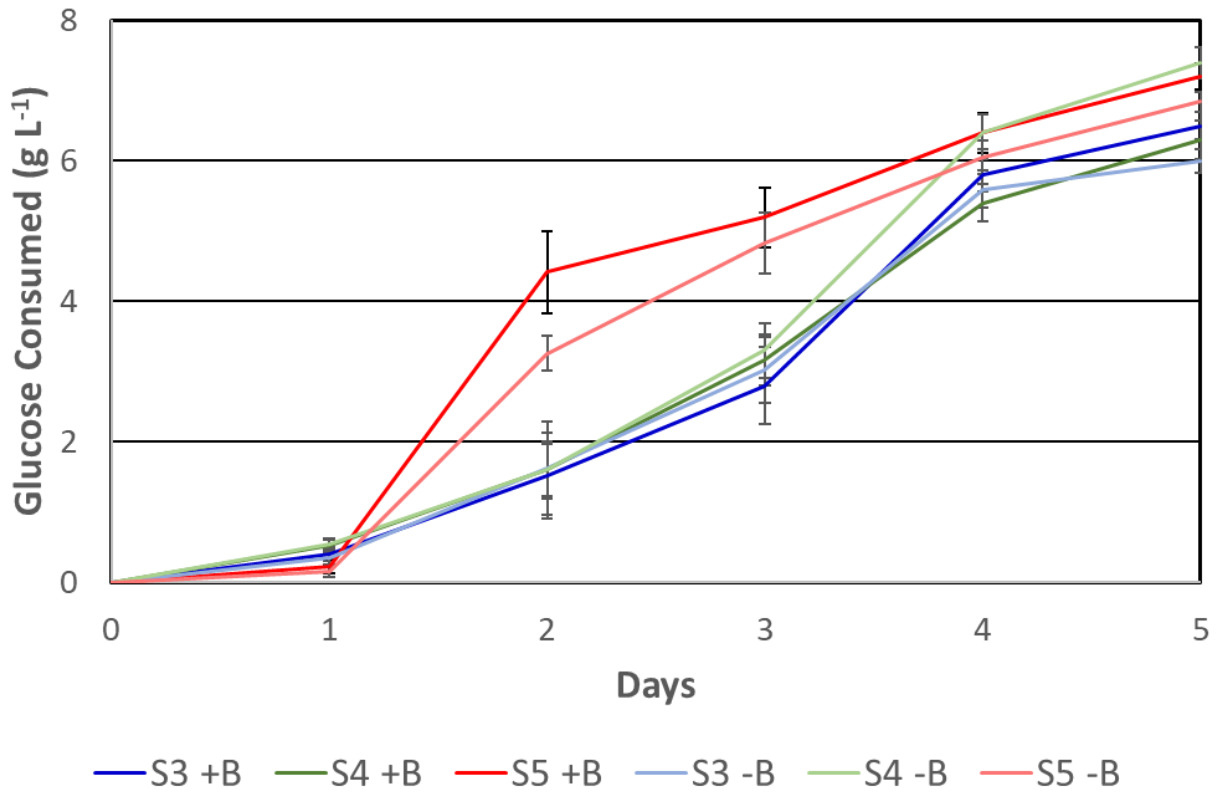
Figure 2.S1. Glucose consumption of Strains 3 through 5

Glucose consumed over the time course of the experiment for Strains 3 through 5 with or without 20 mM bicarbonate (+B or –B). Error bars indicate s.d. (n = 3 biological replicates). Experiment was performed in 1x BG-11 with 10 g L^{-1} glucose.

Figure 2.S2. Glucose consumption and OD$_{730}$ of Strains 5 through 7

a) Glucose consumed over the time course of the experiment for Strains 5 through 7. **b)** OD$_{730}$ for Strains 5 through 7 over the time course of the experiment. Error bars indicate s.d. (n = 3 biological replicates). Experiment was performed in 1x BG-11 with 10 g L^{-1} glucose and 20 mM bicarbonate.
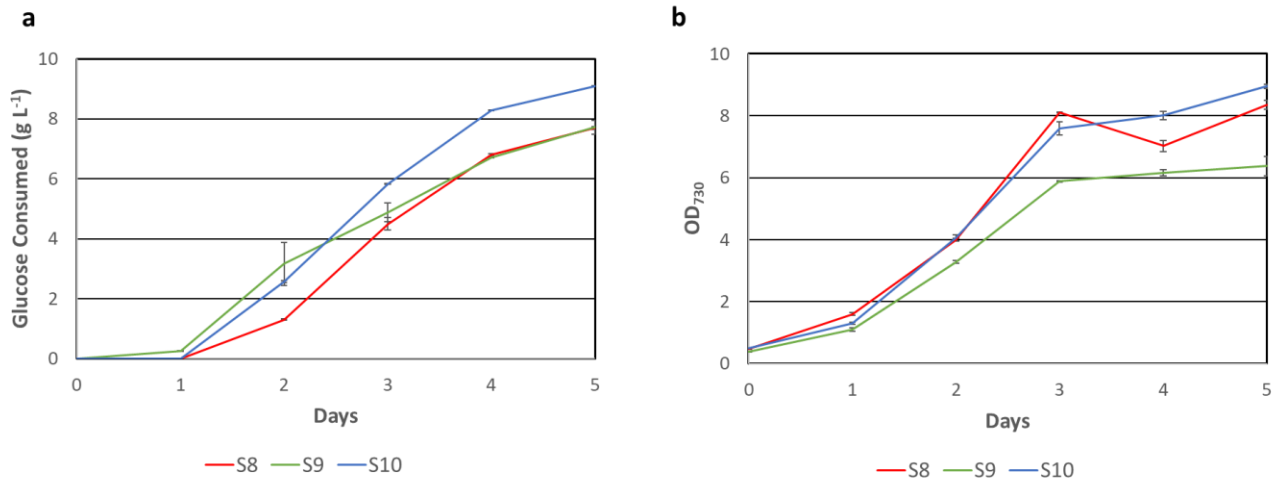
Figure 2.S3. Glucose consumption and OD$_{730}$ of Strains 8 through 10

a) Glucose consumed over the time course of the experiment for Strains 8 through 10. **b)** OD$_{730}$ for Strains 8 through 10 over the time course of the experiment. Error bars indicate s.d. (n = 3 biological replicates). Experiment was performed in 1x BG-11 with 10 g L^{-1} glucose and 20 mM bicarbonate.
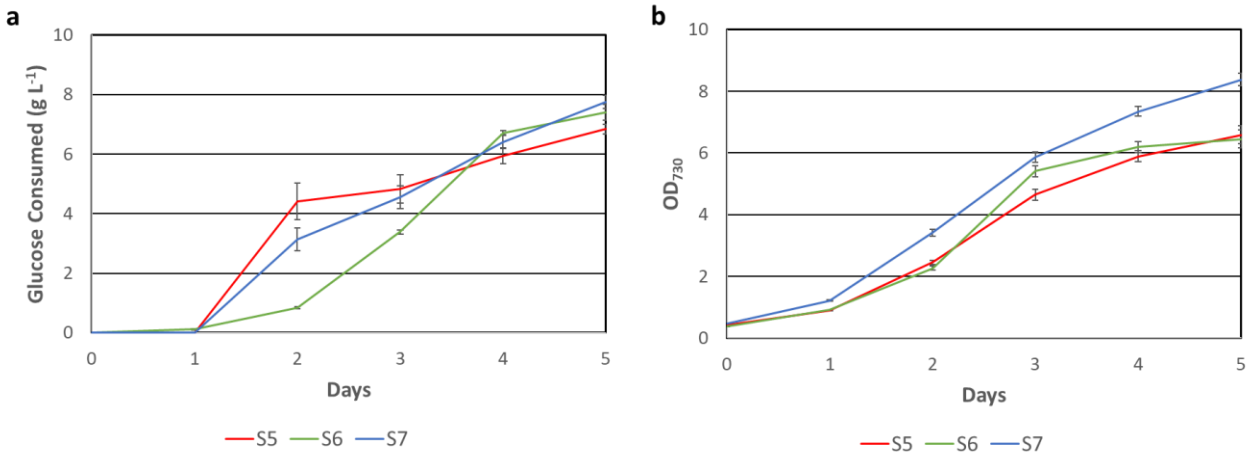
Figure 2.S4. Glucose consumption and OD$_{730}$ of Strains 11 through 13

a) Glucose consumed over the time course of the experiment for Strains 11 through 13. **b)** OD$_{730}$ for Strains 8 through 13 over the time course of the experiment. Error bars indicate s.d. (n = 3 biological replicates). Experiment was performed in 1x BG-11 with 10 g L^{-1} glucose and 20 mM bicarbonate.
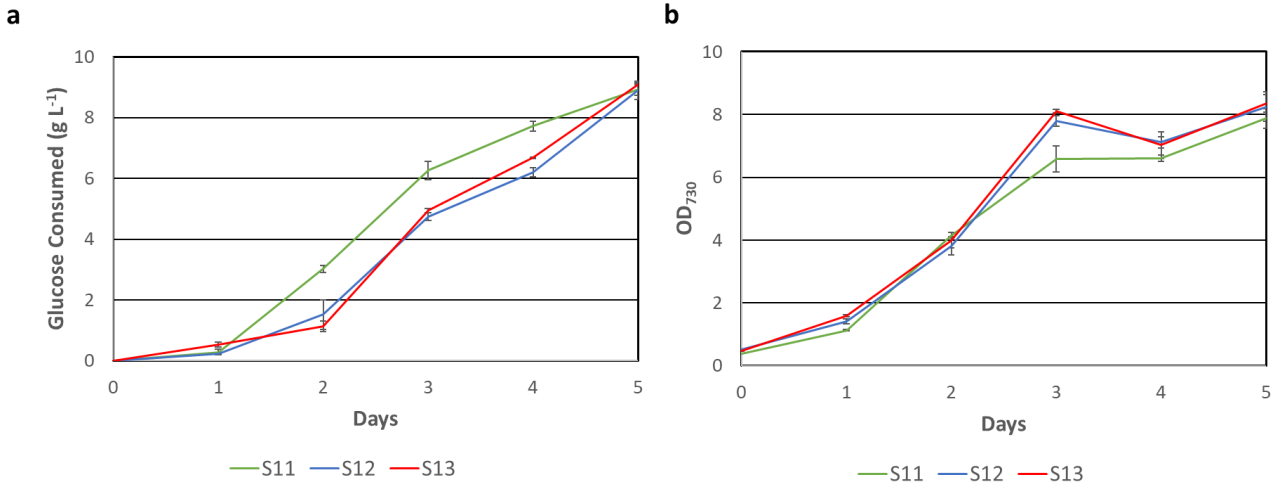
Chapter 3: Carbon Efficient Isobutanol Production in *Escherichia coli*

3.1 Abstract

Developed in this work is an electrical-biological hybrid system wherein engineered *Escherichia coli* consumes formate produced electrocatalytically from CO_2 to supplement bioproduction of isobutanol. Biological CO_2 sequestration is notoriously slow compared to electrochemical CO_2 reduction, while electrochemical methods struggle to generate carbon-carbon bonds. A hybrid system is promising for combining the benefits of biology and electrochemistry. *E. coli* was engineered to assimilate formate and CO_2 in central metabolism using the reductive glycine pathway. We have shown that chemical production in *E. coli* can benefit from single carbon substrates when equipped with the RGP. In this work the engineered strain of *E. coli* that can consume formate from an electrocatalytic bioreactor and produce isobutanol at a yield of >100% of theoretical maximum from glucose. Our results demonstrate that carbon produced from electrocatalytically reduced CO_2 can bolster chemical production in *E. coli*.

3.2 Introduction

The current global climate crisis has been largely fueled by our reliance on fossil fuels, leading to unprecedented levels of greenhouse gases in the atmosphere[1]. This ongoing crisis has driven an increased demand for sustainable chemical production from renewable sources. Developing methods to use atmospheric carbon dioxide for the production of chemical commodities has garnered particular attention in recent years as a solution that can both reduce current greenhouse gas levels and provide an alternative to petroleum-based chemistry[2,3]. Biological systems of engineered microorganisms have been studied to either indirectly or directly use atmospheric CO_2 for the production of valuable chemical commodities[2,4]. Traditional biological fermentation strategies perform indirect CO_2 sequestration by feeding sugar feedstocks sourced from various crops to heterotrophic microorganisms such as yeast or *Escherichia coli*. This methodology has the drawback of directly competing with the global food supply[5]. Using photosynthetic production systems for direct CO_2 reduction also has drawbacks such as slow growth and lower production rates compared to heterotrophic microbes[2]. Inorganic strategies for CO_2 sequestration have similarly been investigated and provide an efficient means to convert CO_2 into more useful single carbon molecules[6–11]. However, inorganic methods cannot efficiently create carbon-carbon bonds[7]. These drawbacks to both biological production and inorganic CO_2 conversion have motivated research into various hybrid strategies where single carbon molecules produced from electrocatalytically reduced CO_2 are fed to biological hosts, providing a production platform that circumvents the aforementioned drawbacks[12,13]. Here, in the model organism *E. coli* we built upon the reductive glycine pathway (RGP) and have shown that *E. coli* can efficiently convert the electrochemically relevant molecule, formate, into the value-added product, isobutanol, a gasoline substitute and a precursor for jet fuel and polymers[14,15].

In a previous study, the theorized RGP was shown to function effectively in *E. coli,* enabling growth in a serine auxotrophic strain[13]. Other studies using a similar strategy to the RGP have shown that *E. coli* can be engineered to grow on formate and CO_2 alone, but the resultant chemoautotrophic *E. coli* suffers from slow growth and lower overall chemical

production[12]. One study hypothesized that intracellular NADH and NADPH levels contributed to the slower growth phenotype. Two genes encoding for variants of the enzyme formate dehydrogenase were installed to generate additional reducing equivalents, however, the engineered strain still lagged behind standard growth rates for *E. coli*[12].

The RGP requires two carbon inputs: formate and CO_2. In an electrocatalytic setting CO_2 can be reduced to formate, simplifying the carbon inputs for the RGP[6,13]. In a previous study, it was demonstrated that *E. coli* is capable of growing and assimilating CO_2 and formate in the cathode of an electrochemical bioreactor where CO_2 is readily converted to formate, reducing the carbon inputs down to CO_2 alone[13]. The previous study required the use of the rare metal indium for the working electrode for the reduction of CO_2 to formate[13]. In this study, we demonstrate that an iron carbonyl cluster can alternatively be used to reduce CO_2 to formate in the hybrid system. There are several benefits to using this iron-based catalysis compared to indium. Iron is Earth-abundant metal and the iron carbonyl cluster can perform catalysis for longer durations[6]. Additionally, this iron-based catalyst has the highest observed catalytic rates at neutral pH, making this catalyst ideal for a biological hybrid system[6]. Using a carbon electrode in the working compartment of the catalysis prevents the use an otherwise toxic metal electrode that impacts the overall health of the biocatalysis. The catalyst used in this study is highly stable and specific to formate production, as such it does not produce other side products such CO, H_2, oxalate, methanol, or formaldehyde making it superior to other catalysts in the context of electrical-biological systems[6].

The downstream chemical of choice in this study, isobutanol, is a relevant polymer and jet fuel precursor[16,17]. Isobutanol production in *E. coli* is well established[17]. Connecting the RGP to isobutanol production provides an ideal signal for determining if the RGP is capable of incorporating formate and CO_2 into a biologically derived chemical product[17]. An important study for this field determined that the chemolithotrophic bacterium, *Ralstonia eutropha,* could produce isobutanol from electrochemically produced formate[18]. However, *R. eutropha* is an obligate aerobe and susceptible to damage from the reactive oxygen species that are generated in an electrocatalytic setting where oxygen is present. While isobutanol provides a robust indicator of *E. coli*'s ability to efficiently convert formate into a value-added chemical, many

other chemical commodities can be generated using this system. Due to the ability of the RGP to incorporate formate and CO_2 into pyruvate, any downstream chemical production pathway that relies on intracellular pyruvate pools could potentially benefit from the RGP[13].

This study represents the ability of an electrical-biological hybrid system to provide a more renewable platform for chemical production in *E. coli* compared to traditional heterotrophic fermentations while also providing a more efficient method for CO_2 sequestration compared to Ribulose-1,5-bisphosphate carboxylase/oxygenase (RubisCO) based carbon capture.

3.3 Methods

3.3.1 Reagents

All enzymes involved in the molecular cloning experiments were purchased from New England Biolabs (NEB). All synthetic oligonucleotides were synthesized by Integrated DNA Technologies. Sanger Sequencing was provided by Genewiz from Azenta Life Sciences.

3.3.2 Strains and Plasmids

All strains and plasmids used in this study are listed in Table 3.1 and Table 3.S1, respectively. All oligonucleotides are listed in Table 3.S2. Plasmids were constructed using sequence and ligation independent cloning (SLIC)[33]. The constructed plasmids were verified via Sanger Sequencing. A guide to the construction of plasmids used in this study is detailed in Table 3.S3. The plasmid (pAL2244, **Table 3.S1**) containing the linear fragment for the integration of the gene formate dehydrogenase from *Arabidopsis thaliana* (hereafter *At*) expressed under the Biobricks strong constitutive promoter P_{BBa_J23119} was integrated into safe site 9[40] of *E. coli* using Clustered Regularly Interspaced Short Palindromic Repeats (CRISPR)/Cas9[41] and was codon optimized and purchased from Genewiz from Azenta Life Sciences.

Table 3.1 List of key strains used in this study

Strain no.	Name	Key genotype	Ref
1	YT151	BW25113/F'[*traD36*, *proAB+*, *lacI^q* ZΔM15 *Tn*10(Tet^R)] $\Delta serA$	13
2	AL4068	1 + SS9::P_{BBa_J23119}:*fdh* (*At*)	This work
3	AL17	BW25113/F'[*traD36*, *proAB^+*, *lacI^q* ZΔM15 *Tn*10(Tet^R)] $\Delta adhE$ $\Delta frdBC$ Δfnr-*ldhA* Δpta $\Delta pflB$	17
4	AL4014	3 + $\Delta serA$	This work
5	AL4101	4 + SS9::P_{BBa_J23119}:*fdh* (*At*)	This work
6	AL4159	4 + SS9::P_{BBa_J23119}:*fdh* (*Cb*)	This work
7	AL4160	4 + SS9::P_{BBa_J23119}:*fdh* (*Sc*)	This work
8	AL4214	6 + P_{sdaA}::P_{LlacO1}	This work

3.3.3 CRISPR

Genome modifications such as gene deletion and gene insertion were constructed using CRISPR-Cas9-mediated homologous recombination[41]. Linear DNA repair fragments for gene deletions and insertions were constructed by amplifying genomic or plasmid DNA via PCR assembly[42]. Plasmids encoding sgRNA for CRISPR-Cas9-mediated homologous recombination were constructed using Q5 site-directed mutagenesis (New England Biolabs) using pTargetF plasmid (Addgene #62226) as a template. All genomic modifications were verified via Sanger Sequencing. A guide for CRISPR-Cas9-mediate gene deletions and insertions used in this study is detailed in Table 3.S4.

3.3.4 Culture Conditions

Overnight cultures were prepared in 3 mL of Luria-Bertani (LB) media containing appropriate antibiotics. Antibiotic concentrations were as follows: tetracycline (5 μg mL^{-1}), spectinomycin (25 μg mL^{-1}), kanamycin (25 μg mL^{-1}), ampicillin (100 μg mL^{-1}). Low density isobutanol experiments were carried out in 5 mL M9P: M9 minimal media (33.7 mM Na$_2$HPO$_4$,

22 mM KH_2PO_4, 8.6 mM NaCl, 9.4 mM NH_4Cl, 1 mM $MgSO_4$, 0.1 mM $CaCl_2$) including A5 trace metal mix (2.86 mg L^{-1} H_3BO_3, 1.81 mg L^{-1} $MnCl_2 \cdot 4H_2O$, 0.079 mg L^{-1} $CuSO_4 \cdot 5H_2O$, 49.4 µg L^{-1} $Co(NO_3)_2 \cdot 6H_2O$) supplemented with 5 g L^{-1} yeast extract (Research Products International) and 10 g L^{-1} glucose (Fisher Bioreagents) with additional appropriate carbon sources. Overnight culture in LB media was spun down at 6,000 g for 1 min. The cell pellet was re-suspended with 5 mL M9P media with 10 g L^{-1} glucose. The M9P culture was grown to an OD_{600} of ~0.4 and subsequently spun down at 6,000 g for 1 min. The pellet was resuspended in 5 mL M9P supplemented with appropriate carbon sources and was induced with 1 mM IPTG and 10 µg L^{-1} aTc. Cultures were incubated at 37 °C. Cell growth was monitored by measuring OD_{600} in a Synergy HTX Plate Reader (BioTek Instruments, Inc.).

For high density experiments, overnight culture was used to inoculate a 250 mL screw cap flask containing 50 mL M9P. The 50 mL culture was allowed to grow to an OD_{600} of ~0.4 and was induced with 1 mM IPTG and 10 µg L^{-1} aTc. The culture was allowed to grow for an additional 1.5 h to an OD_{600} of ~1. The 50 mL culture was centrifuged at 6,000 g for 5 min and resuspended in 1 mL of M9P with appropriate carbon sources for an OD_{600} of ~50.

3.3.5 Preparation of Catalyst

The catalyst $[Na(diglyme)_2][Fe_4N(CO)_{12}]$ was prepared according to a reported procedure[43].

3.3.6 Electrochemical Measurements

Cyclic voltammograms (CV's) were recorded under a N_2 or CO_2 gas (N_2) (99.998%, Praxair) atmosphere using an electrochemical analyzer (CH Instruments, Model 620D or Model 1100B), a glassy carbon working electrode (CH Instruments) with a nominal surface area of 0.0707 cm^2), and a platinum wire auxiliary electrode. Controlled electrode potential (CPE) experiment was performed on a multichannel Biologic VSP 300 potentiostat. The glassy carbon working electrode was polished on a felt pad with alumina paste (0.05 µm, BASi), sonicated in deionized water, rinsed with MeOH, and dried with a Kimwipe prior to each experiment. As the reference electrode, a Ag/AgCl(sat.) electrode was used form aqueous measurements. All

reported potentials are referenced to the SCE couple, and were determined using ferrocene (Aldrich) as an internal standard, where $E_{1/2}$ (Fc$^{+1/0}$) is +0.159 V vs SCE in water[43]. Milli-Q water (18 MΩ) was used for measurements performed in aqueous solution. Buffer solutions were 0.1 M phosphate buffer adjusted to pH 7.4. Reagents for buffer preparation were purchased from EMD, VWR, and Sigma, and were used as received. In all cases, CV sweeps were initiated at the open circuit potential and recorded in quiescent solution.

3.3.7 Controlled Potential Electrolysis (CPE)

CPE experiments were performed in a gas-tight glass cell (working electrode compartment volume of 60 mL) under 1 atm of static N_2 (Praxair, 99.998%) or carbon dioxide (Praxair, 99.5%) with a stirred solution. The cell was custom made by Adams & Chittenden Scientific glass (**Fig. S4**). The counter electrode compartment was separated from the working electrode compartment by a glass frit of medium porosity. In a typical experiment, 20 mL of degassed 0.1 M phosphate buffer solution (made from 0.05 M Na_2HPO_4/0.05 M NaH_2PO_4 was used in the working electrode compartment along with 0.5 mM Na(diglyme)$_2$[Fe$_4$N(CO)$_{12}$] (diglyme: bis(2-methoxyethyl) ether). In control experiments performed with the same solutions absent the iron catalyst no formate was detected, only ~ 2 C of charge were passed over 1 h and low levels of H_2 were detected, consistent with our prior reports[6].

The working electrode was a glassy carbon plate with an area of 8 cm^2 (Tokai Carbon), while the counter electrode was a coiled Pt wire ~70 cm in length (0.5 mm diameter, 99.997% metals basis from Alfa aesar). The reference electrodes employed for CPE experiments were of similar design to those used for CV measurements, using a longer glass tube to fit the H-cell. Between CPE experiments, the glass cell, the stir bar, the working electrode, and the counter electrode were cleaned via sonication in 5% (v/v) nitric acid for 5 min, rinsed with deionized (DI) water, sonicated in DI water for 5 min, rinsed with DI water, and then sonicated in acetone for 5 min, rinsed with DI water, and allowed to dry in an oven before use. Every two weeks the frit was checked and baked out or changed by a glassblower. The glassy carbon plate had an additional initial step of being thoroughly sanded on all surfaces with 300 grit SiC paper and then 600 grit SiC paper and rinsed with water prior to sonication steps. The counter electrode

(Pt coil) was flame annealed prior to each experiment. For longer CPE runs (more than 20 h) both the cathodic and anodic compartment was purged with humidified CO_2 in each hour and the anode chamber was purged with N2 gas. A home-built intermittent purging valve set up was used for purging. During CPE the pH of the solution was monitored by a Bluelab pH controller (Bluelab USA). In those longer CPE experiments no headspace measurements were performed to detect H_2 gas. Faradaic Efficiency (FE) was determined by calculating the amount of charge required in production of each product divided by total charge passed during each experiment.

Quantification of headspace gases and solution-phase products were performed separately[6]. At the end of an electrolysis, a gaseous sample (0.1 mL) was drawn from the headspace, using a gas-tight syringe (Vici), and injected into a gas chromatography–thermal conductivity detection (GC- TCD) system (Model Varian 3800 GC coupled with a TCD detector and a Carboxen 1010 PLOT fused silica column (30 m × 0.53 mm) (Supelco) using N2 (99.999%, Praxair) as the carrier gas. H_2 concentration was determined using a previously prepared working curve[6]. Analysis of the liquid phase and determination of formate content was achieved by removing 0.5 mL of sample from the CPE experiment and analyzed via high performance liquid chromatography described below.

3.3.8 Bio-electrochemical cultivation for isobutanol production

Following the CPE experiment, a syringe was used to remove 20 mL of solution from the working electrode side of the cell. The CPE solution was supplemented with 50 mM sodium bicarbonate and 10 g L^{-1} glucose. Antibiotics and inducers (IPTG and aTc) were also added in appropriate amounts. Overnight cultures were prepared in 3 mL of Luria-Bertani (LB) media containing appropriate antibiotics. Overnight LB culture was used to inoculate a 250 mL screw cap culture flask containing 50 mL M9P. The culture was grown to an OD_{600} of 0.4 and induced with IPTG and aTc. The culture was allowed to grow for an additional 1.5 hours to an OD_{600} of approximately 1. The culture was then centrifuged at 6,000 g for 5 minutes. The cell pellet was resuspended in 1 mL of the solution made using the reaction mixture following the CPE

experiment. 100 µL was removed from the bacterial culture are regular intervals and subsequently analyzed using GC and High Performance Liquid Chromatography (HPLC).

3.3.9 GC analysis

Concentrations of isobutanol were analyzed by GC–FID. The GC system is a GC-2010 with an AOC-20 S auto sampler and AOC-20i auto injector (Shimadzu). The column used was a DB-WAX capillary column (30 m length, 0.32 mm diameter and 0.5 µm film thickness; Agilent Technologies). The GC oven temperature was held at 225 °C, and the FID was held at 330 °C. The injection volume was 0.5 µl, injected at a 15:1 split ratio. Helium was used as the carrier gas. Retention times from samples were compared with standards.

To prepare samples for GC analysis, 1 ml of cell culture was centrifuged at 20,000 g for 10 min at 25 °C. 100 µL of culture supernatant was diluted with 900 µL MilliQ water.

3.3.10 HPLC analysis

Concentrations of glucose and formate were analyzed by 20A HPLC (Shimadzu) equipped with a differential refractive detector 10A and an Aminex fast acid analysis column (Bio-Rad). The mobile phase was 5 mM of H_2SO_4, maintained at a flow rate of 0.6 ml min^{-1} at 65 °C for 12.5 min.

To prepare bacterial samples for HPLC analysis, 1 mL of cell culture was centrifuged at 20,000 g for 10 min at 25°C. 10 µL of filtered culture supernatant or of the liquid phase from CPE experiments was injected into the column for analysis.

3.3.11 Stable isotype tracer analysis

To prepare samples for metabolomics analysis, 0.5 mL of cell cultures were frozen in liquid nitrogen and stored at -80°C until analysis. Metabolite extraction, derivatization and analysis by GC-TOF-MS was carried out by the West Coast Metabolomics Center at University of California, Davis.

3.4 Results and Discussion

3.4.1 Isobutanol Production in Reductive Glycine Pathway Strain

In the previous study, the RGP was constructed in the *E. coli* strain, YT151 (Strain 1, **Table 3.1**)[13]. The RGP containing a formate assimilation pathway constructed from three genes from *Clostridium ljungdahlii*[19] (hereafter *Cl*): a formate-tetrahydrofolate ligase encoded by *fhs*[20], methenyl-THF cyclohydrolase encoded by *fchA*[21], and methylene-THF dehydrogenase encoded by *folD*[22] was combined with the expression of the glycine cleavage system in the reverse direction (rGCS)[13,23] (pYT100, **Table 3.S1**). The RGP was shown to function in *E. coli*; metabolomics data from this study showed that labelled formate and CO_2 were assimilated into L-alanine via pyruvate[13]. The isobutanol production plasmid (pAL603, **Table 3.S1**)[24] was introduced to Strain 1. The isobutanol production pathway was constructed from five genes: an acetolactate synthase from *Bacillus subtilis* encoded by *alsS*[25], a ketol-acid reductoisomerase and a dihydroxy-acid dehydratase from *E. coli* encoded by *ilvC* and *ilvD*[17], respectively, a ketoacid decarboxylase from *Lactococcus lactis* encoded by *kivD*[26], and an alcohol dehydrogenase from *Lactococcus lactis* encoded by *adhA*[27]. This isobutanol pathway was shown to be efficient at converting pyruvate into isobutanol in previous studies[17,24] (**Fig. 3.1**). The production of isobutanol with and without the RGP plasmids (pYT100 and pAL2236, **Table 3.S1**) was compared in M9P with 50 mM $NaHCO_3$ and 0.2 g L^{-1} formate. Strain 1 with the RGP was not able to produce isobutanol, while Strain 1 without the RGP produced 1.75 g L^{-1} isobutanol in 48 h (**Fig. 3.S1a**). The results suggested that there is metabolic imbalance preventing the synthesis of isobutanol. We hypothesized that intracellular NADH/NADPH levels were not sufficient to provide the energetic requirements for both pathways. Thus, the gene encoding for $NADP^+$-dependent formate dehydrogenase (Fdh) from *Arabidopsis thaliana* (hear after *At*)[12] was integrated into safe site 9 (SS9)[28] in the chromosome of Strain 1, generating Strain 2 (**Table 3.1**). Strain 2 with the isobutanol production and the RGP plasmids was able to produce isobutanol at 2.23 g L^{-1}, suggesting that additional reducing equivalents are required to produce isobutanol with the RGP. These three strains produced formate in the first day and consumed formate

slightly in the second day (**Fig. 3.S1b**). The results suggested inefficiency in the formate
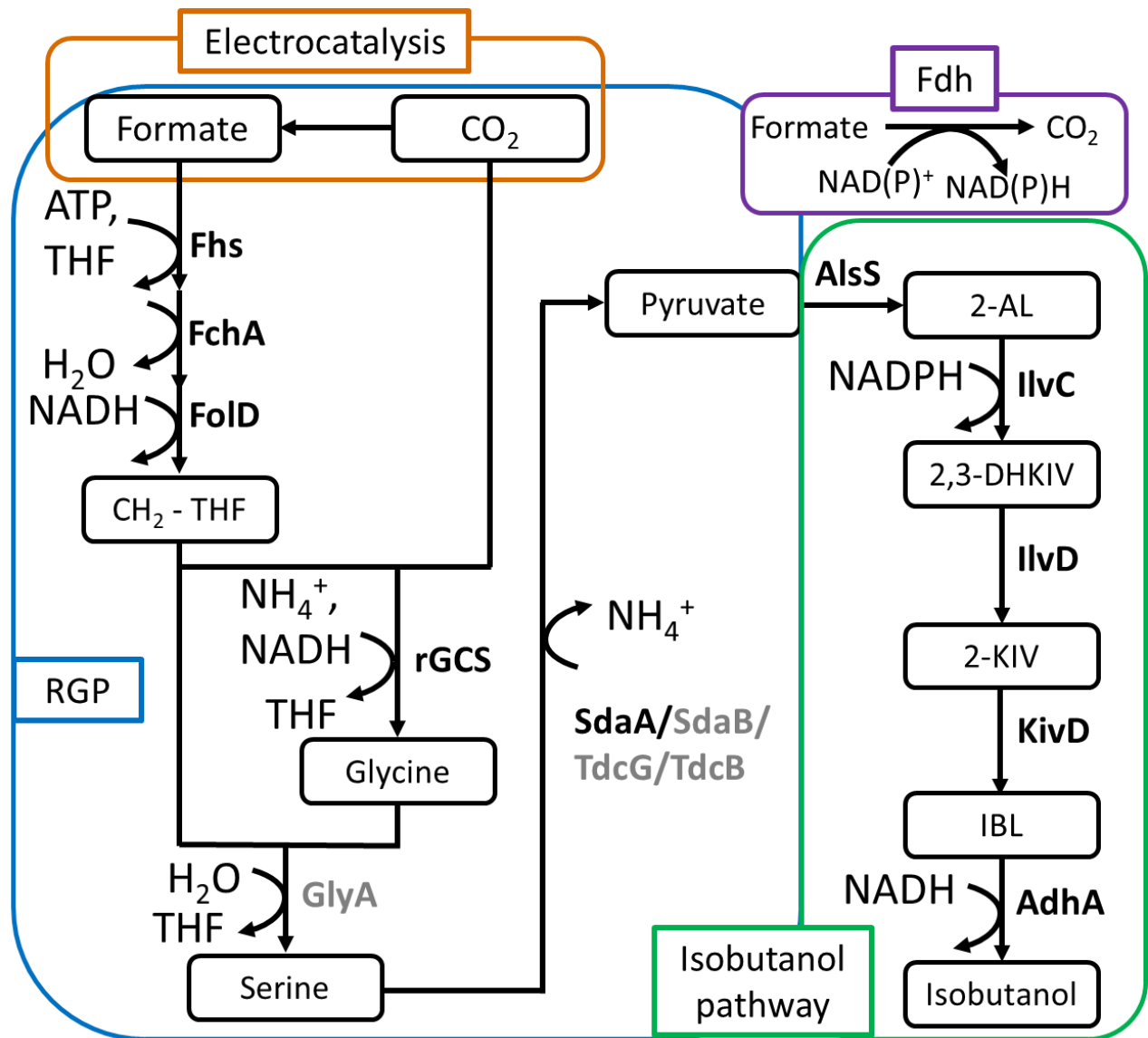
assimilation of the strains.

Figure 3.1 Isobutanol production pathway in electrical-biological hybrid system.

CO_2 is electrocatalytically reduced to formate. Formate is assimilated to methylene-tetrahydrofolate (CH_2-THF). The excess CO_2 is sequestered by the glycine cleavage system acting in the reverse direction to combine with the CH_2-THF to synthesize glycine. Abbreviations: 2-AL (2-acetolactate), 2,3-DHKIV (2,3-dihydroxyketoisovalerate), 2-KIV (2-ketoisovalerate), IBL (Isobutyraldehyde), RGP (Reductive glycine pathway). Enzymes in black are overexpressed in the engineered strain. Enzymes in gray are expressed at native levels.

3.4.2 Engineering Isobutanol Strain with Reductive Glycine Pathway

To improve isobutanol production, this system was moved into AL17 which was designed for isobutanol production (Strain 3, **Table 3.1**)[17]. This strain possesses several gene deletions that were generated to direct flux away from other fermentation products[17,29]. Particularly, the deletion of *pflB*, which encodes for a pyruvate formate-lyase eliminated formate production in Strain 3[29]. The deletion of *pflB* was also used to improve the pyruvate forming flux from formate and CO_2 of an *E. coli* strain by preventing the production of formate from intracellular pyruvate[12]. Notably, Strain 3 harboring the isobutanol production and the RGP plasmids was able to produce 3.19 g L^{-1} isobutanol without the addition of Fdh indicating that the genomic modifications present in AL17 allow for more efficient production of isobutanol (**Fig. 3.2a**). Strain 3 consumed formate, indicating that the formate assimilation inefficiencies present in earlier strains (**Fig. 3.S1b**) were overcome in this strain. In Strain 3, L-serine can be produced by the RGP and the native L-serine biosynthetic pathway. We hypothesized that the increased L-serine pool decreases the efficiency of the RGP. The *serA* gene was deleted from the chromosome of Strain 3, generating Strain 4 (**Table 3.1**). The titer and the yield of isobutanol production were improved in Strain 4 compared to Strain 3 (**Fig. 3.2a**), suggesting that the carbon being assimilated by the RGP is more efficient in aiding the production of isobutanol when glucose metabolism is cut off from L-serine synthesis. This result could be due to flux, by necessity, increasing towards L-serine from formate and CO_2 when serine is unable to be synthesized from glucose.

a)
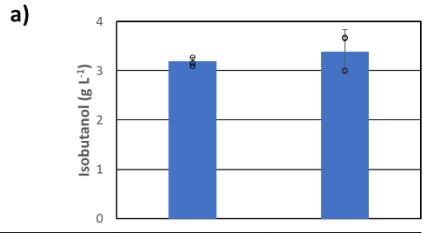
Strain No.	3	4
serA	+	-
Formate Consumed (g L^{-1})	0.62 ± 0.03	0.51 ± 0.04
Yield (g g^{-1})	0.34 ± 0.01	0.37 ± 0.04

b)
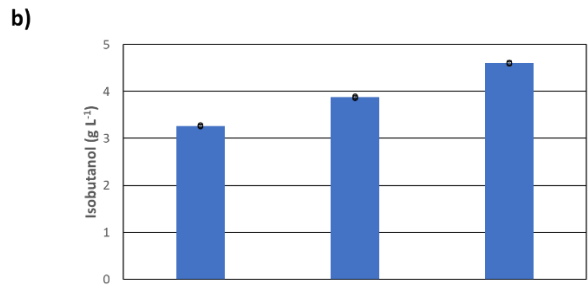
Strain No.	5	6	7
Fdh	At	Cb	Sc
Formate Consumed (g L^{-1})	1.4 ± 0.06	2.5 ± 0.1	1.8 ± 0.2
Yield (g g^{-1})	0.29 ± 0.01	0.35 ± 0.03	0.22 ± 0.01

c)
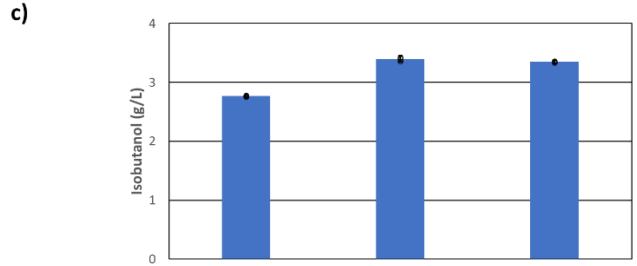
Strain No.	4	6	8
Formate Consumed (g L^{-1})	0.05 ± 0.01	5.5 ± 0.6	5.0 ± 0.9
Yield (g g^{-1})	0.37 ± 0.06	0.39 ± 0.02	0.43 ± 0.01
OD$_{600}$	33.1 ± 0.5	33.3 ± 0.4	33.8 ± 0.5
Productivity (g L^{-1} hr^{-1})	2.8 ± 0.01	3.4 ± 0.02	3.3 ± 0.01

Figure 3.2 Isobutanol production in AL17 Strains

a) Isobutanol production in Strains 3 and 4 with the RGP after 2 days. Cultured in M9P with 10 g L^{-1} glucose 3 g L^{-1} formate, 50 mM sodium bicarbonate with 1 mM IPTG and 10 µg L^{-1} aTc. **b)** Isobutanol production after 2 days in Strains 5 through 7 harboring *fdh* variants. Cultured in M9P with 20 g L^{-1} glucose 3 g L^{-1} formate, 50 mM sodium bicarbonate with 1mM IPTG and 10 µg L^{-1} aTc. **c)** High density isobutanol production in Strains 4, 6 and 8. Isobutanol titer reported after 1 h in Strains 4, 6 and 8. Cultured in M9P with 10 g L^{-1} glucose, 10 g L^{-1} formate, 50 mM

sodium bicarbonate with 1 mM IPTG and 10 µg L^{-1} aTc. Yield is reported as gram isobutanol produced per gram glucose consumed (g g^{-1}). Errors indicate s.d. (n = 3 biological replicates).

3.4.3 Formate Dehydrogenase Screening

The expression of *fdh* (*At*) improved isobutanol production (**Fig. 3.S1a**). We screened two other variants of formate dehydrogenase to determine if there was a similar benefit to either production or yield. The Fdhs from *Candida boidinii* (hereafter *Cb*) and *Saccharomyces cerevisiae* (hereafter *Sc*) are NAD$^+$-dependent[30,31], while Fdh (*At*) is NADP$^+$-dependent. The corresponding gene was cloned under the constitutive promoter P_{BBa_J23119} and integrated into SS9, generating Strains 5 (*At*), 6 (*Cb*), and 7 (*Sc*) (**Table 3.1**). Strain 6 consumed the most formate and produced isobutanol with the best yield of the three strains (**Fig. 3.2b**). Although Strain 7 produced more isobutanol than Strain 6, the yield was the worst of the three strains (**Fig. 3.2b**). Thus, we proceeded with Strain 6 for future experiments.

3.4.4 Strain and Fermentation Optimization

It has been shown that replacing the native promoter of *sdaA* (P_{sdaA}) to P_{LlacO1}[34] enhanced the conversion of formate and CO_2 to pyruvate in the RGP[13]. The gene *sdaA* encodes for an endogenous L-serine deaminase which catalyzes the conversion of L-serine to pyruvate and was previously determined to be the optimal target for overexpression to enhance growth on L-serine[13]. To test if the promoter replacement improves isobutanol production, P_{sdaA} was replaced with P_{LlacO1} in Strain 6, generating Strain 8 (**Table 3.1**). This modification improved the yield (**Fig. 3.S2**), demonstrating that more carbon from the RGP was being incorporated into isobutanol.

To reduce the impact of cell growth on isobutanol production, a high density (Optical Density at 600 nm (OD_{600}) > 30) was conducted to elucidate the ability of the engineered strain to act as a whole cell non-growing biocatalyst[35], capable of converting RGP substrates into isobutanol. In this experiment an induced culture of the strains was grown to an approximate OD_{600} of 1 and subsequently centrifuged and resuspended in 1/50th the volume of fresh experimental media generating a dense non-growing slurry of *E. coli*. Strains 4, 6 and 8 were compared to elucidate the effects of expressing both *fdh* and *sdaA* on isobutanol production. Strains 6 and 8 produced 3.48 and 3.35 g L^{-1} isobutanol respectively, showing that a non-growing

biocatalytic expression system is beneficial for overall chemical production (**Fig. 3.2c**). Strain 8 performed the best with respect to yield, achieving a yield of 0.43 g isobutanol per g glucose (g g^{-1}) which is 101% of the theoretical max yield of isobutanol produced from glucose alone (0.41 g g^{-1}). Achieving above 100% of theoretical maximum yield indicates that the genomic modifications in this strain facilitate the incorporation of formate and CO_2 into isobutanol. An additional experiment was carried out under identical methodology where Strain 8 was cultivated with and without formate and bicarbonate (**Fig. 3.3**). Without formate and/or bicarbonate present in the media resulted in lower yield when compared to the condition where both bicarbonate and formate were present, indicating that formate and bicarbonate aid in the production of isobutanol in this strain (**Fig. 3.3**).
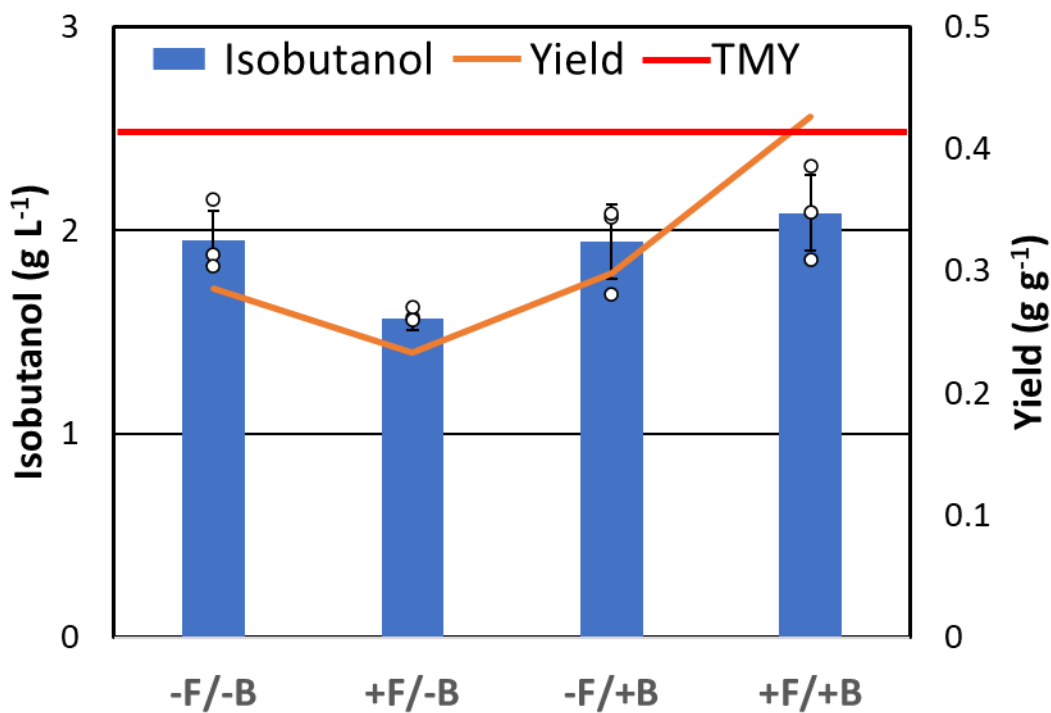
Figure 3.3 High density isobutanol titer and yield in Strain 8

Isobutanol titer after 1 h in Strain 8. Cultured in M9P with 10 g L^{-1} glucose, with or without 3 g L^{-1} formate and 50 mM sodium bicarbonate. Induced with 1 mM IPTG and 10 µg L^{-1} aTc. Yield is reported as gram isobutanol produced per gram glucose consumed (g g^{-1}). The theoretical maximum yield (TMY) is 0.41 g g^{-1}. Errors indicate s.d. (n = 3 biological replicates).

A stable isotype tracer analysis was performed to ensure that the single carbon substrates were indeed incorporated into central metabolism and into the isobutanol production pathway wherein ^{13}C-labeled formate and bicarbonate were fed to Strain 8 under low density conditions. The carbon at position 1 and position 2 in glycine came from CO_2 and formate, respectively (**Fig. 3.4**)[23]. When unlabeled bicarbonate and formate were used, there was no enrichment of M1 and M2 with relative abundance of these ions matching data from the NIST library standards (**Fig. 3.4**). When labeled bicarbonate and formate were used, the M1 and M2 were twice as abundant, indicating that the RGP is functioning as intended (**Fig. 3.4**). The intermediate 2-ketoisovalerate was also analyzed using this stable isotope tracer analysis and it was determined that M1 was enriched by 4.3%, indicating that some of the formate and bicarbonate is flowing through the RGP towards isobutanol. Since the RGP connects to pyruvate much of the labeled formate and bicarbonate is likely flowing to other metabolites unrelated to isobutanol production and further study is required to mitigate this flux away from the product of interest.
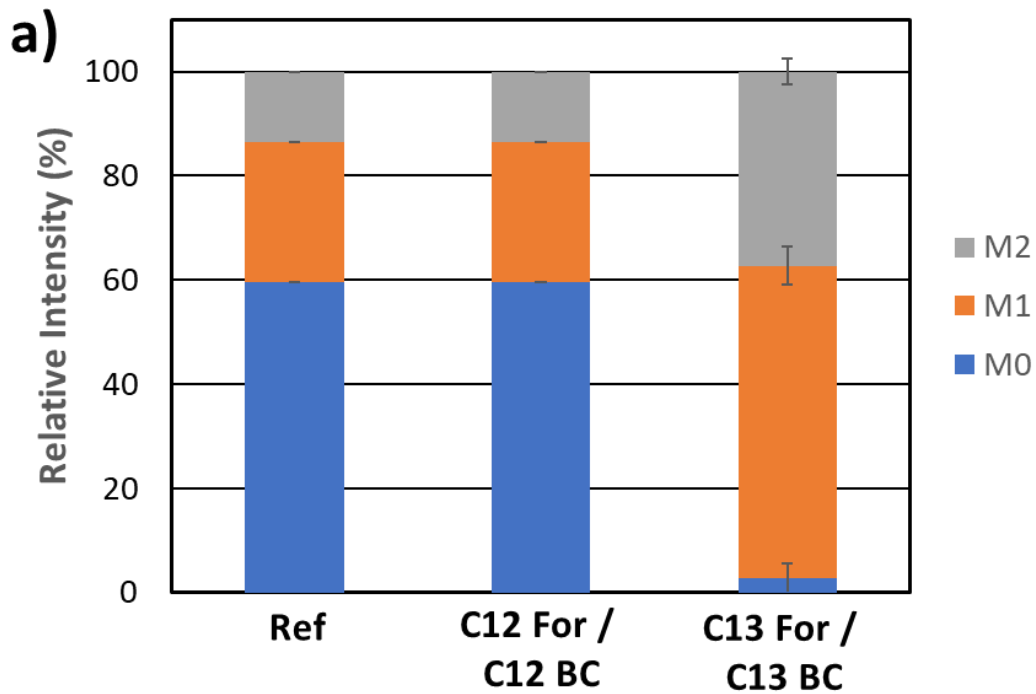
Figure 3.4 ^{13}C-labeling analysis

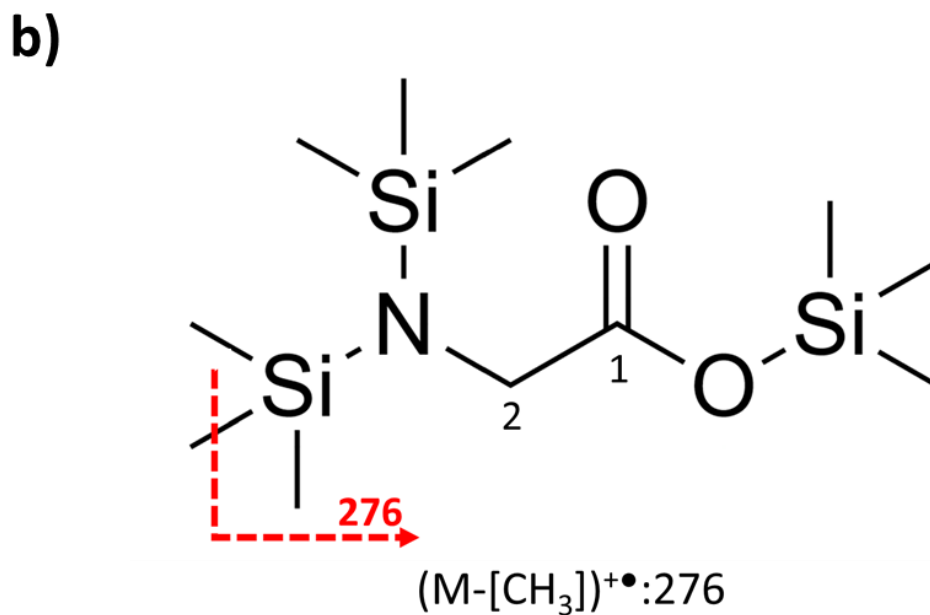**a)** Relative intensity of m/z = 276 (M0), 277 (M1), and 278 (M2) in the glycine produced in Strain 8. Cells were cultured using unlabeled formate and bicarbonate (12For/12BC) or ^{13}C formate and ^{13}C bicarbonate (13For/13BC). Ref indicates data from the NIST library of standards. Errors indicate s.d. (n = 3 biological replicates). **b)** Structure of glycine derivatized with MeOX MSTFA. If

the pathway is active, position 1 and position 2 would be derived from CO_2 and formate, respectively.

To further demonstrate the ability of this engineered strain to leverage formate and CO_2 to produce isobutanol an additional high-density experiment was carried out wherein the only carbon sources were formate and CO_2. Isobutanol production was observed, suggesting that the engineered strain can integrate single carbon substrates into isobutanol (**Fig. 3.S3**).

3.4.5 Coupling Electrocatalysis with Engineered Strain

A series of controlled potential electrolysis (CPE) experiments were performed using the catalyst $[Na(diglyme)_2][Fe_4N(CO)_{12}]$ (**Table 3.2, Fig. 3.S4**). The applied potential was selected by performing a series of CPE experiments over the applied potential range of −1.12 - −1.24 V to determine where formate production rate and selectivity over H_2 production would be highest (**Fig. 3.S5**). A potential of −1.2 V was selected based on those experiments which were run over 1 h each. For production of formate to support isobutanol production the CPE experiments were run over 20 h and the cathode chamber was purged every 1 h with humidified CO_2. Control blank CPE experiments with no added catalyst show significantly lower amounts of charge passed during 20 h CPE experiment (**Table 3.2**). We also ran a CPE experiment with the used glassy carbon working electrode (rinse test) to ensure that deposition of catalyst or other materials was not responsible for the catalysis: no formate was detected from that experiment. The stability and homogeneous nature of the catalyst was tested before and after CPE experiments by recording infrared spectra of CPE solution to make sure that the catalyst is still present in solution. Peaks characteristic of $[Na(diglyme)_2][Fe_4N(CO)_{12}]$ were observed at 2015 and 1989 cm^{-1} and were present before and after CPE experiments indicating that the catalyst was intact for each trial (**Fig. 3.S6**).

Table 3.2 CPE results for control experiments and experiments with catalyst

Experiments	Time/h	Charge (C)	FE(%)	Formate Yield (g L^{-1})
Blank (No Catalyst)	22	160	67% (H$_2$)	Not detected
0.5 mM Catalyst	22	354	84(5) (HCOO$^-$)	4.2 (0.3)
Rinse test	22	180	60% (H$_2$)	Not detected

Applied potential (E_{app}) for CPEs is -1.2 V vs SCE, Detection limit of formate by HPLC is 0.05 g L^{-1}, FE is Faradic Efficiencies for H$_2$ and Formate. High FE for H$_2$ in blank and rinse test are the result of the ability of buffering anions to donate hydrogen directly to the electrode surface.

In CPE experiments, 4.2 g L^{-1} formate was produced after 21 hours using 0.5 mM catalyst (**Table 3.2**) which demonstrates the ability of this catalyst to convert CO$_2$ efficiently into formate. This formate production rate of 0.2 g L^{-1} h^{-1} is relatively slow compared with published work[11] that employs gas diffusion electrodes and heterogeneous electrocatalysts such as tin, bismuth, or lead and operate at > 10 g L^{-1} h^{-1}. However, here we have used a traditional H-cell set up which has slow diffusion kinetics and low solubility of CO$_2$ in the aqueous buffer, and this choice of the electrochemical cell could be modified in future work to access faster formate production rates[36,37]. Formate is the most readily synthesized chemical from CO$_2$ using electrocatalytic methods[6]. The use of an Earth-abundant material such as iron that can continue to produce formate for long periods (> 20 h) also represents one of the more renewable and sustainable methodologies to sequester carbon. To demonstrate the electrocatalytically produced formate could be upcycled into other valuable chemicals, we cultivated Strain 8 using the CPE reaction mixture, supplemented with 50 mM NaHCO$_3$ and 10 g L^{-1} glucose (**Fig. 3.5**). The engineered *E. coli* consumed the formate produced electrocatalytically at a rate of 1.84 g L^{-1} h^{-1} (**Fig. 3.5b**) under high density conditions during the production of isobutanol without the need to purify formate away from the reaction mixture. Strain 8 could produce isobutanol with a high productivity (2.53 g L^{-1} h^{-1}) using an electrocatalytic reaction mixture (**Fig. 3.5c**). This is in contrast to other hybrid systems reported where the produced compound must be purified away from toxic compounds prior to being used as a substrate for an engineered

microorganism[38,39]. This finding demonstrates that efficient electrocatalytic reduction of CO_2 can be coupled to biochemical production to convert formate into the valuable chemical commodity isobutanol. This study represents a significant advance towards sustainably producing chemicals from CO_2.
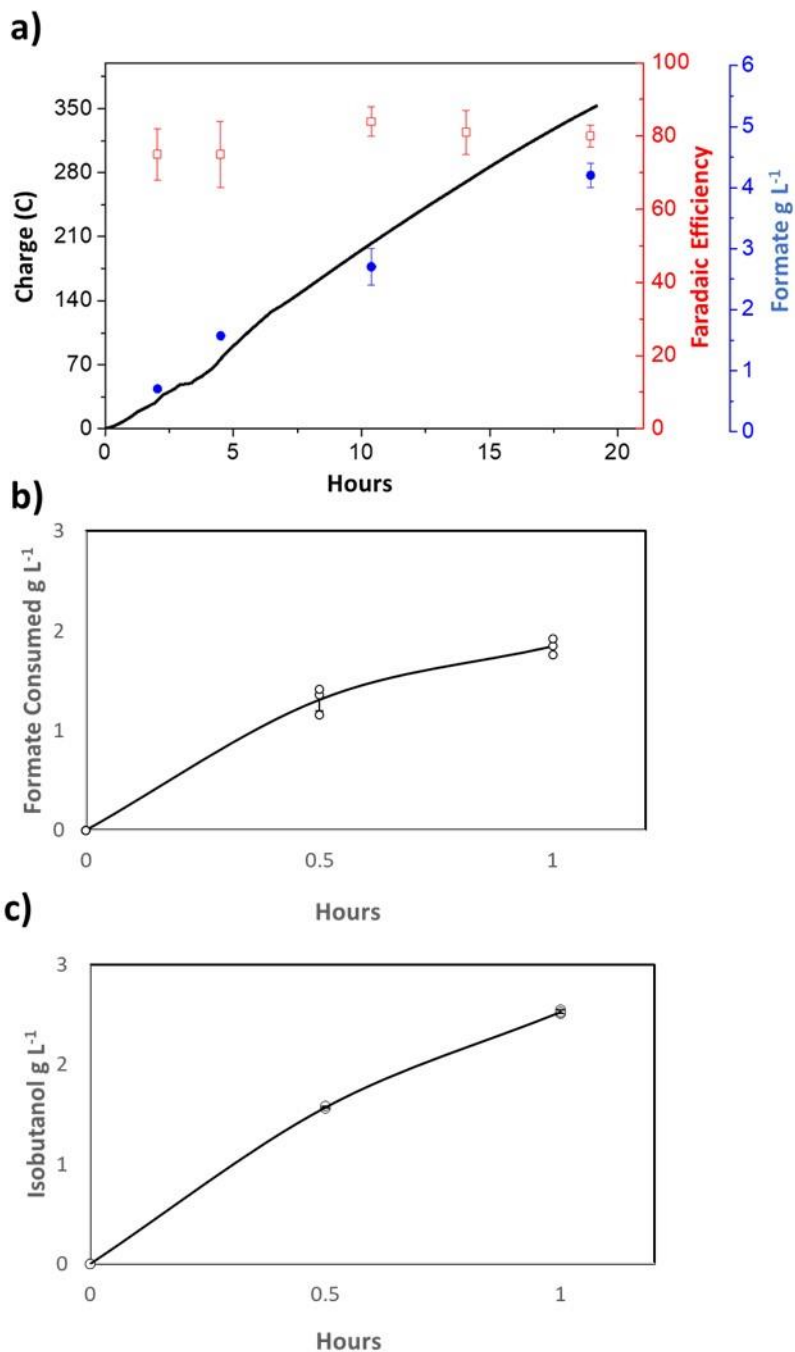
Figure 3.5 Enriched electrochemical broth used for isobutanol synthesis

a) Plot of [formate] vs time (blue), Faradic Efficiency vs time (red) and plot of Current density vs time (black) CPE experiment performed with 0.5 mM catalyst in 0.1 M phosphate buffered aqueous solution at pH 7.2. b) *E. coli* formate consumption of electrocatalytically produced

formate. c) Isobutanol production in *E. coli* using electrochemical broth. Error bars indicate s.d. (n = 3 technical (a) and biological (b & c) replicates).

3.5 Conclusion

Here we have shown that a non-RuBisCO based CO_2 fixation method, the RGP, can be efficiently used to bolster the production of a value-added chemical commodity. By creating a hybrid system, we can link renewable sources of electricity with the production of an energy dense chemical commodity. This electrical-biological hybrid system has several benefits over electrochemical or biological production alone. The production of formate from CO_2 by electrochemical methods has established a more rapid method of carbon sequestration than carbon capture by photosynthesis. The use of formate as a feedstock for *E. coli* has led to an efficient electrocatalysis platform for the production of isobutanol, a stable, high-energy and valuable chemical.

The RGP is a promising platform for CO_2 assimilation in microbes. Additionally, there are several reasons that both *E. coli* and the RGP are promising candidates for future optimization of a hybrid electrical-biological system for CO_2 fixation. First, *E. coli* has been shown to be a viable host for the RGP that requires minimal metabolic perturbations in order to establish a CO_2 fixing strain. Second, two-thirds of the carbons in the RGP come from formate, which can be readily synthesized in an electrocatalytic setting. Third, *E. coli* is a well-established host organism, allowing us to balance various parameters of metabolism and generate metabolic changes quickly as was done when screening and installing formate dehydrogenase.

As renewable sources of energy production become more widespread, a surplus of electricity is generated during the day, resulting in excess unused energy. By using this excess to electrocatalytically capture CO_2 we can improve the environmental impact of renewable energy generation. By combining electrocatalytic systems with microbial production platforms, we can link efficient carbon capture methods with the bio-based production of valuable chemical commodities. Additionally, by showing that *E. coli* can incorporate electrocatalytically produced formate that was generated using a more efficient catalyst into central metabolism, we have shown that as these fields continue to grow, advances in either field can add an overall benefit to the sustainability and efficiency of hybrid systems.

3.6 References

(1)   Chen, L.; Msigwa, G.; Yang, M.; Osman, A. I.; Fawzy, S.; Rooney, D. W.; Yap, P. S. *Strategies to Achieve a Carbon Neutral Society: A Review*; Springer International Publishing, 2022; Vol. 20. https://doi.org/10.1007/s10311-022-01435-8.

(2)   Case, A. E.; Atsumi, S. Cyanobacterial Chemical Production. *J Biotechnol* **2016**, *231*, 106–114. https://doi.org/10.1016/j.jbiotec.2016.05.023.

(3)   Barecka, M. H.; Ager, J. W.; Lapkin, A. A. Carbon Neutral Manufacturing via On-Site CO2 Recycling. *iScience* **2021**, *24* (6), 102514. https://doi.org/10.1016/j.isci.2021.102514.

(4)   Lynd, L. R.; Cushman, J. H.; Nichols, R. J.; Wyman, C. E. Fuel Ethanol from Cellulosic Biomass. *Science* **1991**, *251* (4999), 1318–1323. https://doi.org/10.1126/science.251.4999.1318.

(5)   Cheng, M.-H.; Huang, H.; Dien, B. S.; Singh, V. The Costs of Sugar Production from Different Feedstocks and Processing Technologies. *Biofuels Bioprod Biorefin* **2019**, *13* (3), 723–739. https://doi.org/https://doi.org/10.1002/bbb.1976.

(6)   Taheri, A.; Thompson, E. J.; Fettinger, J. C.; Berben, L. A. An Iron Electrocatalyst for Selective Reduction of CO_2 to Formate in Water: Including Thermochemical Insights. *ACS Catal* **2015**, *5* (12), 7140–7151. https://doi.org/10.1021/acscatal.5b01708.

(7)   Goeppert, A.; Czaun, M.; Jones, J. P.; Surya Prakash, G. K.; Olah, G. A. Recycling of Carbon Dioxide to Methanol and Derived Products-Closing the Loop. *Chem Soc Rev* **2014**, *43* (23), 7995–8048. https://doi.org/10.1039/c4cs00122b.

(8)   Nitopi, S.; Bertheussen, E.; Scott, S. B.; Liu, X.; Engstfeld, A. K.; Horch, S.; Seger, B.; Stephens, I. E. L.; Chan, K.; Hahn, C.; Nørskov, J. K.; Jaramillo, T. F.; Chorkendorff, I. Progress and Perspectives of Electrochemical CO_2 Reduction on Copper in Aqueous Electrolyte. *Chem Rev* **2019**, *119* (12), 7610–7672. https://doi.org/10.1021/acs.chemrev.8b00705.

(9)   Chen, H.; Dong, F.; Minteer, S. D. The Progress and Outlook of Bioelectrocatalysis for the Production of Chemicals, Fuels and Materials. *Nat Catal* **2020**, *3* (3), 225–244. https://doi.org/10.1038/s41929-019-0408-2.

(10)   Loewen, N. D.; Neelakantan, T. V; Berben, L. A. Renewable Formate from C-H Bond Formation with CO2: Using Iron Carbonyl Clusters as Electrocatalysts. *Acc Chem Res* **2017**, *50* (9), 2362–2370. https://doi.org/10.1021/acs.accounts.7b00302.

(11)   Fernández-Caso, K.; Díaz-Sainz, G.; Alvarez-Guerra, M.; Irabien, A. Electroreduction of CO_2: Advances in the Continuous Production of Formic Acid and Formate. *ACS Energy Lett* **2023**, *8* (4), 1992–2024. https://doi.org/10.1021/acsenergylett.3c00489.

(12)   Bang, J.; Hwang, C. H.; Ahn, J. H.; Lee, J. A.; Lee, S. Y. Escherichia coli Is Engineered to Grow on CO_2 and Formic Acid. *Nat Microbiol* **2020**, *5* (12), 1459–1463. https://doi.org/10.1038/s41564-020-00793-9.

(13)   Tashiro, Y.; Hirano, S.; Matson, M. M.; Atsumi, S.; Kondo, A. Electrical-Biological Hybrid System for CO_2 Reduction. *Metab Eng* **2018**, *47*, 211–218. https://doi.org/10.1016/j.ymben.2018.03.015.

(14)   Wang, W. C.; Tao, L. Bio-Jet Fuel Conversion Technologies. *Renew Sustain Energy Rev* **2016**, *53*, 801–822. https://doi.org/10.1016/j.rser.2015.09.016.

(15)   Volanti, M.; Cespi, D.; Passarini, F.; Neri, E.; Cavani, F.; Mizsey, P.; Fozer, D. Terephthalic Acid from Renewable Sources: Early-Stage Sustainability Analysis of a Bio-PET Precursor. *Green Chemistry* **2019**, *21* (4), 885–896. https://doi.org/10.1039/c8gc03666g.

(16)   Geleynse, S.; Brandt, K.; Garcia-Perez, M.; Wolcott, M.; Zhang, X. The Alcohol-to-Jet Conversion Pathway for Drop-In Biofuels: Techno-Economic Evaluation. *ChemSusChem* **2018**, *11* (21), 3728–3741. https://doi.org/10.1002/cssc.201801690.

(17)   Atsumi, S.; Hanai, T.; Liao, J. C. Non-Fermentative Pathways for Synthesis of Branched-Chain Higher Alcohols as Biofuels. *Nature* **2008**, *451* (7174), 86–89. https://doi.org/10.1038/nature06450.

(18)   Li, H.; Opgenorth, P. H.; Wernick, D. G.; Rogers, S.; Wu, T. Y.; Higashide, W.; Malati, P.; Huo, Y. X.; Cho, K. M.; Liao, J. C. Integrated Electromicrobial Conversion of CO_2 to Higher Alcohols. *Science* **2012**, *335* (6076), 1596. https://doi.org/10.1126/science.1217643.

(19)   Köpke, M.; Held, C.; Hujer, S.; Liesegang, H.; Wiezer, A.; Wollherr, A.; Ehrenreich, A.; Liebl, W.; Gottschalk, G.; Dürre, P. Clostridium Ljungdahlii Represents a Microbial Production Platform Based on Syngas. *Proc Natl Acad Sci U S A* **2010**, *107* (29), 13087–13092. https://doi.org/10.1073/pnas.1004716107.

(20)   Paukert, J. L.; Rabinowitz, J. C. [85] Formyl-Methenyl-Methylenetetrahydrofolate Synthetase: A Multifunctional Protein in Eukaryotic Folate Metabolism. *Methods Enzymol* **1980**, *66* (C), 616–626. https://doi.org/10.1016/0076-6879(80)66515-X.

(21)   Clark, J.; Ljungdahl, L. G. Purification and Properties of 5,10-Methenyltetrahydrofolate Cyclohydrolase from Clostridium Formicoaceticum. *J Biol Chem* **1982**, *257* (7), 3833–3836. https://doi.org/10.1016/s0021-9258(18)34857-9.

(22)   Suarez de Mata, Z.; Rabinowitz, J. C. Formyl-Methenyl-Methylenetetrahydrofolate Synthetase from Yeast. Biochemical Characterization of the Protein from an ADE3 Mutant Lacking the Formyltetrahydrofolate Synthetase Function. *J of BiolChem* **1980**, *255* (6), 2569–2577. https://doi.org/10.1016/s0021-9258(19)85930-6.

(23)   Kikuchi, G.; Motokawa, Y.; Yoshida, T.; Hiraga, K. Glycine Cleavage System. *Proc Natl Acad Sci U S A* **2008**, *84* (10), 246–263. https://doi.org/10.2183/pjab/84.246.

(24)   Desai, S. H.; Rabinovitch-Deere, C. A.; Tashiro, Y.; Atsumi, S. Isobutanol Production from Cellobiose in Escherichia coli. *Appl Microbiol Biotechnol* **2014**, *98* (8), 3727–3736. https://doi.org/10.1007/s00253-013-5504-7.

(25)   Gollop, N.; Damri, B.; Chipman, D. M.; Barak, Z. Physiological Implications of the Substrate Specificities of Acetohydroxy Acid Synthases from Varied Organisms. *J Bacteriol* **1990**, *172* (6), 3444–3449. https://doi.org/10.1128/jb.172.6.3444-3449.1990.

(26)   De La Plaza, M.; Fernández De Palencia, P.; Peláez, C.; Requena, T. Biochemical and Molecular Characterization of α-Ketoisovalerate Decarboxylase, an Enzyme Involved in the Formation of Aldehydes from Amino Acids by Lactococcus Lactis. *FEMS Microbiol Lett* **2004**, *238* (2), 367–374. https://doi.org/10.1016/j.femsle.2004.07.057.

(27)   Bolotin, A.; Wincker, P.; Mauger, S.; Jaillon, O.; Malarme, K.; Weissenbach, J.; Ehrlich, S. D.; Sorokin, A. The Complete Genome Sequence of the Lactic Acid Bacterium Lactococcus Lactis Ssp. Lactis IL1403 . *Genome Res* **2001**, *11* (5), 731–753. https://doi.org/10.1101/gr.169701.

(28)   Bassalo, M. C.; Garst, A. D.; Halweg-Edwards, A. L.; Grau, W. C.; Domaille, D. W.; Mutalik, V. K.; Arkin, A. P.; Gill, R. T. Rapid and Efficient One-Step Metabolic Pathway Integration in E. coli. *ACS Synth Biol* **2016**, *5* (7), 561–568. https://doi.org/10.1021/acssynbio.5b00187.

(29)   Atsumi, S.; Cann, A. F.; Connor, M. R.; Shen, C. R.; Smith, K. M.; Brynildsen, M. P.; Chou, K. J. Y.; Hanai, T.; Liao, J. C. Metabolic Engineering of Escherichia coli for 1-Butanol Production. *Metab Eng* **2008**, *10* (6), 305–311. https://doi.org/10.1016/j.ymben.2007.08.003.

(30)   Guo, Q.; Gakhar, L.; Wickersham, K.; Francis, K.; Vardi-Kilshtain, A.; Major, D. T.; Cheatum, C. M.; Kohen, A. Structural and Kinetic Studies of Formate Dehydrogenase from Candida Boidinii. *Biochemistry* **2016**, *55* (19), 2760–2771. https://doi.org/10.1021/acs.biochem.6b00181.

(31)   Overkamp, K. M.; Ktter, P.; Van Hoek, R. Der; Schoondermark-Stolk, S.; Luttik, M. A. H.; Van Dijken, J. P.; Pronk, J. T. Functional Analysis of Structural Genes for NAD+ -Dependent Formate Dehydrogenase in Saccharomyces Cerevisiae. *Yeast* **2002**, *19* (6), 509–520. https://doi.org/10.1002/yea.856.

(32)   Jeong, J. Y.; Yim, H. S.; Ryu, J. Y.; Lee, H. S.; Lee, J. H.; Seen, D. S.; Kang, S. G. One-Step Sequence-and Ligation-Independent Cloning as a Rapid and Versatile Cloning Method for Functional Genomics Studies. *Appl Environ Microbiol* **2012**, *78* (15), 5440–5443. https://doi.org/10.1128/AEM.00844-12.

(33)   Lutz, R.; Bujard, H. Independent and Tight Regulation of Transcriptional Units in Escherichia coli via the LacR/O, the TetR/O and AraC/I1-I2 Regulatory Elements. *Nucleic Acids Res* **1997**, *25* (6), 1203–1210. https://doi.org/10.1093/nar/25.6.1203.

(34)   Shiloach, J.; Fass, R. Growing E. coli to High Cell Density - A Historical Perspective on Method Development. *Biotechnol Adv* **2005**, *23* (5), 345–357. https://doi.org/10.1016/j.biotechadv.2005.04.004.

(35)   Alinejad, S.; Quinson, J.; Wiberg, G. K. H.; Schlegel, N.; Zhang, D.; Li, Y.; Reichenberger, S.; Barcikowski, S.; Arenz, M. Electrochemical Reduction of CO_2 on Au Electrocatalysts in a Zero-Gap, Half-Cell Gas Diffusion Electrode Setup: A Systematic Performance Evaluation and Comparison to an H-Cell Setup. *ChemElectroChem* **2022**, *9* (12), 1–11. https://doi.org/10.1002/celc.202200341.

(36)   Hernandez-Aldave, S.; Andreoli, E. Fundamentals of Gas Diffusion Electrodes and Electrolysers for Carbon Dioxide Utilisation: Challenges and Opportunities. *Catalysts*. 2020, pp 1–34. https://doi.org/10.3390/CATAL10060713.

(37)   Zheng, T.; Zhang, M.; Wu, L.; Guo, S.; Liu, X.; Zhao, J.; Xue, W.; Li, J.; Liu, C.; Li, X.; Jiang, Q.; Bao, J.; Zeng, J.; Yu, T.; Xia, C. Upcycling CO_2 into Energy-Rich Long-Chain Compounds via Electrochemical and Metabolic Engineering. *Nat Catal* **2022**, *5* (5), 388–396. https://doi.org/10.1038/s41929-022-00775-6.

(38)   Orella, M. J.; Brown, S. M.; Leonard, M. E.; Román-Leshkov, Y.; Brushett, F. R. A General Technoeconomic Model for Evaluating Emerging Electrolytic Processes. *Energy Technol* **2020**, *8* (11), 1–12. https://doi.org/10.1002/ente.201900994.

(39)   Bassalo, M. C.; Garst, A. D.; Halweg-Edwards, A. L.; Grau, W. C.; Domaille, D. W.; Mutalik, V. K.; Arkin, A. P.; Gill, R. T. Rapid and Efficient One-Step Metabolic Pathway Integration in E. coli. *ACS Synth Biol* **2016**, *5* (7), 561–568. https://doi.org/10.1021/acssynbio.5b00187.

(40)   Jiang, Y.; Chen, B.; Duan, C.; Sun, B.; Yang, J.; Yang, S. Multigene Editing in the Escherichia coli Genome via the CRISPR-Cas9 System. *Appl Environ Microbiol* **2015**, *81* (7), 2506–2514. https://doi.org/10.1128/AEM.04023-14.

(41)   Xiong, A. S.; Yao, Q. H.; Peng, R. H.; Li, X.; Fan, H. Q.; Cheng, Z. M.; Li, Y. A Simple, Rapid, High-Fidelity and Cost-Effective PCR-Based Two-Step DNA Synthesis Method for Long Gene Sequences. *Nucleic Acids Res* **2004**, *32* (12). https://doi.org/10.1093/nar/gnh094.

(42)   Noviandri, I.; Brown, K. N.; Fleming, D. S.; Gulyas, P. T.; Lay, P. A.; Masters, A. F.; Phillips, L. The Decamethylferrocenium/Decamethylferrocene Redox Couple: A Superior Redox Standard to the Ferrocenium/Ferrocene Redox Couple for Studying Solvent Effects on the Thermodynamics of Electron Transfer. *J Phys Chem B* **1999**, *103* (32), 6713–6722. https://doi.org/10.1021/jp991381+.

(43)   Zhang, A.; Sun, L.; Bai, Y.; Yu, H.; McArthur, J. B.; Chen, X.; Atsumi, S. Microbial Production of Human Milk Oligosaccharide Lactodifucotetraose. *Metab Eng* **2021**, *66* (April), 12–20. https://doi.org/10.1016/j.ymben.2021.03.014.

3.7 Supplementary Information

Table 3.S1 List of plasmids used in this study

Plasmid name	Contents	Origin	Marker	Ref
pCas	P_{cas}:*cas9* P_{araB}:*Red lacI^q* P_{trc}:*sgRNA*	pMB1	KanR	addgene #62225
pTargetF	P_{J23119}:*sgRNA-pmB1*	pMB1	SpecR	addgene #62226
pYT048	P_{LlacO1}: *gcvTHP*	ColE1	AmpR	[13]
pYT100	P_{LtetO1}: *fhs-fchA-folD* (*Cl*)	p15A	KanR	[13]
pAL603	P_{LlacO1}:*kivD-adhA*, PLlacO1:*alsS-ilvCD*	ColE1	AmpR	[24]
pAL1023	P_{LtetO1}	ColA	KanR	[43]
pAL1851	*pTargetF-lacZ*	ColE1	AmpR	[43]
pAL1853	*sgRNA-ss9*	pMB1	AmpR	[43]
pAL1899	*sgRNA-serA*	pMB1	AmpR	This work
pAL2235	P_{LtetO1}: *gcvTHP*	ColA	KanR	This work
pAL2236	P_{LtetO1}: *gcvTHP*	ColA	SpecR	This work
pAL2244	P_{J23119}:*fdh* (*At,* codon optimized for *E. coli*)	pUC-GW	AmpR	Genewiz
pAL2342	*sgRNA-P$_{sdaA}$*::P_{LlacO1}	pMB1	AmpR	This work

Cl, Clostridium ljungdahlii; *At, Arabidopsis thaliana*

Table 3.S2 Oligonucleotides used in this study

Name	Sequence 5' to 3'	Plasmid(s) or fragment(s) produced	Used for sequencing
MM40	GAGTCAGTGAGCGAGGAAGC		pAL1899, pAL2342
MM60	AGTTAAATCGGTTTTAGAGCTAGAAATAGC	pAL2342	
MM62	AATATTGCGAACTAGTATTATACCTAGGACTG	pAL2342	
MM63	AGCAACTGGAGAAGTAAGACG	P_{sdaA}::P_{LlacO1} repair fragment	
MM64	TCGTCGATCTCTTTCTTGCTG	P_{sdaA}::P_{LlacO1} repair fragment	
MM274	GCGGATGCAAATCCGCACACAACATTTCAAAAGACAGGATTGGGTAAATGCGCGCCC	Δ*serA* repair fragment	
MM275	CCTGCCCGTTGATTTTCAGAGAAGGGGAATTAGTACAGCAGACGGGCGCGCATTTACCC	Δ*serA* repair fragment	
MM276	AAGCGCACCGGTTTTAGAGCTAGAAATAGC	pAL1899	
MM277	TAGCATTGGCACTAGTATTATACCTAGGAC	pAL1899	
TT530	CGATTAGCGAATACCAGTAAACGCGTGCTAGAGGCATCAAATAAAACG	pAL2235	
TT531	AAAGGAGTCTGTTGTGCCATGGTACCTTTCTCCTCTTTAATGAATTCGGTCAGTG	pAL2235	
TT532	TTAAAGAGGAGAAAGGTACCATGGCACAACAGACTCCTTTGTAC	pAL2235	
TT533	TTGATGCCTCTAGCACGCGTTTACTGGTATTCGCTAATCGGTACG	pAL2235	
TT534	CGGCTTGAACGAATTGTTAGAC	pAL2236	
TT535	AGCTCTCGGGTAACATCAAGG	pAL2236	
TT536	CTAACAATTCGTTCAAGCCGGACTCCTGTTGATAGATCCAGTAATGACCTC	pAL2236	
TT537	CTTGATGTTACCCGAGAGCTGGCGCCCCAGCTGGCAATTC	pAL2236	
TT552	GCTTGGTTGAGAATACGCCGAAGTTAAAATCAGC	SS9 repair fragment	SS9
TT553	GCCTACGATTACGCATGGCTTGCC	SS9 repair fragment	SS9
TT577	TTAGCGATACTGCGGCGCCAG		*fdh* (*Cb*)
TT580	TAGCACGCGTATTTGATGCCTCTAGCACGCGTTTACTTTTTATCATGTTTTCCGTACGCTTTGGTCACG	*fdh* (*Cb*)	
TT586	TTCTCCTCTTTAATGAATTCAACTAGTATTATACCTAGGACTGAGCTAGCTGTCAAC	SS9 repair fragment	
TT593	CATTGCACAAGGACTCAAGG		*fdh* (*Sc*)
TT594	AAAATTGTGGCCATAACGTG		*fdh* (*Sc*)
TT609	TTATGCCACCAGAGCTTATGGACAGAAGAAATAAACGCGTGCTAGAGGCATCAAATACG	SS9 repair fragment	
TT613	CTTCGACATCTAGTATTTCTCCTCTTTCACTAGTAACTAGTATTATACCTAGGACTGAG	SS9 repair fragment	
TT614	AATACTAGTTACTAGTGAAAGAGGAGAAATACTAGATGTCGAAGGGAAAGGTTTTGCTG	*fdh* (*Sc*)	
TT615	GCACGCGTATTTGATGCCTCTAGCACGCGTTTATTTCTTCTGTCCATAAGCTCTGGTGG	*fdh* (*Sc*)	

TT616	ACCAAAGCGTACGGAAAACATGATAAAAAGTAAACGCGTGCTAGAGGCAT CAAATACGC	SS9 repair fragment	
TT617	TTGACAGCTAGCTCAGTCCTAGGTATAATACTAGTTGAATTCATTAAAGA GGAGAAAGG	*fdh* (*Cb*)	

Cb, Candida boidinii; Sb, Saccharomyces cerevisiae

Table 3.S3 Plasmid construction guide

Plasmid	Vector PCR			Insert(s) PCR			
	Primer (F)	Primer (R)	Template	Primer (F)	Primer (R)	Template	Insert description
pAL1899*	MM276	MM277	pAL1851				
pAL2235	TT530	TT531	pAL1023	TT532	TT533	pYT048	rGCS
pAL2236	TT534	TT535	pTargetF	TT537	TT536	pAL2235	rGCS
pAL2342*	MM60	MM62	pAL1851				

*Q5 Site-Directed Mutagenesis (NEB)

Table 3.S4 Guide for CRISPR-Cas9-Mediated gene deletions and insertions

Modification	pTargetF		Linear repair fragment assembly PCR primers and PCR Template
	Plasmid	20 bp sgRNA targeting sequence 5' to 3'	
Δ*serA*	pAL1899	GCCAATGCTAAAGCGCACCG	MM274, MM275 Template: YT151
P_{sdaA}::P_{LlacO1}	pAL2342	TCGCAATATTAGTTAAATCG	MM63, MM64, Template: YT276
SS9::P_{J23119}:*fdh* (*At*)	pAL1853	TCTGGCGCAGTTGATATGTA	TT552, TT553 Template: pAL2244
SS9::P_{J23119}:*fdh* (*Cb*)	pAL1853	TCTGGCGCAGTTGATATGTA	TT552, TT553, TT586, TT616 Template: pAL2244 TT617, TT580 Template: *Cb gDNA*
SS9::P_{J23119}*fdh* (*Sc*)	pAL1853	TCTGGCGCAGTTGATATGTA	TT552, TT553, TT609, TT613 Template: pAL2244 TT614, TT615 Template: *Sc gDNA*

At, *Arabidopsis* thaliana; *Cb, Candida boidinii*; *Sb, Saccharomyces cerevisiae*
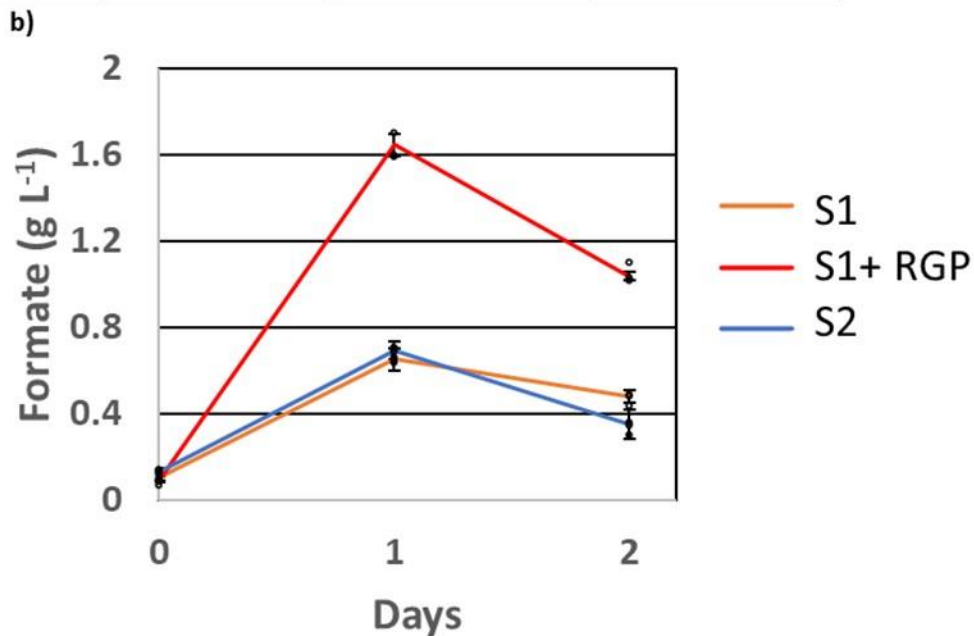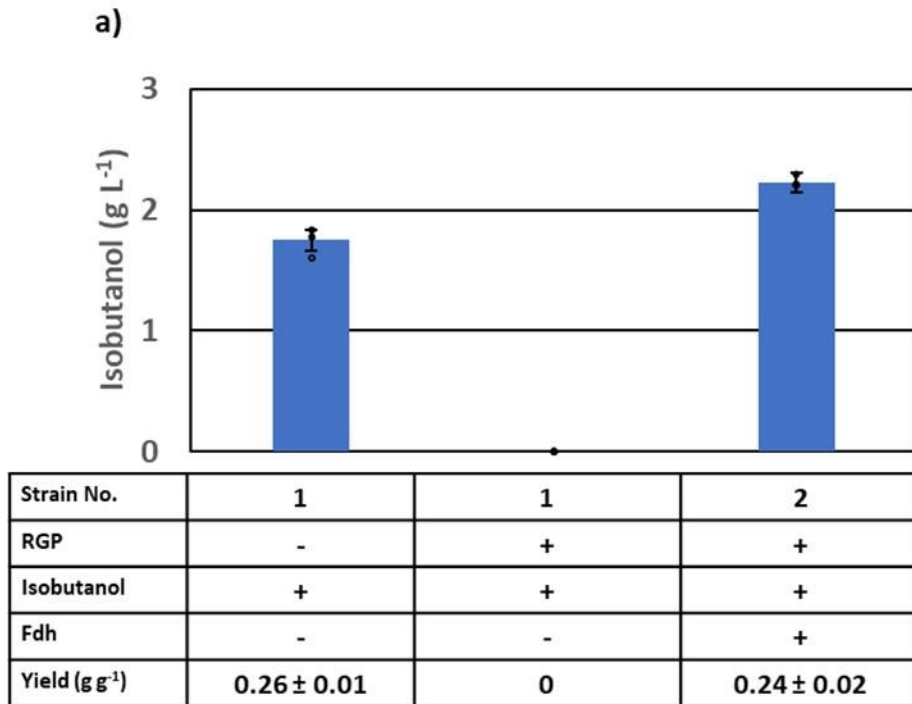
Figure 3.S1 Isobutanol in YT151 strains

a) Isobutanol production in Strain 1 with or without the presence of the RGP and Strain 2 with

the RGP and *fdh* after 2 days. Cultured in M9P with 10 g L^{-1} glucose 0.2 g L^{-1} formate, 50 mM

sodium bicarbonate with 1 mM IPTG and 10 μg L^{-1} aTc. **b)** Formate concentration in media over

time in Strain 1 with and without the presence of the RGP and Strain 2. Errors indicate s.d. (n = 3 biological replicates).
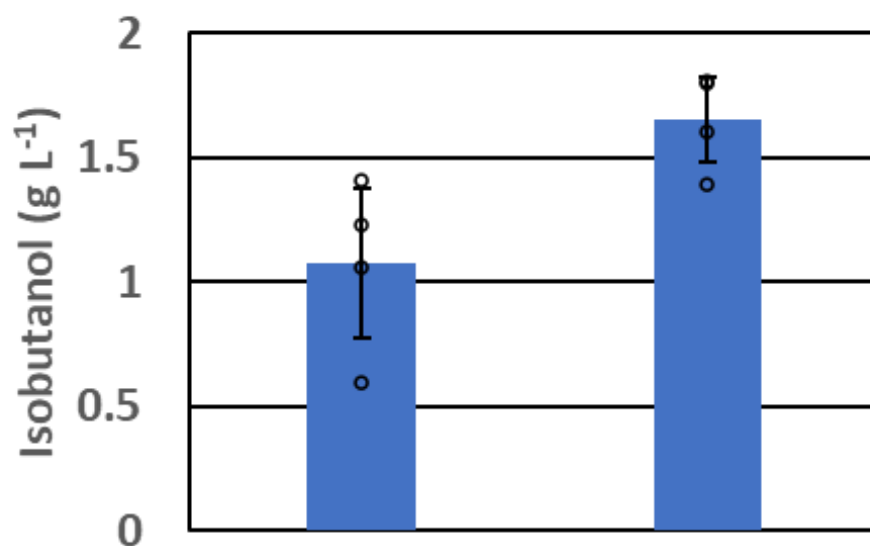
Strain No.	8	8
RGP	-	+
Formate Consumed (g L^{-1})	2.8 ± 0.01	2.9 ± 0.06
Yield (g g^{-1})	0.32 ± 0.04	0.38 ± 0.03

Figure 3.S2 Isobutanol production in Strain 8 with and without RGP

Isobutanol production after 3 days in Strain 8 with or without the RGP. Cultured in M9P with 10 g L^{-1} glucose 3 g L^{-1} formate, 50 mM sodium bicarbonate with 1 mM IPTG and 10 µg L^{-1} aTc. Errors indicate s.d. (n = 3 biological replicates).

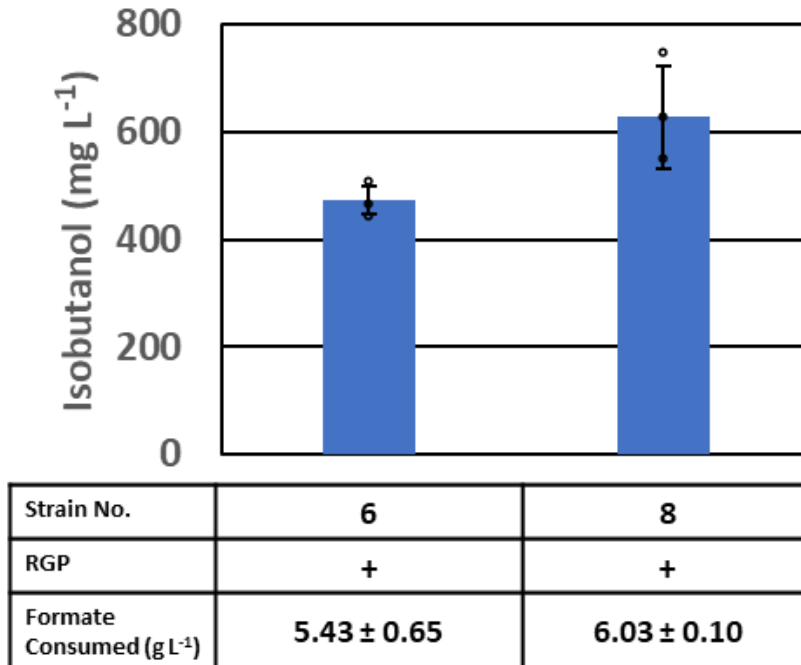| Strain No.	6	8
RGP	+	+
Formate Consumed (g L^{-1})	5.43 ± 0.65	6.03 ± 0.10

Figure 3.S3 High density isobutanol production without glucose

Isobutanol titer after 1 hour in Strains 6 and 8. Cultured in M9P with 10 g L^{-1} formate, 50 mM sodium bicarbonate with 1mM IPTG and 10 µg L^{-1} aTc. Errors indicate s.d. (n = 3 biological replicates).
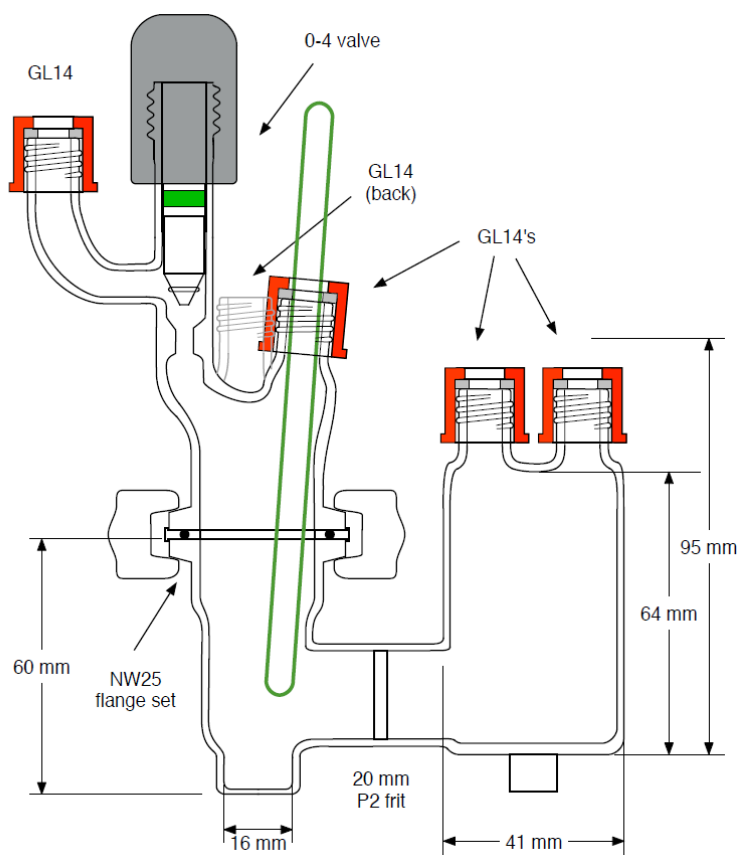
Figure 3.S4 Schematic of H-cell used in CPE experiments to produce formate.
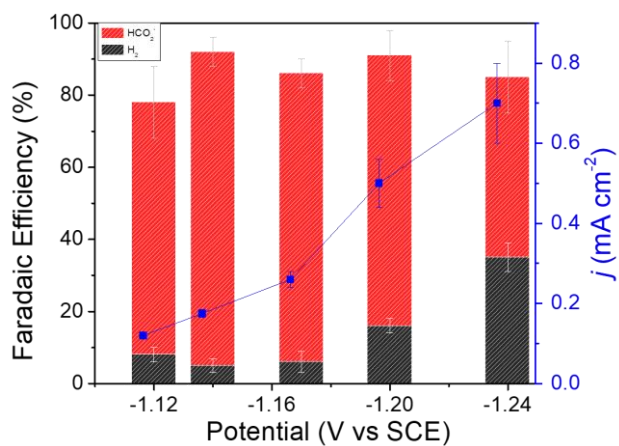
Figure 3.S5 CPE experiments

Plot of faradaic efficiency (%) and current density (j) vs applied potential (V vs SCE) during controlled potential electrolysis over 1 h with 0.5 mM [Na(diglyme)][Fe$_4$N(CO)$_{12}$] in 0.1 M phosphate buffer (pH 7.4). Errors indicate s.d. (n = 3 replicates).
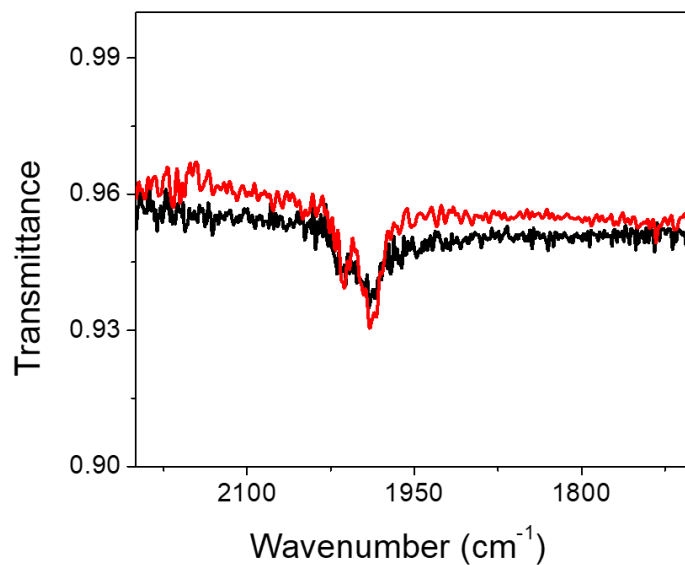
Figure 3.S6 Infrared spectra of [Na(diglyme)$_2$][Fe$_4$N(CO)$_{12}$]

IR spectra of [Na(diglyme)$_2$][Fe$_4$N(CO)$_{12}$] recorded before (red) and after (black) CPE experiment in 0.1 M Phosphate buffer. The peak at 2015 and 1989 are characteristic of [Na(diglyme)$_2$][Fe$_4$N(CO)$_{12}$] reported elsewhere[6].

Chapter 4: Conclusion

The research presented in these works represents the ability of metabolic engineering to enable renewable methodologies for chemical commodity synthesis from renewable sources. These bioproduction systems are able to use renewable feedstocks such as sugars or carbon dioxide to generate the same chemical commodities that have been historically sourced from petrochemical methods. With each advance in the field of bioproduction we drive towards a more sustainable economy that is less dependent on fossil fuels. As this field progresses it is highly important to continue efforts to make these chemical production platforms more sustainable through investigating various production hosts that can enable novel synthesis routes for these products.

Succinate production in 7942, addressed in chapter two, is a promising step towards a more sustainable bioproduction system. While succinate can be readily produced in other host organisms, cyanobacteria offer a means for carbon dioxide to be directly converted into succinate. By continuing to investigate cyanobacteria as production hosts, any increase in our understanding of these organisms will progress our ability to use these photosynthetic hosts as alternative bioproduction systems that offer several benefits over their heterotrophic counterparts. Photomixotrophy, in particular, is a system that is relatively new to the field of metabolic engineering and due to its positive benefits on both production and growth of 7942 requires further study. By continuing to investigate photomixotrophy we may continue to optimize this altered form of metabolism to better utilize photosynthetic hosts to produce everyday chemical commodities.

Similarly, developing carbon sequestration pathways in traditionally heterotrophic organisms, such as *E. coli,* is another important route for metabolic engineering as a field to explore. As addressed in chapter three, developing a *de novo* carbon fixation pathway improves the sustainable effects of using bioproduction systems. While isobutanol is a well established product of these engineered microorganisms, we can continue to improve upon these synthetic routes by investigating novel pathways such as the reductive glycine pathway to bolster chemical production from single carbon substrates.

With each new finding, the field of metabolic engineering is driving closer to the end goal of solving the sustainability challenges we are facing globally. As we move on from the systems and processes of the industrial revolution to mitigate the ongoing climate crisis, it is of paramount importance to look to nature for solutions and to ensure the longevity of life on this planet.

Appendices

Appendix A: Exploring Various Pathways for the Production of 1,4 – Butanediol in Cyanobacteria

1,4-butanediol is a valuable platform chemical commodity that has uses in synthesizing important materials or industrial chemicals. However, like many traditional routes for synthesizing platform chemicals, the route to produce 1,4-butanediol relies on petrochemical and energy-intensive methods. Synthesizing 1,4-butanediol using bio-based methods are one approach to alleviate the environmental impact of generating platform chemicals that the economy relies on. In our current work to produce 1,4-butanediol using 7942 we have attempted to engineer three distinct pathways into cyanobacteria. The first pathway was provided by the Golden Lab at UCSD. This pathway contains the following genes under the control of the IPTG inducible promoter Ptrc: 4*hbd* which encodes for a 4-hydroxybutyrate dehydrogenase from *Porphyromonas gingivalis, kgd* which encodes for an alpha-ketoglutarate dehydrogenase from *Synechococcus elongatus* PCC 7002, *cat2* which encodes for a 4-hydroxybutyrate CoA transferase from *Porphyromonas gingivalis*, *ald* which encodes for an aldehyde dehydrogenase from *Clostridium beijerinckii*, and *adh1* which encodes for an alcohol dehydrogenase from *Geobacillus thermoglucosidasius*. These five enzymes are responsible for converting alpha-ketoglutarate to 1,4-butanediol. However, when we installed this pathway in 7942, generating Strain 1, no 1,4-butanediol was detected.

Rather than investigating the potential bottlenecks or side products of this pathway, we instead constructed an alternative strain using a different pathway known as the Weimberg pathway, in an effort to efficiently convert extracellular xylose into alpha-ketoglutarate. This pathway consists of a xylose transporter from *Escherichia coli* encoded by the gene *xylE*, and four genes from *Caulobacter crescentus*: *xdh* which encodes for a xylose dehydrogenase, *xylC* which encodes for a D-xylonolactonase, *xylD* which encodes for a D-xylonate dehydrogenase, and *xylX* which encodes for a 2-keto-3-deoxy-D-xylonate dehydratase. Alpha-ketoglutarate is then leveraged to produce 1,4-butanediol through the enzymes alpha-ketoisovalerate decarboxylase (*kivD*) from *Lactococcus lactis* and an alcohol dehydrogenase (*yqhD*) from *Escherichia coli.* The final strain (Strain 2) which was constructed to possess both the Weimberg pathway along with *kivD* and *yqhD,* was able to consume extracellular xylose (~5g/L over 5 days) and produce 1,4-butanediol in small quantities, approximately 50mg/L. As a control, a strain was also constructed with the genes *kivD* and *yqhD* alone (Strain 3) and this strain was unable to produce 1,4-butanediol. These results suggest that the Weimberg pathway functions and may increase the

intracellular amount of 2,5-dioxopentanoate to the concentration required to synthesize 1,4-butanediol via this route but due to the low yield (0.01 gram 1,4-butanediol produced per gram xylose consumed) we believe that the Weimberg pathway intermediates may interact with central metabolism, thus funneling our substrate intended for 1,4-butanediol to other metabolites. This hypothesis requires further investigation, but due to the lower than anticipated titer of 1,4-butanediol made by Strain 2 we decided our efforts would be better spent investigating a third pathway for 1,4-butanediol production.

This final pathway involves leveraging succinate semialdehyde pools that are produced through the reaction catalyzed by the enzyme alpha-ketoglutarate dehydrogenase which was shown to be functional in our own succinate production studies. Succinate semialdehyde is converted to 4-hydroxybutyrate by an alcohol dehydrogenase encoded by the gene *yqhD* from *Escherichia coli.* 4-hydroxybutyrate is then converted to 4-hydroxybutyraldehyde by a carboxylic acid reductase encoded by the gene *car* from *Mycobacterium marinum.* We also engineered our strain to house the gene *sfp,* which encodes an apoprotein from *Bacillus subtilis* that has been shown to improve the activity of the carboxylic acid reductase. 4-hydroxybutyraldehyde is then ultimately converted to 1,4-butanediol by the alcohol dehydrogenase. When this pathway was installed into 7942, Strain 4 was generated. Strain 4 produced ~90mg/L 1,4-butanediol in 5 days under photoautotrophic conditions, suggesting that this 1,4-butanediol production pathway is more efficient in the context of global 7942 metabolism. Future work with this strain is planned to include engineering photomixotrophic strains using this pathway that can utilize both glucose and/or xylose to increase the carbon flux towards 1,4-butanediol. We hypothesize that like in our previous studies, photomixotrophy will be beneficial for 1,4-butanediol production.

Appendix B: Electrical-Biological Hybrid System for Polymer Precursor Production in Collaboration with Zymochem

As reported in the above study regarding electrical-biological hybrid production of isobutanol we worked in collaboration with Zymochem to use this hybrid system to produce formate in an effort to power the redox requirements of their polymer precursor pathway in *Escherichia coli*. Several experiments were conducted to establish this hybrid system. First, the iron carbonyl cluster used as a catalyst to reduce carbon dioxide to formate was tested in media in various concentrations to determine if any toxic effects on growth or production were observed. We determined that growth of *E. coli* was inhibited by the presence of the catalyst in the optimal concentration for catalysis (0.5mM). We determined that 0.1mM was nontoxic to *E. coli* and thus further experiments were conducted using this concentration.

Using 0.5mM catalyst concentration, the production of ~4g/L formate was observed over the course of 20 hours. Using the 0.1mM concentration ~100mg/L (2.2mM) formate was produced in the same time period. The Zymochem strain requires one equivalent of formate to generate one equivalent of NADH using a formate dehydrogenase (FDH) from *Saccharomyces cerevisiae.* One NADH is required for one equivalent of substrate in this pathway. The molar mass of the substrate is ~146g/mol, upon feeding *E. coli* 10g/L in a 25mL fermentation inside of the active electrical bioreactor, ~2.5g/L of the product (molar mass of ~147g/mol) was produced. When the same experiment was conducted outside of the electrical bioreactor without any formate added to solution, no product formation was observed suggesting that the formate produced by the electrocatalysis is responsible for the necessary reducing equivalents to power this step of the polymer precursor pathway. These experiments provided clear proof of concept that an electrical-biological hybrid system can be used to provide an alternative and environmentally conscious way of harnessing atmospheric carbon dioxide to produce chemical commodities.